

2607

1809

JPL Publication 84-28

DOE/ET 29372-4
Distribution Category UC-97b

Power System Applications of Fiber Optics

H. Kirkham
A. Johnston
G. Lutes
T. Daud
S. Hyland

(NASA-CR-176831) POWER SYSTEM APPLICATIONS
OF FIBER OPTICS (Jet Propulsion Lab.) 180 p
HC A09/MF A01 CSCL 10A

N86-25875

Unclas
G3/44 43039

March 1984

Prepared for
Electric Energy Systems Division
U.S. Department of Energy
Through an Agreement with
National Aeronautics and Space Administration
by
Jet Propulsion Laboratory
California Institute of Technology
Pasadena, California

1. Report No. 84-28	2. Government Accession No.	3. Recipient's Catalog No.	
4. Title and Subtitle Power System Applications of Fiber Optics		5. Report Date March 1984	6. Performing Organization Code
7. Author(s) H. Kirkham, A. Johnston, G. Lutes, T. Daud, S. Hyland		8. Performing Organization Report No.	
9. Performing Organization Name and Address JET PROPULSION LABORATORY <i>5574450</i> California Institute of Technology 4800 Oak Grove Drive Pasadena, California 91109		10. Work Unit No.	11. Contract or Grant No. NAS7-918
12. Sponsoring Agency Name and Address NATIONAL AERONAUTICS AND SPACE ADMINISTRATION Washington, D.C. 20546		13. Type of Report and Period Covered JPL Publication	
15. Supplementary Notes Sponsored by the U.S. Department of Energy through Interagency Agreement DE-AI01-79ET29372 with NASA; also identified as DOE/ET 29372-4 (RTOP or Customer Code 778-12-01).		14. Sponsoring Agency Code	
<p>16. Abstract</p> <p>Power system applications of optical systems, primarily using fiber optics, are reviewed. The first section of the report reviews fibers as components of communication systems. Recent development in the technology, the present state of the art and power system applications and experience are covered.</p> <p>The second section deals with fiber sensors for power systems, reviewing the many ways light sources and fibers can be combined to make measurements. Methods of measuring electric field gradient are discussed, in some depth, and some experimental work done at the Jet Propulsion Laboratory in this area is reported.</p> <p>Optical data processing is the subject of the third section, which begins by reviewing some widely different examples and concludes by outlining some potential applications in power systems: fault location in transformers, optical switching for light-fired thyristors and fault detection based on the inherent symmetry of most power apparatus.</p> <p>The fourth and final section is concerned with using optical fibers to transmit power to electronic equipment in a high-voltage situation, potentially replacing expensive high-voltage low-power transformers. JPL has designed small photodiodes specifically for this purpose, and fabricated and tested several samples. This work is described.</p>			
<p>17. Key Words (Selected by Author(s))</p> <p><i>ENERGY</i> Conversion Techniques <i>ELECTRIC</i> Power Sources <i>SUPPLIES</i> Energy Production TECHNOLOGY <i>FIBER OPTICS</i> OPTICAL COMMUNICATION</p>		<p>18. Distribution Statement</p> <p>Remote SENSORS LIGHT SOURCES ELECTRIC FIELDS DATA PULSE TRANSFORMER OPTICAL SWITCHING</p> <p>THYRISTORS PHOTO DIODES</p> <p>Unclassified-unlimited</p>	
19. Security Classif. (of this report) Unclassified	20. Security Classif. (of this page) Unclassified	21. No. of Pages 186	22. Price

Power System Applications of Fiber Optics

H. Kirkham
A. Johnston
G. Lutes
T. Daud
S. Hyland

March 1984

Prepared for
Electric Energy Systems Division
U.S. Department of Energy
Through an Agreement with
National Aeronautics and Space Administration
by
Jet Propulsion Laboratory
California Institute of Technology
Pasadena, California

Prepared by the Jet Propulsion Laboratory, California Institute of Technology,
for the U.S. Department of Energy through an agreement with the National
Aeronautics and Space Administration.

This report was prepared as an account of work sponsored by an agency of the
United States Government. Neither the United States Government nor any
agency thereof, nor any of their employees, makes any warranty, express or
implied, or assumes any legal liability or responsibility for the accuracy, com-
pleteness, or usefulness of any information, apparatus, product, or process
disclosed, or represents that its use would not infringe privately owned rights.

Reference herein to any specific commercial product, process, or service by trade
name, trademark, manufacturer, or otherwise, does not necessarily constitute or
imply its endorsement, recommendation, or favoring by the United States
Government or any agency thereof. The views and opinions of authors
expressed herein do not necessarily state or reflect those of the United States
Government or any agency thereof.

This publication reports on work performed under NASA Task RE-152, Amend-
ment 203 (change 7, paragraph II.A.(7)) and sponsored through DOE/NASA
Interagency Agreement No. DE-AI01-79ET 29372 (Mod. A009).

POWER SYSTEM APPLICATIONS OF FIBER OPTICS
H. Kirkham, A. Johnston, G. Lutes, T. Daud, S. Hyland

ABSTRACT

Power system applications of optical systems, primarily using fiber optics, are reviewed. The first section of the report reviews fibers as components of communications systems. Recent development in the technology, the present state-of-the-art and power system applications and experience are covered.

The second section deals with fiber sensors for power systems, reviewing the many ways light sources and fibers can be combined to make measurements. Methods of measuring electric field gradient are discussed in some depth, and some experimental work done at the Jet Propulsion Laboratory in this area is reported.

Optical data processing is the subject of the third section, which begins by reviewing some widely different examples and concludes by outlining some potential applications in power systems: fault location in transformers, optical switching for light-fired thyristors and fault detection based on the inherent symmetry of most power apparatus.

The fourth and final section is concerned with using optical fibers to transmit power to electronic equipment in a high-voltage situation, potentially replacing expensive high-voltage low-power transformers. JPL has designed small photodiodes specifically for this purpose, and fabricated and tested several samples. This work is described.

ACKNOWLEDGMENTS

This report is a combination of four reports prepared for the Electric Energy Systems Division of the Department of Energy in 1983 as part of the JPL project 'Communications and Control in Electric Power Systems'. Thanks are due to Ken Klein of that office for his continued interest and support, and his helpful suggestions throughout the work.

Each section of the report corresponds to one of the four reports delivered to DOR. The first deals with communications applications of fiber optics and was written largely by George Lutes who, as part of his responsibilities at the Jet Propulsion Laboratory has installed optical fibers between the various antennae at the Goldstone Deep Space Communications Complex. These links will be used for high-accuracy timing signals to make possible long baseline interferometry.

Section 2 covers sensor applications, reviewing the measurement of electric fields in particular. Most of the section was written by Alan Johnston, a group supervisor in Section 364, with wide experience in optical systems. A fiber optics experiment with Dr. Johnston as principal investigator is scheduled to fly on the Space Shuttle in 1984.

Hoshyar Sayah fabricated the electrometer field sensor described in Section 2, and did the experimental work to furnish the calibration data.

As task manager, I participated in the writing of all the sections. Section 3, which introduces optical data processing, was, unlike the other sections, a solo effort on my part.

The transmission of power over optical fibers is covered in Section 4. The ability to transmit power to supply remote electronics could save the expense of a high-voltage transformer in some power system applications. The design study and the photocells that were fabricated were the work of Sandra Hyland and Taher Daud, who wrote most of Section 4.3.

Contributions to Section 4 were also made by Kevin Jones of California Polytechnic University, Pomona, California.

An Appendix describes in detail the solution of Poisson's equation in cylindrical coordinates, and the computer program written to find numerical values for the impact of ion current on the gradient distribution in a high-voltage test cage. I am grateful to Radhe Das of California State University at Long Beach, California, for his valuable help with this material.

I would like to express my appreciation to all of the people mentioned above for their contributions to the work and to this report. Credit must also be given to the administration at the Jet Propulsion Laboratory for providing time to prepare this document. In particular, thanks are due to John Klein, who served both as Project Manager and Group Supervisor during 1983-1984.

Harold Kirkham
March 1984

CONTENTS

1.	POWER SYSTEM APPLICATIONS OF FIBER OPTICS COMMUNICATIONS	1-1
1.1	Introduction	1-1
1.2	Optical Fiber Technology	1-1
1.2.1	Optical Fiber	1-2
1.2.2	Types of Fiber	1-2
1.2.3	Fiber Parameters	1-4
1.2.4	Optical Fiber Cable	1-7
1.2.5	Optical Fiber Communications System	1-9
1.2.6	Advantages of Optical Fiber	1-11
1.2.7	Splices	1-11
1.2.8	Connectors	1-15
1.2.9	Modulation	1-15
1.2.10	Multiplexing	1-18
1.2.11	Signal-to-Noise Ratio	1-18
1.2.12	Delay Stability	1-19
1.2.13	Optical Transmitters	1-19
1.2.14	Optical Receivers	1-21
1.2.15	Future Developments	1-21
1.3	State of the Art in Fiber Optics Communications.	1-23
1.3.1	Bandwidth and Distance	1-23
1.3.2	Delay Stability	1-23
1.3.3	Commercial Installations	1-23
1.4	Electric Utility Applications.	1-25
1.4.1	Substation Applications of Optical Fibers	1-25
1.4.2	Intra-System Communication using Fiber Optics	1-28
1.4.3	Optical Fibers in Power Conductors	1-28
1.4.4	Concluding Remarks	1-32
1.5	References	1-33
2.	POWER SYSTEM APPLICATIONS OF FIBER OPTICS SENSORS	2-1
2.1	Introduction	2-1
2.1.1	Optical Fiber Technology	2-1
2.1.2	Fibers as Sensors	2-2
2.1.3	General Sensor Types	2-3
2.1.4	Distributed vs Point Sensing	2-8
2.2	Power-System Sensors.	2-9
2.2.1	General Criteria for a Power System Sensors	2-9
2.2.2	Measurement Quantities	2-9
2.2.3	Voltage Measurement	2-10
2.3	E-Field Measurement.	2-13
2.3.1	Background	2-13
2.3.2	General Consideration for E-Field Measurement	2-14
2.4	Optical Building Blocks.	2-25
2.4.1	Input and Output Coupling Considerations	2-25
2.4.2	Lenses	2-25
2.4.3	Couplers	2-26

2.4.4	Polarizers	2-26
2.4.5	Isolator	2-29
2.4.6	Connectors and Splices	2-29
2.4.7	Integrated Optics	2-29
2.4.8	Sources and Detectors	2-30
2.5	Direct Fiber Optic Sensing of E-Field.	2-31
2.5.1	Linear Electro-Optic Effect Sensors	2-31
2.5.2	Kerr Effect	2-35
2.5.3	Piezoelectric Jacketed Fiber	2-37
2.5.4	Fused Silica Electrometer	2-39
2.5.5	Other Optical Techniques	2-42
2.6	Electronic Sensing Techniques with Fiber Readout	2-47
2.6.1	The Influence of Microelectronics-Microtransducer Technology	2-47
2.6.2	Power Considerations for Microcircuit Fiber Transmitter	2-49
2.6.3	Electrometer Amplifier E-Field Sensor	2-49
2.6.4	The Electret	2-50
2.6.5	Vibrating Plate Electrometer	2-54
2.6.6	Other Electronic Field Sensor Concepts	2-55
2.7	Summary and Conclusions.	2-56
2.8	References	2-60
3.	POWER SYSTEM APPLICATIONS OF OPTICAL DATA PROCESSING	3-1
3.1	Introduction	3-1
3.2	Background	3-2
3.2.1	Optical Computers	3-2
3.2.2	Special-Purpose Optical Computing	3-7
3.2.3	Fourier Transform	3-15
3.2.4	Concluding Remarks	3-23
3.3	Power System Applications of Optical Data Processing	3-24
3.3.1	Introduction	3-24
3.3.2	Transformer Protection	3-24
3.3.3	Transformer Fault Location	3-26
3.3.4	HVDC Control Pulse Generation	3-31
3.3.5	Concluding Remarks	3-34
3.4	References	3-37
4.	POWER SYSTEM APPLICATIONS OF OPTICAL POWER TRANSFER	4-1
4.1	Introduction	4-1
4.1.1	Other Applications	4-4
4.2	System Description	4-6
4.2.1	Overall Design	4-6
4.2.2	Electrical to Optical Conversion	4-6
4.2.3	Source to Fiber Coupling	4-7
4.2.4	Fiber	4-9
4.2.5	Receiving End	4-9
4.3	Device for Energy Conversion at 0.85 μm	4-11

4.3.1	Review	4-11
4.3.2	Device Design	4-11
4.3.3	Device Fabrication and Measurements	4-14
4.3.4	Test Results	4-16
4.4	Future Work.	4-20

APPENDIX	Solutions of Poisson's Equations in Cylindrical Coordinates	A-1
----------	---	-----

Figures

1-1	Diagram showing the critical angle and the acceptance cone half-angle for a step index fiber	1-3
1-2	Staircase output amplitude due to modal dispersion and the different arrival times it causes	1-6
1-3	Typical fiber construction methods	1-8
1-4	Fiber optic communication system	1-10
1-5	Bandwidth versus cable length for some optical fibers and coaxial cables	1-12
1-6	Attenuation versus frequency for some optical fibers and coaxial cables	1-13
1-7	Two methods of splicing fiber optic cables. (a) Fusion splice (b) Chemical bond splice	1-14
1-8	Optical fiber connector	1-16
1-9	Fiber end preparation. (a) Lapped (b) Cleaved	1-17
1-10	Optical link in oil-filled insulator	1-27
1-11	Possible designs for composite cable	1-30
2-1	Interferometer sensor configurations	2-4
2-2	An example of an optical sensor based on intensity. The fiber-optic microbend transducer	2-7
2-3	High impedance amplifier configuration	2-16
2-4	Rotating-vane field mill	2-19

2-5	(a) Electric field gradient as a function of radius of various values of ion current, cylindrical geometry	
	(b) Electric field gradient at the conductor surface and the ground as a function of ion current	2-24
2-6	(a) Four-port fused tapered multimode fiber coupler	
	(b) Stanford single-mode four-port fiber coupler	2-28
2-7	The elements of an electro-optic field sensor.	
	(a) for transverse geometry	
	(b) for longitudinal geometry	2-32
2-8	An Electric field sensor based on piezoelectric jacketed fibers	2-38
2-9	A concept for implementing a fused silica fiber electroscope with integral optical fiber readout	2-40
2-10	Transmitted light intensity for fiber electrometer as a function of directly applied voltage	2-41
2-11	A concept for field sensing using deflection of thin membranes	2-44
2-12	An all-dielectric torsion balance for field measurements	2-45
2-13	Functional diagram of a representative electronic sensor-fiber readout field measurement system	2-48
2-14	Cutaway view of electret microphone	2-52
3-1	Fabry-Perot interferometer	3-3
3-2	Transfer curve of nonlinear Fabry-Perot interferometer	3-5
3-3	Two input nonlinear Fabry-Perot interferometer	3-6
3-4	Optical logic array processor	3-9
3-5	Overlapping of projections of the ij cell	3-11
3-6	Nine-by-nine image region for sixteen logic operations on two binary variables using bright-true logic	3-12
3-7	Experimental results, 64 x 64 array processor	3-14
3-8	Transforming lens/object configuration	3-17
3-9	Diffraction geometry	3-20
3-10	Optically obtained Fourier spectrum of the character '3'	3-22

3-11 Transformer Construction	3-25
3-12 Fault location using two sensors	3-27
3-13 Conceptual diagram of three-dimensional fault identification and location system	3-30
3-14 Generation of optical firing pulses. (a) by switching light source on and off. (b) by optical switching	3-32
3-15 Mach-Zehnder ipterferometer with electro-optic delay arm . .	3-33
3-16 Fabry-Perot interferometer as an electro-optical switch . .	3-35
3-17 Polarization-type optical switching. (a) electro-optical (b) magneto-optical	3-36
4-1 Digital data link in high voltage bus	4-2
4-2 Optical data link. (a) power supplied over separate fiber (b) power supplied over separate fiber	4-3
4-3 Optically-transmitted power in HVDC application	4-5
4-4 Block diagram of optical power transfer system	4-8
4-5 Light Cone Emerging From The End Of An Optical Fiber	4-10
4-6 Device Design	4-12
4-7 Current-Voltage Curves, Measured and Theoretical	4-15

SECTION ONE

**POWER SYSTEM APPLICATIONS
OF
FIBER OPTICS COMMUNICATIONS**

by

George Lutes and Harold Kirkham

SECTION 1

POWER SYSTEM APPLICATIONS OF FIBER OPTIC COMMUNICATIONS

1.1 INTRODUCTION

The present widespread interest in optical fibers began in the communications industry, and it is largely through the efforts of laboratories tied to the telephone companies of the industrial nations (particularly the United States, England, Germany and Japan) that fibers have come down in cost and gone up in performance to their present competitive levels. It is therefore fitting that we begin this report with a review of optical fibers for communications purposes.

Because not all readers will be familiar with optical fiber technology, we have attempted to present in this section, in addition to a review of fiber communications technology, material which can serve as background to the concepts presented later, for example in Section 2 (Sensors) or Section 3 (Data Processing).

Section 1.2 begins with a discussion of optical fibers, how they work, how they are assembled into cables, and how communication systems are built using them. Section 1.3 presents a short review of the state of the art in fiber-based communication systems (as of late 1983) and Section 1.4 concludes the first part of the report by describing utility applications and experience.

1.2 OPTICAL FIBER TECHNOLOGY

The possibility of using glass fibers for communications was conceived as far back as 1910 when Hondros and Debye [1-1]¹ showed analytically that a circularly symmetrical transverse magnetic (TM) mode can be guided by a dielectric cylinder situated in free space. The existence of this wave was demonstrated experimentally by Zahn, Rueter and Schreiver in 1916 [1-2]. The observation of waveguide modes in optical fibers was first reported by Snitzer and Hicks in 1959, but the loss in this fiber was more than 1000 dB/km [1-3], making its use for communications impractical.

In the mid-1960s Kao and Hockam [1-4], then of Standard Telecommunication Laboratories in England, realized that optical waveguide attenuation was not a function of any basic property of the glass, but rather of impurities. Optical fibers became a viable medium for communications in 1970 when Kapron, Keck, and Maurer announced the fabrication of glass fibers having less than 20 dB loss per kilometer [1-5]. The fiber loss has since rapidly decreased and now is approaching the theoretical limit of 0.2 dB/km for glass fiber at 1500 nm optical wavelength.

¹Numbers in brackets indicate references.

Light Emitting Diodes (LEDs) were developed in the 1960s for displays and later became the highly reliable light sources needed for optical fiber communications. By the late 1970s a more efficient and more concentrated light source, the semiconductor laser diode operating at 850-nm wavelength, had achieved adequate reliability for use in optical fiber communications systems. Laser diodes permitted optical fiber links to operate over distances in the tens of km. More recently, laser diodes operating at 1300 nm wavelengths have been developed. This wavelength is desirable because it is near the minimum dispersion wavelength of glass fibers, and losses less than 0.5 dB/km can be achieved. Systems operating at this wavelength have demonstrated data rates in excess of 400 Mb/s over distances greater than 100 km without repeaters.

1.2.1 Optical Fiber Construction

An optical fiber consists of a core of transparent material surrounded by a cladding of transparent material having a lower index of refraction than the core. When light is launched into the core at an angle nearly parallel to the axis of the fiber, it is trapped. There is a critical angle at the core-cladding interface. If the incoming light is sufficiently oblique at this interface, it will be reflected. The critical angle and acceptance angle are explained in Figure 1-1.

A glass fiber coated with a reflective coating would not work as well. No conventional mirror can reflect all of the light striking it. A glass fiber with a shiny coating, such as silver, would have a large loss because much of the light in a multimode glass fiber is reflected hundreds of times per meter back and forth in the core. Some of the light would be absorbed at each reflection, and in a short distance the input power would be dissipated to an unusable level.

1.2.2 Types of Fiber

1.2.2.1 Step-Index Fiber. In step-index fiber there is a sharp transition in refractive index between the core and the cladding. If the core in this type of fiber is large enough in diameter to support many modes, that is to say, if light can enter the fiber at a variety of angles and be reflected various numbers of times, it is called multimode fiber. The intermodal dispersion in this type of fiber is large and limits its modulation bandwidth to about 20 MHz-km (see section 1.2.3).

1.2.2.2 Single-mode Fiber. If the core diameter is small enough, only the one mode traveling straight down the center of the fiber is transmitted. This is called single-mode fiber.

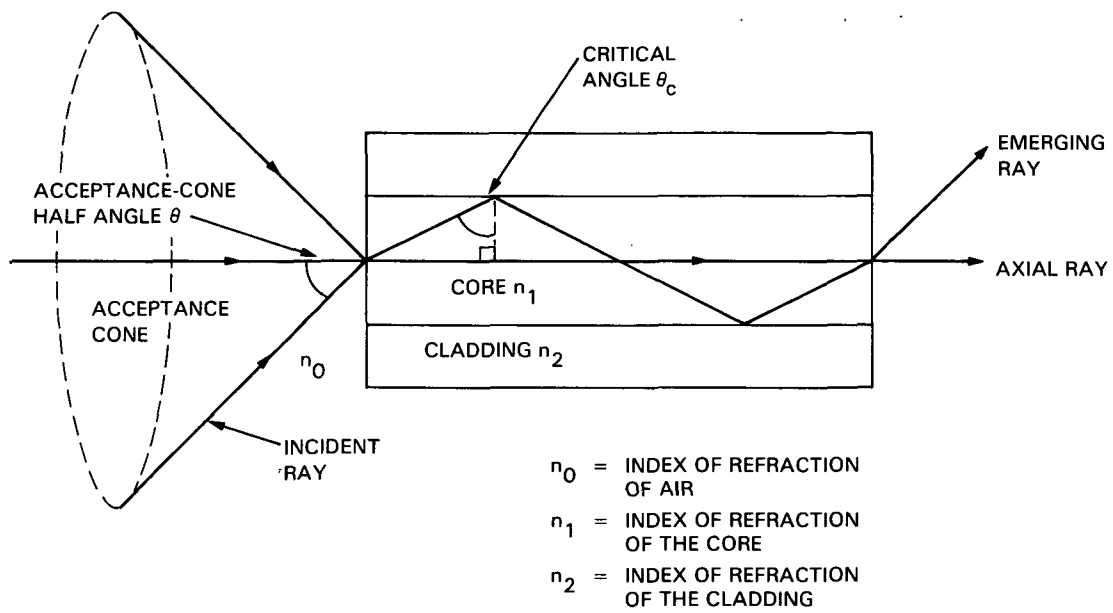


Figure 1-1. Diagram showing the critical angle and the acceptance cone half-angle for a step index fiber

1.2.2.3 Graded Index Fiber. In graded index fiber the index of refraction of the core increases gradually toward the center. Since light travels faster in material having a lower index of refraction, the higher order modes which travel farther in the core also travel proportionately faster. As a result, all of the modes reach the far end of the fiber at the same time. It is theoretically possible to eliminate intermodal distortion in multimode fiber if the index grading is perfect. In practice, intermodal dispersion is always present in multimode fiber. Bandwidth-distance products greater than 3 GHz-km in multimode fiber have been achieved, but bandwidths for 'off-the-shelf' multimode fibers are usually less than 1.5 GHz-km. Nevertheless, it is clear that this kind of fiber has more information-carrying capacity than multimode step-index fiber.

1.2.2.4 Fiber Material. There are three types of fiber construction: all-glass, glass core with plastic cladding and all-plastic. All-glass fiber is by far the best functionally, but also the most expensive. Fiber with a glass core and plastic cladding is less expensive but is characterized by temperature instability and loss. All-plastic fiber is the least expensive, but it is very lossy and is therefore used only over short distances.

As an indication of quality, it may be noted that plate glass used in windows has about 50,000 times more loss than the glass used in optical fibers.

1.2.3 Fiber Parameters

1.2.3.1 Modes. Modes can be thought of as individual rays of light traveling through the fiber. Some of them will bounce back and forth in the fiber at various angles and others will travel straight down the center of the fiber without touching the core/cladding interface. The modes bouncing back and forth at the greatest angle are the highest-order modes and the modes traveling straight down the fiber are the lowest-order modes. Discontinuities in the fiber, such as a splice or a sharp bend, can convert some of the lower-order modes to higher-order modes. If the discontinuity is too great, the angle of some of the modes can become smaller than the critical angle and light will escape through the side of the fiber. (This is how some optical fiber sensors work. The escaping light or the extra loss in the fiber can be measured).

1.2.3.2 Dispersion. Dispersion in a medium spreads out a wave front that is traveling through the medium. This results in rounding out of pulses that are transmitted. The effect is much the same as transmitting the signal through a low-pass filter. In severe cases the signal can be completely lost.

There are three kinds of dispersion in optical fibers: intermodal dispersion, material dispersion, and waveguide dispersion.

Intermodal dispersion occurs in multimode fibers, fibers that support more than one mode. When many modes travel through a fiber, the ones bouncing back and forth at the greatest angle travel farther than the modes going more directly through the fiber, so they reach the far end at different times. If, for example, we assume a pulse of light with a fast risetime is launched into

a fiber in 10 modes at the same instant, that each mode contains 10% of the total optical power and that the times the modes reach the far end of the fiber are evenly spaced, then a plot of the output power would look like Figure 1-2. The fast risetime at the input has become a staircase ramp at the output. In practice there are hundreds of modes in the fiber that reach the far end at time intervals that follow a standard distribution around the mean time of arrival. The result is a relatively smooth rounded curve that resembles a fast risetime transition that has passed through a low-pass filter.

If we assume all of the modes in the above example are traveling straight down the core of the fiber with none bouncing back and forth, then they will all get to the far end at the same time. The risetime in this case should be the same at the output as it is at the input, but in practice it is not because of material dispersion. Material dispersion has the same effect as intermodal dispersion but on a smaller scale in most systems. It is a result of the fact that light at different wavelengths travels through a fiber at different speeds. Light sources do not generate light at a single wavelength, but rather over a band of wavelengths. This band is extremely narrow for some sources and is often considered to be a single wavelength, but in reality it is not. Even the best lasers are not truly monochromatic.

If we now assume that the 10 different 'packets' of light traveling straight down the fiber are different wavelengths of light instead of modes, and that the times they reach the far end of the fiber are evenly spaced, we again get a ramp at the far end. This is the effect of material dispersion. The risetime of this ramp decreases as the number of wavelengths in the band decrease until there is only one wavelength. At this point the risetime at the output will be the same as the risetime at the input. Now, the refractive index does not change uniformly with wavelength. Aside from using a monochromatic input, the effect of material dispersion can, therefore, be reduced by operating at a wavelength at which the velocity does not change rapidly with wavelength. This occurs near 1300 nm for most fibers.

Waveguide dispersion is a result of the paths of some of the modes being altered by imperfections in the fiber. For example, high-order modes travel farther in a larger diameter fiber, so if the diameter of the fiber varies through its length, the arrival time of these modes at the far end of the fiber will be affected by the variation in diameter.

The longer a fiber is, the more effect dispersion has on the risetime because the time difference between the arrival of the different modes or wavelengths at the far end of the cable increases with length.

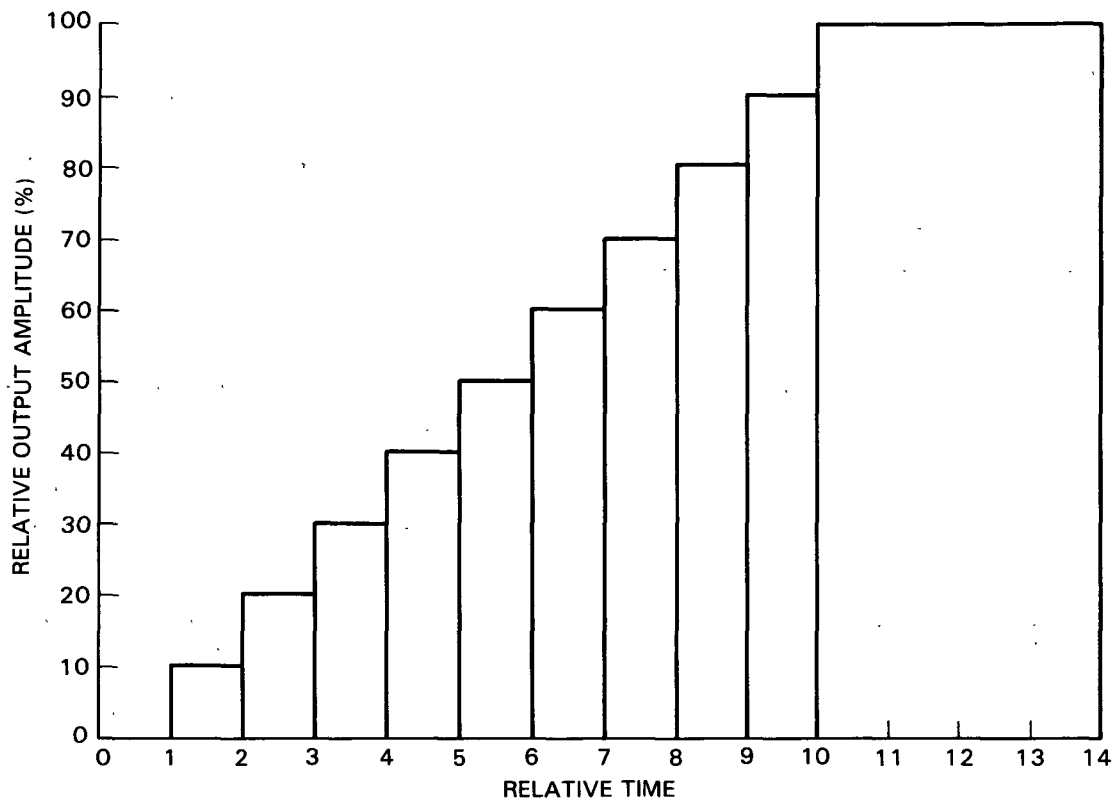


Figure 1-2. Staircase output amplitude due to modal dispersion and the different arrival times it causes

1.2.3.3 Fiber Bandwidth. There are two bandwidths associated with optical fiber, the optical bandwidth and the modulation bandwidth.

The optical bandwidth is the optical band contained between the two optical frequencies, one on each side of the minimum loss frequency, at which the loss has increased by 3 dB. This bandwidth can be several hundred thousand GHz.

The modulation bandwidth is the bandwidth specified by the manufacturer and is the modulation frequency at which the modulation index has decreased to 70.7% of the modulation index of the signal at the input to the fiber. This bandwidth is a result of dispersion in the fiber and is limited to a few GHz-km in multimode fiber and tens of GHz-km in single-mode fiber. Modulation bandwidth decreases approximately proportionately to the length of the fiber because of the increased effect of dispersion over longer distances, as discussed previously. For this reason, optical fiber bandwidth is specified in terms of MHz-km, which is the bandwidth for 1 km of fiber. The bandwidth for other lengths of fiber can be determined by dividing the specified bandwidth by the length in kilometers. For example, a 100 MHz-km fiber 5 km long would have 20 MHz bandwidth.

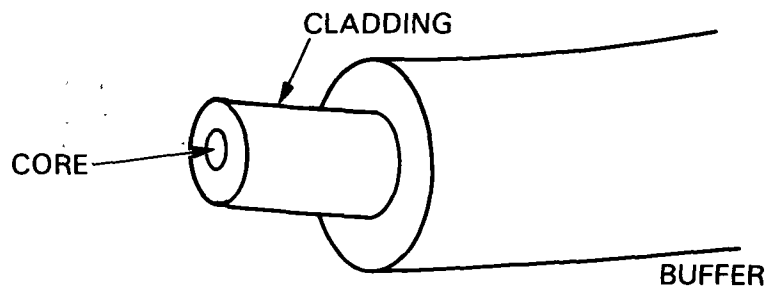
1.2.4 Optical Fiber Cable

The protection directly around the optical fiber comes in three forms: loose-tube, soft-buffer, and hard-buffer.

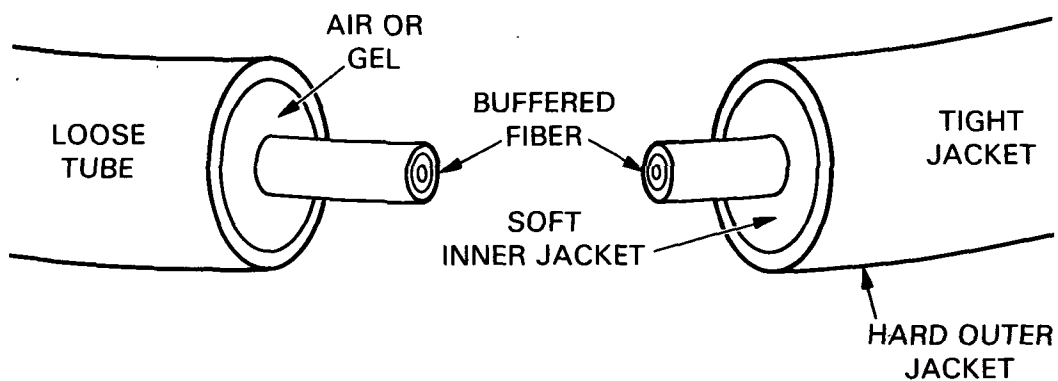
Loose-tube construction has the fiber enclosed in a tube that is many times the diameter of the fiber. The fiber, which is coated with a thin layer of soft buffering material such as epoxy or plastic, lies loosely within this tube and is longer than the tube which contains it. This leaves an allowance for the cable to stretch before the fiber is stressed. The ratio between the length of the fiber and the length of the tube is called the packing factor. This type of construction gives the greatest protection to the fiber, protecting it from external stresses that can cause excessive loss in the fiber. This construction should not be used for a cable that is hung vertically and moved or vibrated because the fiber can slide down the loose tube and pull out of the connector at the high end.

Soft-buffered fiber is coated with a thin layer of soft buffering material next to the fiber over which a hard coating similar to that used on copper wire is added. The buffer itself in this kind of construction can stress the fiber. Microbends in the fiber can be created if it is bunched up because of a difference in the temperature coefficient of expansion between the fiber and the buffer. This problem has been reduced to acceptable levels for most applications by some manufacturers.

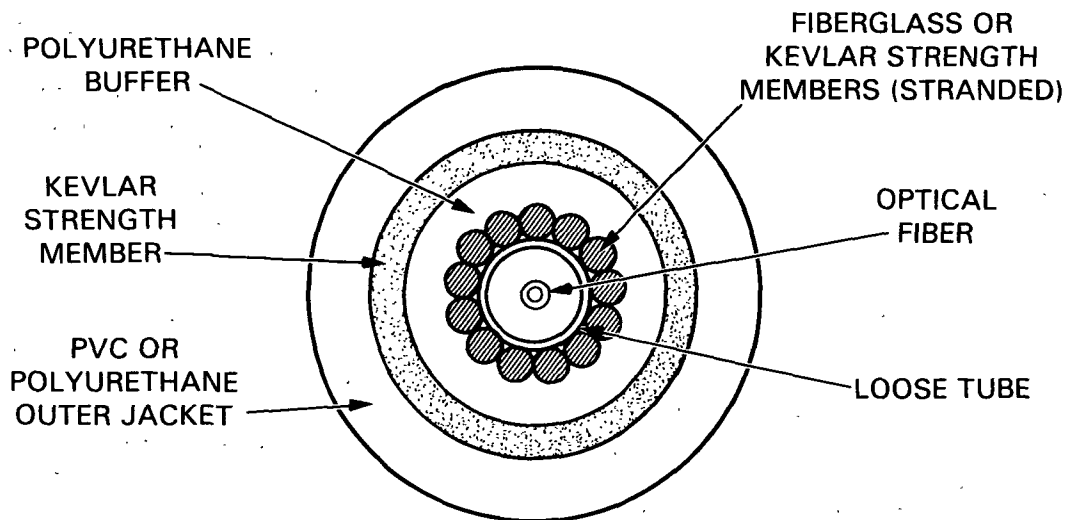
Hard-buffered fiber is covered directly with a material similar to that used on copper wire. Loss and delay changes related to temperature variations in this type of construction are a problem and it should generally not be used. Figure 1-3 shows typical optical fiber construction methods.



a) FIBER CONSTRUCTION



b) PRIMARY PROTECTION



c) CABLE CONSTRUCTION

Figure 1-3. Typical Fiber Construction Methods

Optical fiber cables are made in many forms, as are copper conductor cables. Three major categories are aerial, duct, and direct burial cables.

Aerial cable is designed to be strung on telephone poles and almost always has a steel strength member running through the center of the cable. This cable is available with a nonmetallic strength member for special applications, but it is more expensive.

Duct cable is designed for installation in ducts or conduits either inside buildings or outdoors. It usually has nonmetallic strengtheners and is less durable than the other types.

Cable designed to be buried directly in the ground usually contains a rodent shield directly under the outer jacket. The strength member is usually steel and the cable is sturdily constructed. This type of cable is available in a completely dielectric form with a nonmetallic rodent shield and strength member but is quite expensive.

1.2.5 Optical Fiber Communications Systems

In an optical fiber communications system a light beam, which is generated by a Light Emitting Diode (LED) or a laser diode (LD), is amplitude modulated by the signal to be transmitted. It is then launched down an optical fiber and detected with a photodetector at the far end of the fiber. The output of the photodetector is a reproduction of the signal that was transmitted. The arrangement is shown in Figure 1-4.

The largest users of optical fiber systems are the telephone companies. Companies such as American Telephone and Telegraph (AT&T) in the United States, Nippon Telegraph and Telephone (NTT) in Japan, and British Telecom in Great Britain have already installed thousands of miles of optical fiber cable. All new major telephone trunk lines in these countries will be optical fiber.

In the United States much of an East Coast corridor optical fiber system from Boston to Miami is completed. A West Coast route from Sacramento to San Diego is also near completion. A northern and a southern route across the country is being planned by AT&T. This will join major cities such as Philadelphia, Pittsburg, Cleveland, Chicago, Des Moines, Omaha, Denver, Salt Lake City, and San Francisco in the north. In the south it will link Atlanta, Birmingham, Jackson, Dallas, Houston, Tucson, Phoenix, and Los Angeles.

In Japan and Great Britain links are being installed through the lengths of the countries. Links across the Atlantic and Pacific Oceans are being planned. Construction on the Atlantic Link will begin in 1985.

At the Jet Propulsion Laboratory, optical fiber links are used to communicate between Deep Space Stations within a Deep Space Complex or tracking station, such as the one at Goldstone, California. These links carry telephone signals, monitoring and control signals, and frequency and timing reference signals.

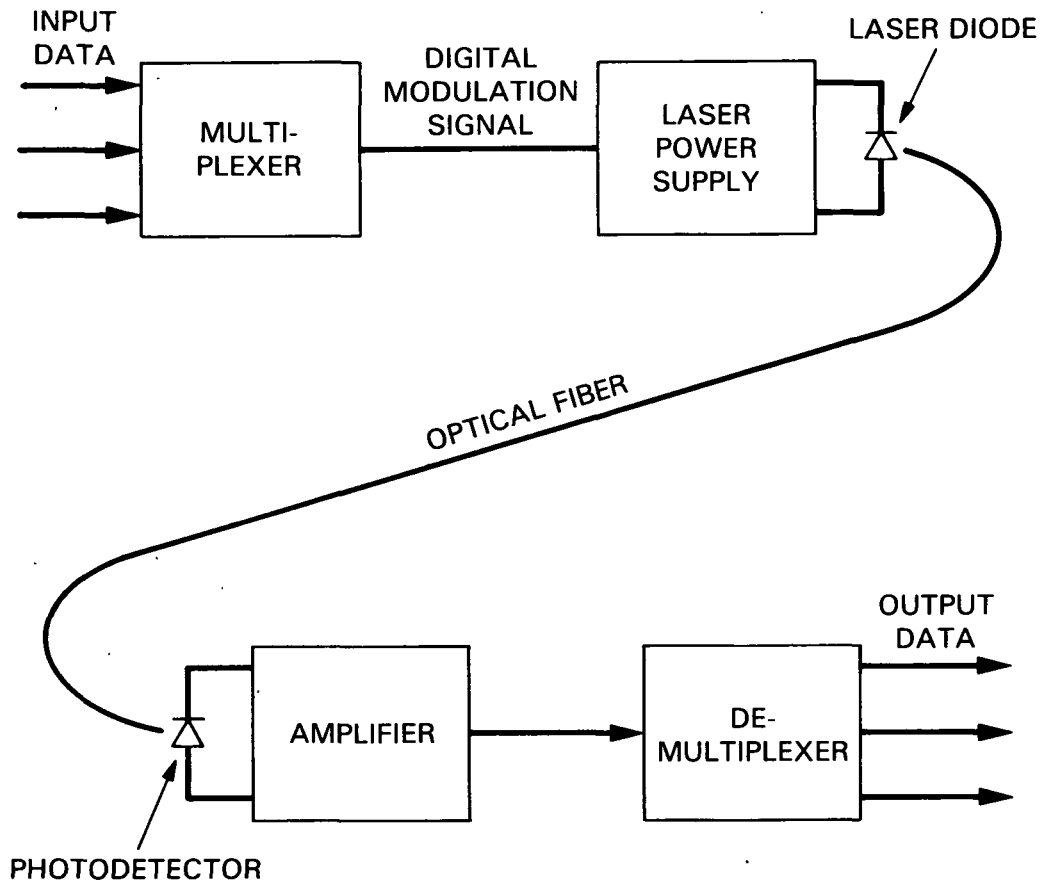


Figure 1-4. Fiber optic communication system

1.2.6 Advantages of Optical Fiber

Optical fibers generally have greater bandwidth and lower loss than do coaxial cables. This is shown in Figures 1-5 and 1-6, in which attenuation and bandwidth data from manufacturer specifications for common types of optical fibers and coaxial cables have been plotted together. This means that much greater channel capacity can be handled over much longer distances without repeaters than any other medium with the exception of radio and microwave transmission.

Optical fibers do not radiate or pickup RFI or EMI. Electrical isolation may be maintained between the optical transmitter and receiver, thereby eliminating ground loops and reducing the possibility of short circuits.

Optical fiber cables are small, lightweight and corrosion resistant. The cost of optical fiber cables is very low compared to the cost of coaxial cables when the capacity is taken into account.

The change in delay as a result of temperature change for commercial optical fiber cable is as good as the best coaxial cable. Optical fibers with much lower temperature coefficients of delay have been fabricated. This is important when a fault is to be located precisely by means of time domain reflectometry.

1.2.7 Splices

Currently there are three splicing methods commonly used: the fused splice, the chemically bonded (glued) splice and the elastomeric splice.

In a fused splice the glass fiber is melted together end-to-end either by an electric arc or a gas flame. The electric arc is most often used. Splice losses on the order of 0.1 dB or less can be achieved using this method. The strength of this splice approaches the strength of the unspliced fiber. This method is preferred for multimode fiber.

The chemically bonded splice is achieved by butting the fiber together end-to-end and gluing it in place with a polymer or epoxy. The adhesive is generally a type that is cured with ultraviolet light. This is used for convenience, because it can be cured in a few seconds and does not require mixing. The unprotected splice is not as strong as a fused splice, but protection is added in the form of a glass tube. The protected splice is then much stronger than the original fiber. This is the preferred splicing method for single-mode fiber and can achieve splice losses on the order of 0.1 dB. Figure 1-7 shows fusion and chemical bond splices.

In the elastomeric splice two fibers are butted together within an elastomer tube with matching index gel between them. They are then held together mechanically. This method is generally used for temporary splicing. Losses on the order of 1 dB are common. The splice can be microphonic and may deteriorate with age.

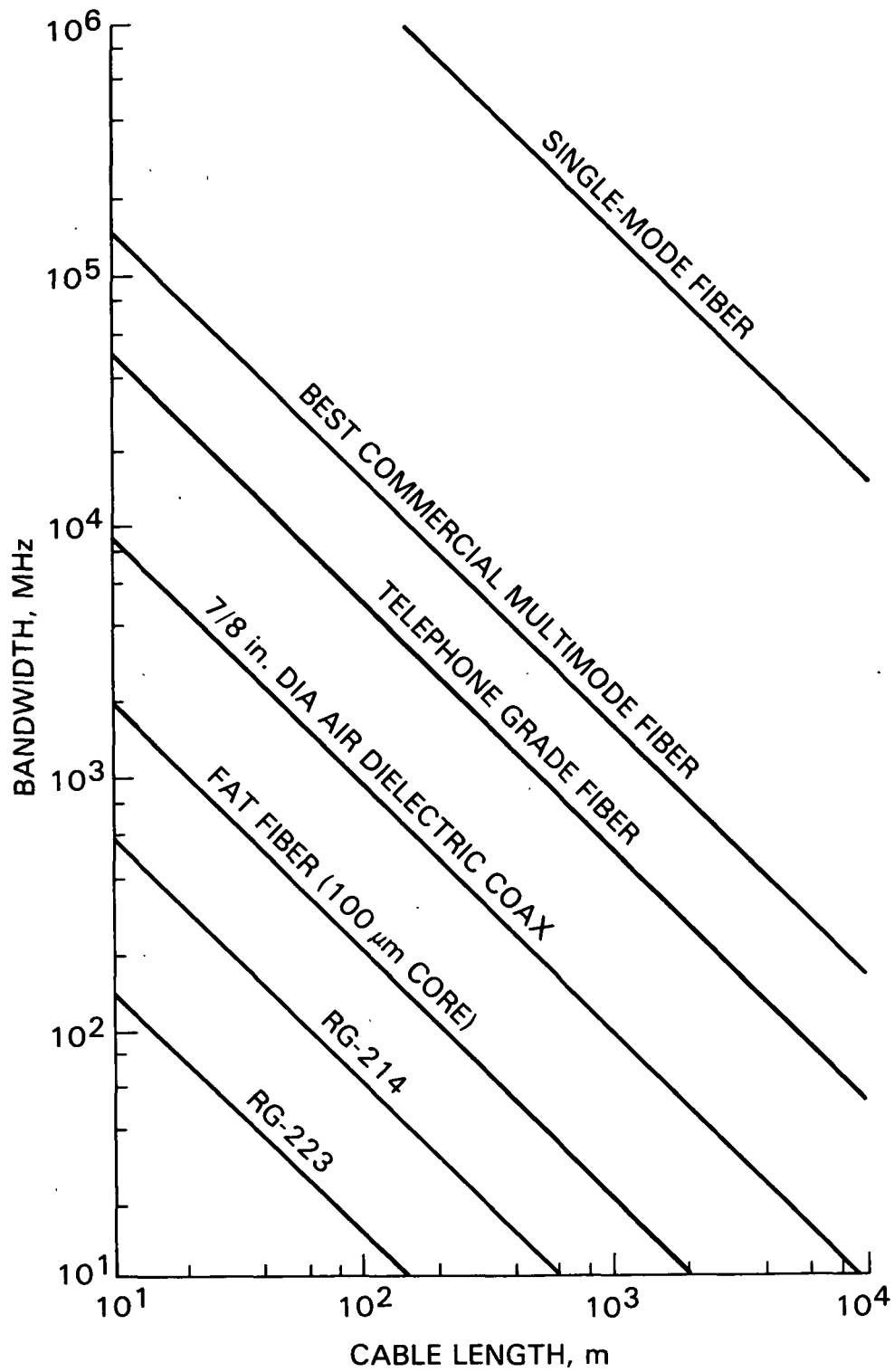


Figure 1-5. Bandwidth versus cable length for some optical fibers and coaxial cables

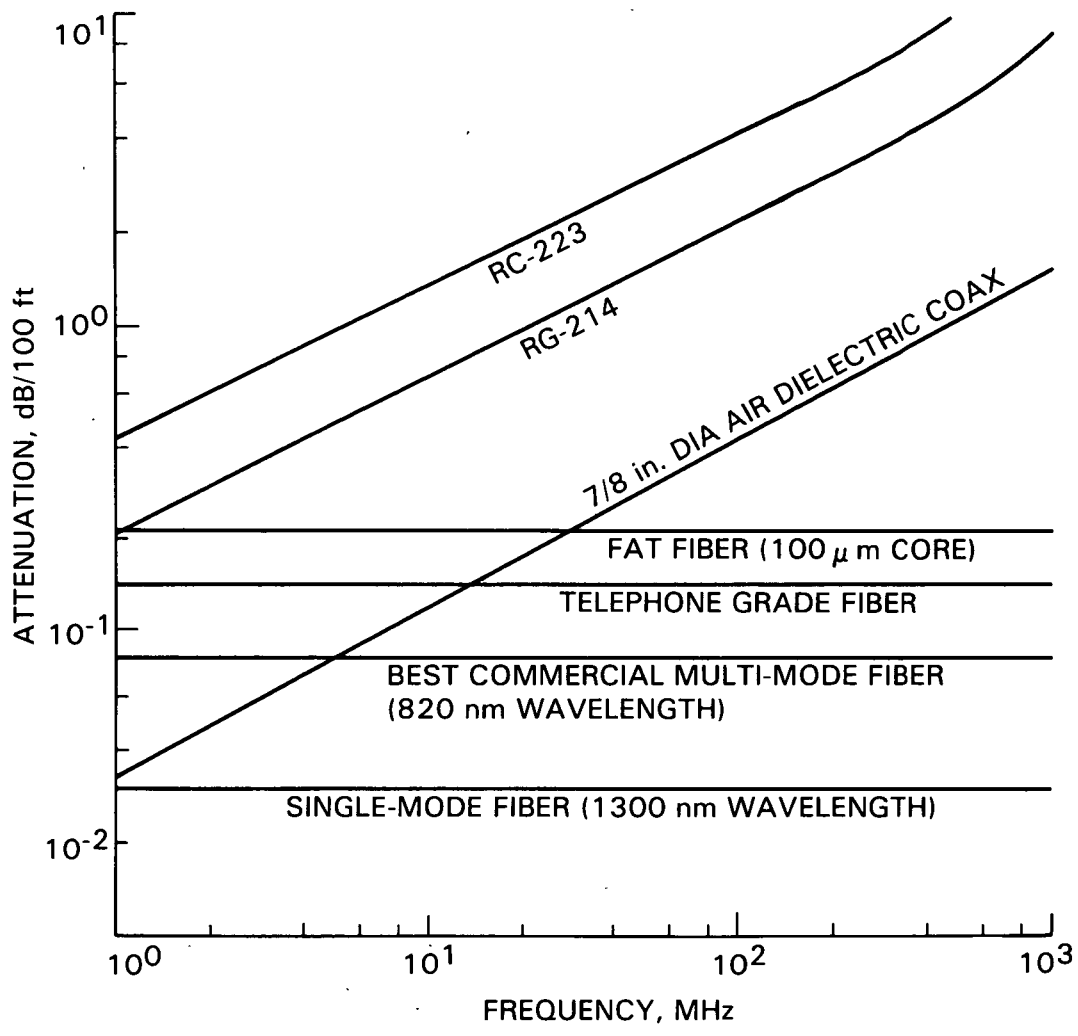


Figure 1-6. Attenuation versus frequency for some optical fibers and coaxial cables

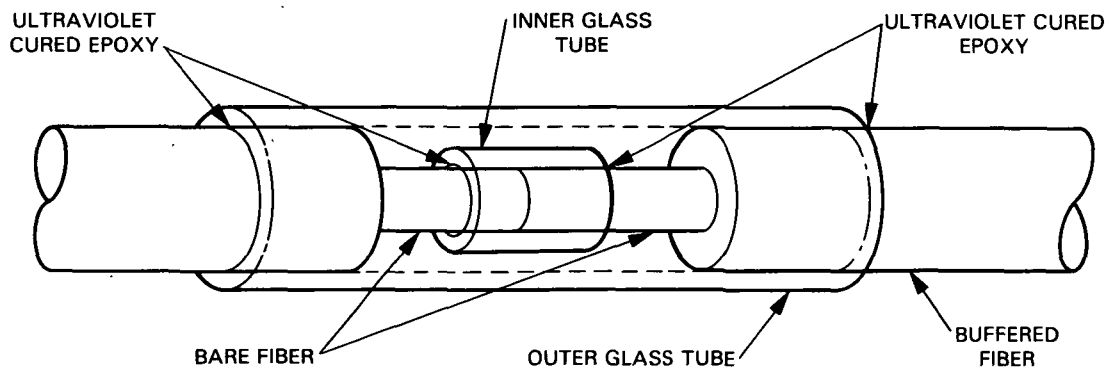
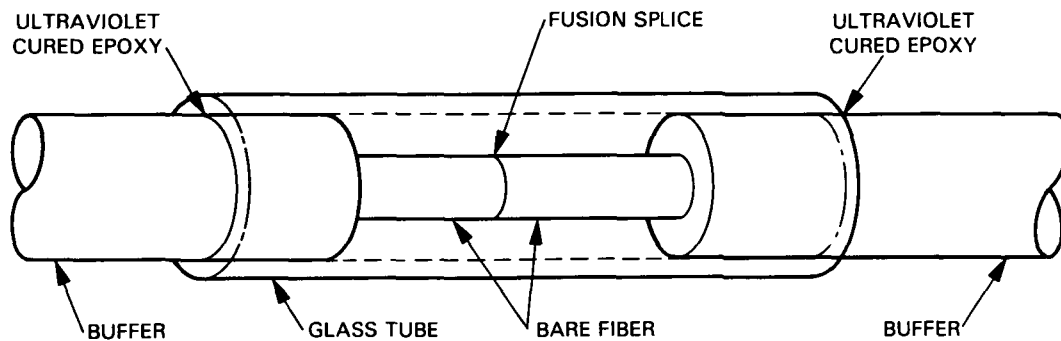


Figure 1-7. Two methods of splicing fiber optic cables
a) Fusion splice
b) Chemical bond splice

1.2.8 Connectors

A wide variety of connectors is available for optical fiber cable. Good connectors tend to be very complicated (see Figure 1-8) and expensive, but such expense is often warranted. If the cost of a connector is calculated on the basis of how many channels are transmitted through it, the optical fiber cable connector cost may be less than that for the coaxial cable connector.

A description of all of the different connector types is beyond the scope of this report, but one important class should be mentioned. Most connectors added after installation of the optical fiber require the end of the fiber to be polished. This is a tedious, time-consuming process. Connectors have been developed recently which permit breaking the fiber off with a perpendicular smooth face, eliminating the need for polishing. This type of connector should be used whenever possible. Figure 1-9 shows details.

1.2.9 Modulation

As far as a communication system is concerned, a steady light level contains no information. In order to transmit information, the light must be changing, which may be accomplished by direct modulation of the optical source or by indirect modulation, which modulates the light beam after it has left the source.

Solid-state light sources do not produce optical output until a certain threshold current is passed through them. Direct modulation is achieved by applying the signal directly to the LED or laser which has been biased near the threshold (so that the modulation signal turns the light source on and off) for digital signals or in the linear region of its optical power-out versus current curve for linear signals.

Indirect modulation is achieved in a device such as a Kerr cell (see Section 2), which attenuates the light passing through it as a function of an applied voltage.

Direct modulation is used in nearly every optical fiber communications system currently in use. However, external modulators capable of operation at frequencies as high as 10 GHz have been demonstrated in the laboratory and should soon be available commercially.

Direct modulation results in a lower noise figure for analog systems than does indirect modulation. This is because the noise of the LED or laser diode is a function of the average current in the diode, which is lower when direct modulation is used.

In many systems the optical carrier is AM modulated with an RF subcarrier and, in turn, the RF subcarrier is modulated using FM or some other form of modulation. Using this scheme, bandwidth can be traded off for improved signal-to-noise ratio in linear systems.

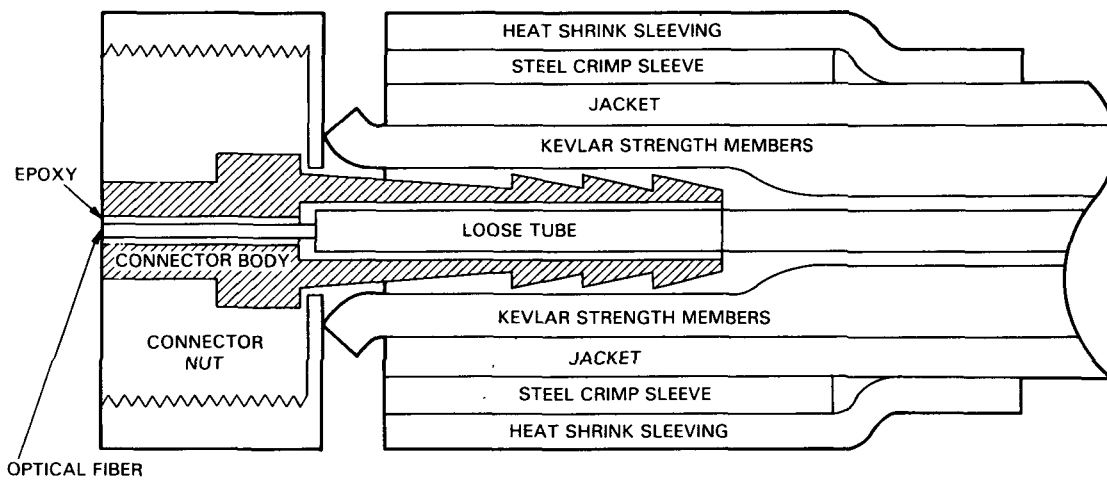


Figure 1-8. Optical fiber connector

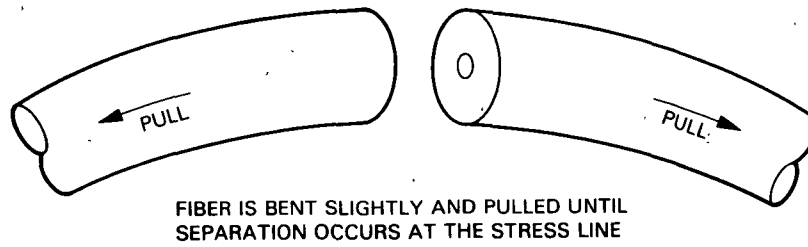
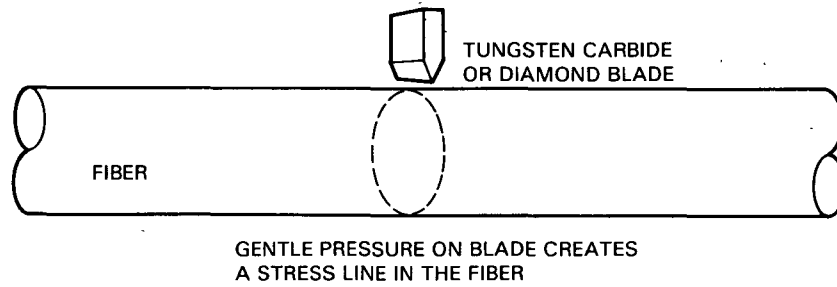
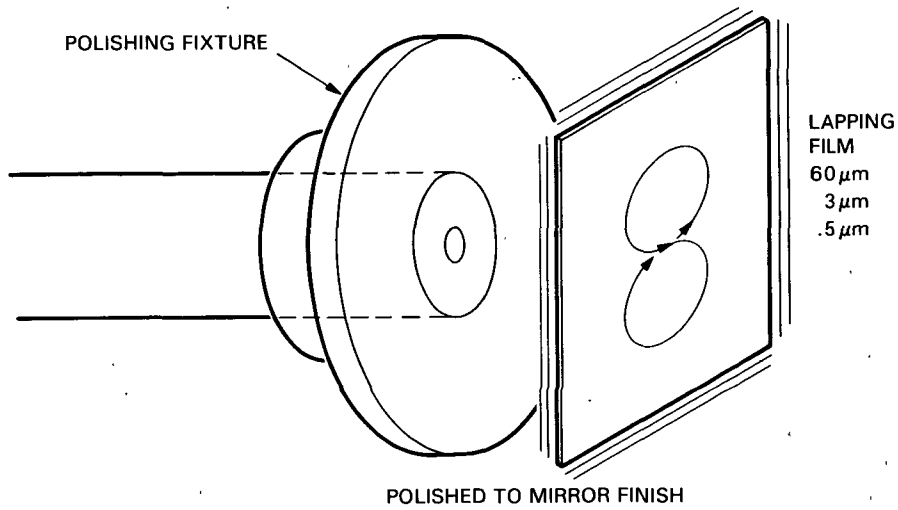
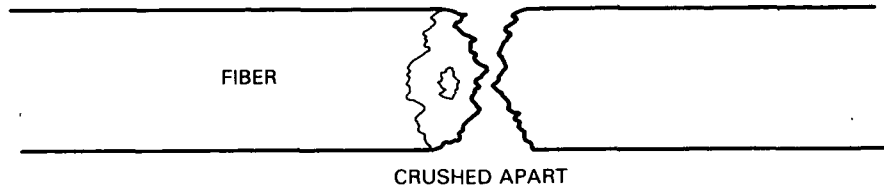


Figure 1-9. Fiber end preparation

- a) Lapped
- b) Cleaved

1.2.10 Multiplexing

One of the major advantages of optical fibers over coaxial cable is the much larger bandwidth over long distances. In order to exploit this advantage, it is often necessary to multiplex many signals onto one optical fiber. Multiplexing can be accomplished three ways: RF frequency division multiplexing, time division multiplexing, and optical wavelength multiplexing.

RF frequency division multiplexing is done electronically and the composite signal is then applied to the optical fiber transmitter. This composite signal is recovered at the output of the optical detector and is demultiplexed or separated electronically.

Time division multiplexing is also done electronically and applied to the optical transmitter. The composite signal is recovered at the output of the optical detector and demultiplexed.

Optical wavelength division multiplexing is achieved by applying a number of optical transmitters operating at different optical wavelengths to a single optical fiber. At the receiving end the different wavelengths are divided with optical filters into separate optical output channels. Each optical output channel is then detected and converted to an electrical signal. Each of these channels has the same bandwidth, so the capacity of the fiber is multiplied by the number of optical channels used. The total capacity of this type of system is limited by how narrow a bandwidth can be achieved in the optical filters and the total optical bandwidth of the fiber.

A two-wavelength system, operating at 1200 and 1300 nm (and another version at 810 and 890 nm) has been reported [1-6]. The data rate in this NTT demonstration in Japan was 6.3 Mb/s, using conventional optical (color) filters.

A detection system analogous to the familiar superheterodyne (which has been the choice of radio receiver designers for decades) has recently been built and tested [1-7]. In this system the intermediate frequency (i.f.) was 1.5 GHz, and the data rate 8.4 Mb/s over 280 m of fiber. This type of detection is especially difficult since heterodyne detection requires a local oscillator to match the incoming signal in frequency, phase, and polarization. The magnitude of the problem may be understood by recognizing that most semiconductor lasers have spectral line widths of hundreds of MHz, and fibers do not preserve a predictable polarization at the output. The effort is justified, however, by a 10-20 dB improvement in receiving level in comparison with intensity modulation and direct detection, and the possibility of multichannel systems using selective i.f. filters.

1.2.11 Signal-to-Noise Ratio

The signal-to-noise ratio (S/N) of a typical linear optical fiber system is laser diode-limited to approximately 120 dB/Hz [1-8]. This is not as high as found in many coaxial systems. For a 100-MHz bandwidth, the S/N would be 40 dB:

$$120 \text{ dB} - 10 \log 10^8 \text{ Hz} = 120 \text{ dB} - 80 \text{ dB} = 40 \text{ dB}$$

This can be increased by using wideband FM modulation of the RF subcarrier as described earlier.

Commercial optical fiber CATV systems are available which carry up to seven TV channels over distances in the tens of km without repeaters and achieve S/N of greater than 50 dB [1-9].

In a typical linear system the major noise contribution comes from the laser diode until the cable loss exceeds about 30 dB [1-8]. This means that the S/N is fairly constant out to a distance of 30 km for a system using fiber having 1 dB/km loss.

1.2.12 Delay Stability

The signal delay (or transit time) through an optical fiber changes as a result of temperature change as it does through any transmission medium.

Optical fibers cabled in loose tubes have been measured at JPL and the temperature coefficient of delay has been found to change about 7 ppM/°C. This is as good as the best coax cable and is substantially better than other types of construction, which in some cases are several orders of magnitude worse.

Delay stability is important where the location of faults or sensor disturbances must be determined accurately.

1.2.13 Optical Transmitters

Optical fiber communications systems almost always use semiconductor light sources because of their high reliability. Two types of devices are used, Light Emitting Diodes (LED) and laser diodes.

LEDs made with gallium arsenide and operating in the short wavelength region, 800 to 900 nm, were first developed for use in displays. They became the logical source for use with optical fibers because they were already available and demonstrated good reliability. The problem with LEDs is that the light is emitted from a relatively large area and cannot be concentrated to the small beam required for good efficiency with optical fibers. In most cases not more than 100 microwatts can be launched into a practical fiber from an LED. This power level is adequate for many applications, however, and LEDs are used extensively in systems less than 2 km in length.

Laser diodes operating in the short wavelength region were developed by the late 1970s using the same gallium arsenide technology already used for LEDs. These devices emitted a much narrower concentrated light beam than did LEDs which made it possible to launch several milliwatts of optical power into a fiber, resulting in systems operating over distances of tens of km. The spectral purity (usually expressed in terms of spectral linewidth) of lasers is also narrower than that of LED and results in less dispersion in a fiber. This permits wider modulation bandwidths on long fibers. The widest bandwidth requires the fastest response, and for this a laser is the required source.

Won-Tien Tsang of Bell Labs has invented a laser which does not change frequency when modulated. This is accomplished by cutting a section off the end of a semiconductor laser, and then aligning the two parts to provide optical coupling between them, but with electrical isolation. The two parts are connected to separate current sources and the short section is biased below threshold current. This section is a frequency controller. The long section is biased above threshold and the modulation current is superimposed on this bias.

The modes propagating in the long section interact with those in the short section. Modes of the same frequency will travel through both sections while modes at other frequencies are filtered out.

These lasers have very narrow bandwidths and therefore reduce pulse spreading (dispersion) in a fiber because dispersion in a fiber is proportional to the bandwidth of the source.

Other types of lasers, such as the periodic-structure laser, can achieve similar results. External cavities consisting of fibers can also stabilize a laser.

By changing the bias on the short section of the laser, it can be made to operate at different stable frequencies within a range of about 15 nm. This makes frequency shift keying modulation possible as well as wavelength division multiplexing.

LEDs and lasers currently available off-the-shelf can be modulated at rates as high as 100 MHz and 1 GHz respectively. Lasers capable of modulation rates to 4 GHz have been demonstrated in the laboratory and should be available soon.

LEDs and lasers operating at longer wavelengths, 1300 nm and 1500 nm, utilizing gallium arsenide-indium phosphide (GaAs-InP) technology have been developed recently. These wavelengths are desirable because optical fiber dispersion is lowest at about 1300 nm and the losses are lowest at about 1500 nm.

Lasers are thermally less stable than LEDs and are usually temperature controlled. Because the lifetime of these devices degrades rapidly as the temperature is elevated, they are typically cooled for stabilization. This is usually accomplished with solid-state thermoelectric coolers which are simple and reliable.

In most optical transmitters utilizing lasers, a negative feedback loop is used to hold the laser's optical output power constant because it diminishes gradually with age. The increase in current required to hold the output constant can be monitored and used as an indication of the remaining lifetime of the laser.

Efficient coupling of the light from the source to the optical fiber is the most difficult task involved in the fabrication of optical transmitters. This is particularly a problem with single-mode fiber because of the small core

diameter, usually less than 10 micrometers. With simple butt coupling, efficiencies of 50% can usually be achieved with multimode fiber and 15% with single-mode fibers. This coupling efficiency can be increased to better than 70% and 50% respectively using lenses.

1.2.14 Optical Receivers

The device which converts the optical signal to electrical form should be efficient at the wavelength in use and operate at a suitable data rate. There are several semiconductor devices that can be used, including various kinds of photodiodes and phototransistors. The choice depends on the application. Optical receivers usually consist of a suitable optical detector, an amplifier, and power supplies to provide power to the amplifier and biasing for the detector. For communications, two types of photodetectors are commonly used, PIN photodiode detectors and Avalanche Photodiode Detectors (APD).

The PIN detector, which has no internal gain, is generally used except in long links where the optical signal levels are very low. It requires a low reverse bias voltage, approximately 20 volts, and is quite stable with temperature.

On the other hand, an APD requires a high bias voltage (which must be stabilized in the area of 150 volts) and is much less stable with temperature. It is a more sensitive device because it has internal gain and produces many electrons per absorbed photon. For this reason, it is used mostly on long optical links having very low signal levels. Bandwidths on the order of 500 MHz can be achieved with PIN diode receivers and 3 GHz with APD receivers. Receiving devices are also discussed in Section 2.4.8, in reference to sensing applications, and also in Section 4.3 where photodiode design for maximum power transfer is described.

1.2.15 Future Developments

Development is needed on systems operating at wavelengths greater than 3 μm . Losses in optical fibers on the order of 10^{-3} dB/km may be possible at these wavelengths. The size of the fiber core would also be larger for single-mode fiber, making it easier to work with. Distances between repeaters could be as far as 30,000 km. These fibers would not darken appreciably when exposed to large amounts of radiation. Small amounts of power for signal processing or sensors could be transmitted over distances on the order of 3,000 km.

Even though it would be beneficial to have very long wavelength systems, communications in a power system could be readily handled using current technology. Workmanship standards need further development and more attention must be given to standardization of components. A program to evaluate connectors for possible use would be beneficial. Single-mode fiber splicing techniques need improvement if the fiber is to be used for distributed sensing.

Another area for future development is optical heterodyne detection, similar in principle to practically all recent radio receivers. This approach has the advantage that selectivity is provided by an intermediate frequency (i.f.)

filter which can be optimized because its frequency is fixed. There are difficulties with optical heterodyne detection due to the fact that the local oscillator must match the incoming signal rather precisely.

A group of German research engineers at the Heinrich-Hertz-Institut fuer Nachrichten Technik in Berlin have reported (Electronics Letters, August 18, 1983) the development of an experimental fiber-optic digital transmission experiment with heterodyne detection in a coherent single-channel, single polarization system at 830 nm wavelength. The receiver has an intermediate-frequency of 1.5 GHz and proved capable of receiving 8.4 Mbit/s digital signals over 280m of fiber.

It is recognized that the use of superhet-type techniques could not only reduce the minimum receiving level by 10-20dB in comparison with systems using intensity modulation and direct detection but also open the way to multichannel systems utilizing the relatively high selectivity of i.f. filters. A second laser is used as the local oscillator in the receiver. The work is being supported by the Deutsche Bundespost.

Another area for future work is the use of solitons for communication. Solitons are pulses which propagate without dissipating. Solitons are not, strictly speaking, immune from dispersion rather they are waves in which the effects of dispersion are exactly cancelled by some compensating phenomenon. This can occur if the equations of motion are nonlinear, and if the amplitude as well as the shape of the pulse is correct.

The first recorded observation of a soliton was made about 150 years ago by John Scott Russell, an engineer and naval architect, who observed a mass of water moving up a narrow channel.

Akira Hasegawa of Bell Labs predicted that this phenomenon could occur in optical fibers. Two colleagues, Roger Stolen and Linn Mollenauer, discovered a way to generate solitons with a semiconductor laser. They demonstrated an optical fiber link utilizing the effect.

The soliton laser discovery was announced in the January, 1984, 'Optics Letter'.

1.3 STATE OF THE ART IN FIBER OPTICS COMMUNICATIONS

1.3.1 Bandwidth and Distance

Most bandwidth and distance records in fiber optics communications are now held by single-mode fibers. The following are examples of the kinds of data rates and distances that have been reported [1-10], and some proposed applications.

British Telecom (England) - 140 Mb/s over 102 km in May 1982. No repeater, dual-laser system. Wavelength was 1.52 μm and error rate was 10^{-9} . This data-rate/bandwidth record has since been surpassed.

Kokusai Denshin Denwa R&D Laboratories (Japan) - 280 Mb/s over 21.7 km. Feedback-stabilized laser at 1.53 μm .

Bell Laboratories (United States) - 274 Mb/s over 101 km at 1.31 μm . Total attenuation over 101 km was 38 dB.

Nippon Telegraph and Telephone (NTT) (Japan) - 400 Mb/s over 104 km at 1.53 μm . Total attenuation, including nine splices, was 35 dB.

Several laboratories are working at improving the data rates of fiber communication links.

Heinrich Herz Institut fuer Nachrichten Technik (Institute for Communication Technology) (Germany) - 2.24 Gb/s over 21 km at 1.304 μm .

NTT (Japan) - 2 Gb/s over 51.5 km, error rate better than 10^{-9} .

Bell Laboratories announced at the August 1983 SPIE Conference in San Diego, California, the achievement of 1 Gb/s over 101 km.

1.3.2 Delay Stability

A single-mode fiber is used to transmit frequency and timing signals within the NASA Deep Space Network Communication Complex at Goldstone, California. The signals are used for long baseline interferometry, and stability and accuracy are crucial. It is hoped that this system, designed and installed by JPL, will eventually achieve stability of one part in 10^{17} for 1000-second averaging times, and timing accuracy of 100 ps over 20 km. This is equivalent to a one-second error in three billion years! At present, JPL has achieved three parts in 10^{15} for 1000 second averages over 3 km.

1.3.3 Commercial Installations

Telecommunications companies in several countries have installed fiber cables for trunk lines, sometimes for submarine trunks [1-11].

NTT (Japan) has a six-fiber, 80-km section in service, with repeaters 10-20 km apart in suburban Tokyo. They have also tested submarine links

(and submarine repeaters) with the objective of linking some of the islands in the Japanese archipelago by fiber trunks.

During 1983 tenders were presented for TAT8, the eighth telephone cable across the North Atlantic. This will be the first long distance ocean cable using fiber optics technology and should be capable of carrying up to 36,000 simultaneous telephone connections.

An optical fiber cable is due to be in service between France and Corsica in 1985.

A 25-km cable to be installed by British Telecommunications across the Solent will link Portsmouth and Ryde by optical fiber by 1985. The cable will be supplied by Standard Telephone and Cable (STC) and operate at 140 Mb/s, carrying a variety of information technology services as well as speech.

1.4 ELECTRIC UTILITY APPLICATIONS

The electric utilities have applied fiber optics in three important and distinct ways. First, optical fibers have been used to transmit information within an electric substation. In this application the main advantage of the optical fiber is its insulating property. Second, fibers have been used to transmit information from point to point in the operating area of the utility. In this application the fiber is used in exactly the same way as it would be by any telecommunications company. Third, a few utilities have attempted to combine an optical fiber for transmitting information with an electrical power conductor. This combination makes the optical fiber more difficult to use, and significant problems are encountered.

Each of the three areas mentioned will be dealt with in turn.

1.4.1 Substation Application of Optical Fibers

An optical fiber, along with the necessary transmitting and receiving equipment, may seem like an expensive way to move a small amount of information between two points. Within an electric substation, the total rate of information that must be transmitted is almost certain to be orders of magnitude less than the capability of even the poorest optical fiber. Nevertheless, the fact that the optical fiber is inherently immune to the influence of common-mode voltages or electromagnetic disturbances makes its use attractive, especially where there are likely to be surges or electrical noise. Further advantages may accrue from the fact that special ground mats or special isolating transformers are unnecessary with optical fibers performing data communication, and optical fibers are so light that, in some instances, they can simply be laid in existing trenches or ducts in a substation by a very small crew.

Consequently, although the apparent cost of a fiber may be rather high compared with metallic conductor for the small amount of information typically involved, the installed cost in a substation may be quite competitive and easily justified in many applications.

An excellent introduction to the topic is given in the paper 'Fiber Optic Applications in Electrical Substations' prepared jointly by the IEEE Microwave Radio Subcommittee and the Research Subcommittee of the Power Systems Communications Committee [1-12].

Malewski and Nourse [1-13] have applied optical fibers in a transient measurement system for extra-high voltage (EHV) systems. In this application, advantage was taken of the isolation afforded by the optical coupling in reducing the effect of interference due to the physical separation between the measurement sensors and the recording apparatus. Ground circulating currents are no longer effective in producing shield currents, which in turn would become common-mode voltages in the measurement.

This is a particularly acute problem in transient situations, where the transient voltage between the grounds at various locations in the station may

be several kilovolts, and indeed may be higher than the signal which is being recorded.

Following an idea first developed and applied by Mike Comber of Project UHV in Pittsfield, Massachusetts, one of the authors of this report (Kirkham) has used an optical fiber to transmit information from an Ultra-High Voltage bus to ground, at the AEP-ASEA UHV station in North Liberty, Indiana. This installation was made to replace a free-space infrared light link [1-14] which was suffering from an insufficient gain margin. The optical fiber, encased in Kevlar, was wrapped around the outside of a porcelain bus-support insulator. In this case the installation operated for about two years without maintenance, at the end of which time there was a flashover, presumably caused by tracking along the pollution built up on the Kevlar.

Further applications of optical fibers within substations for routine (rather than experimental) purposes will depend upon a number of factors. Progress would be facilitated by the development of sensors suited to the task of producing information in optical form (or in a form which could be readily applied to an optical fiber), by the development of power sources which do not degrade the isolation afforded by the optical fiber, and by the development of receiving equipment which is sufficiently robust and reliable to be used in a power substation. Some of these topics are discussed later in this report, specifically in Section 2 (dealing with sensors) and Section 4 (dealing with power transfer).

In a permanent installation in an electric substation, no doubt a significant part of the cost of bringing information from a high-voltage bus is the permanent weatherproofing required for the optical fiber. In the past permanent fibers of this kind have been installed in an oil-filled cavity in a porcelain insulator complete with rain sheds - ASEA, for example, has installed a transformer protection scheme using such an optical link at the AEP-ASEA UHV station. This kind of hardware is expensive, both to buy and to install. Figure 1-10 shows an example.

The development of fiberglass-and-neoprene insulators with optical fibers embedded in the fiberglass would undoubtedly reduce costs. Although such insulators are presently available as strain insulators, the application envisaged here would result in very little strain on the fiberglass, and it should be possible to produce a sufficiently high tensile strength tube which could contain a large number of optical fibers embedded in a water-repellent silicone grease. There then would remain only the problem of suitable terminations at the end of the insulator, and it seems possible that a number of standard-length modules could be produced to cover a wide variety of spans.

The improved availability of these various components should lead to the routine application of optical fibers for substation measurements for monitoring and protection as well as experimental and test purposes.

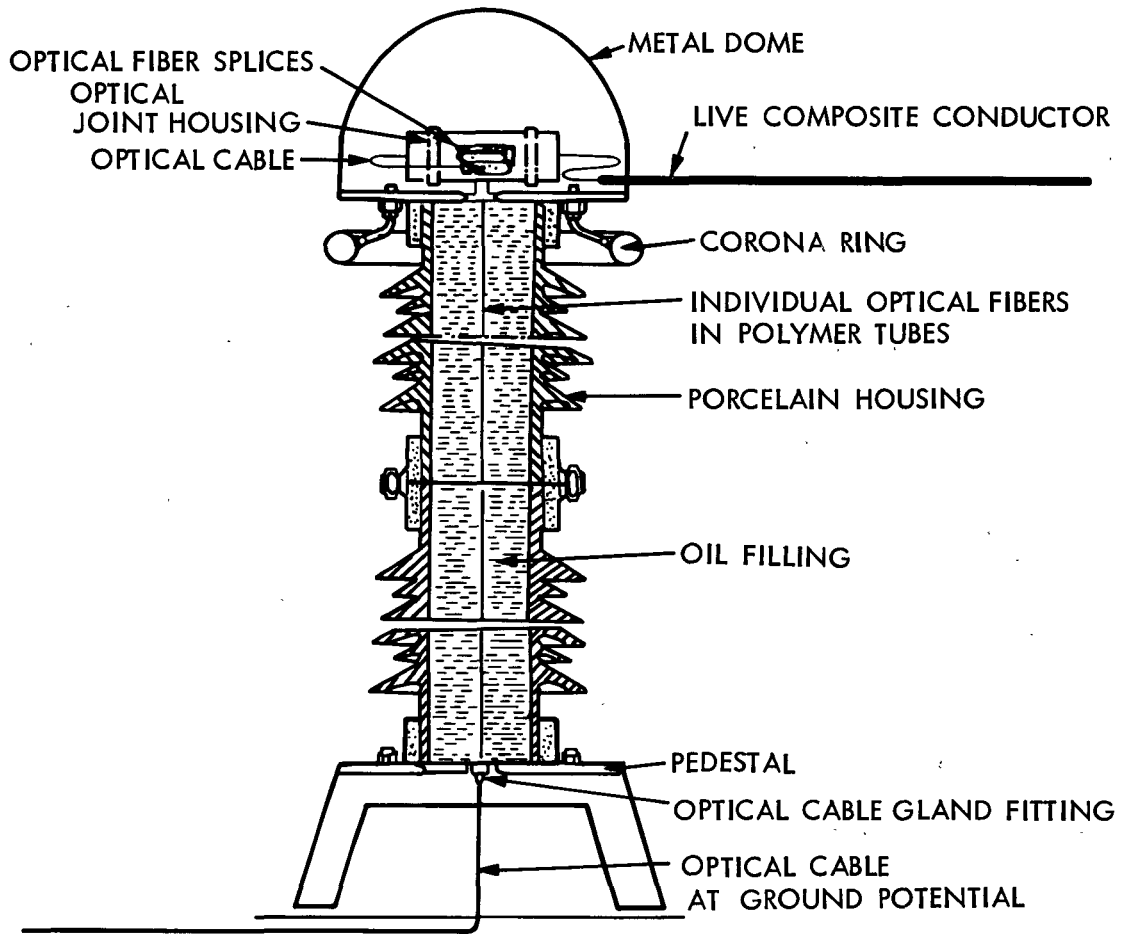


Figure 1-10. Optical link in oil-filled insulator

1.4.2 Intra-system Communication Using Fiber Optics

Several utilities have used fiber optics for communicating information within their operating area, at least on a trial basis. Most notably, fiber optics have been used for this purpose in Japan, where 40 systems are in use in 10 power companies [1-15]. At least one American utility has tested optical fibers to link its control centers [1-16].

In Japan, cooperative development of fiber optics system was started in 1974, by the Tokyo Electric Power Company and the Kansai Electric Power Company (operating in Osaka). The first operational system was installed in 1978 by the Tokyo Electric Power Company. Other companies in Japan followed suit in subsequent years. Systems were installed for general communications, for supervision and control, for protection, to link computers and for video. A variety of cable structures has been used, and data rates have been as low as 1200 bits/s (Kansai Electric Power) and as high as 32 Mb/s (Tokyo Electric Power). Reliability is reported as excellent.

In the United States, Niagara Mohawk Power Corporation, which has an operating area in upstate New York, installed a demonstration fiber optics system, transmitting data, voice, and video between its corporate headquarters, the district operator's office and the power control center.

Applications such as this may be regarded in some ways as duplicating the telecommunication function of organizations such as the telephone company. However, one difference is that the utility-installed fiber is totally under the control of the utility - it is dedicated to them. The final part of this section describes applications of fiber optics in which the fiber is not only dedicated to the utility, but is on its existing right-of-way, strung as part of a power circuit.

1.4.3 Optical Fibers in Power Conductors

The combination of an optical fiber and a transmission line conductor is unique in that it can provide a high-capacity communication link which is immune to electromagnetic interference and the problems of ground potential, uses an existing right-of-way and is independent of FCC regulation. The incremental cost (that is, the cost of providing a communication link in addition to the power circuit) may be quite small.

It is quite possible that the transmission capacity of the communication link is comfortably above the requirements of the utility itself. This may be especially likely if the optical communication system includes spare circuits and automatic switching in the event of link failure. In such cases, there is a good chance that the spare communication capacity could be leased to non-utility users, thereby increasing the cost-effectiveness to the utility. This kind of leasing arrangement has been in use in some U.S. railroads, taking advantage of the widespread nature of their networks.

Power conductors containing optical fibers could be used for transmission or distribution systems. In the transmission system it should be more convenient to use the shield wire (because there is nominally no isolation problem). On

the distribution system, shield wires are not common, and the use of a neutral conductor will depend on the system in question and the voltage level. At least some installations would find it necessary to use the phase conductors in the communication link. The problem of how to bring an optical fiber out of a high voltage cable has already been solved.

1.4.3.1 Cable Construction. Power cables can readily provide mechanical strength and shielding so that within them a large number of optical fibers could be run. In 1982 a British paper [1-17] described cables of the loose-tube type in power conductors. The tube was filled with a protective and water-repellent gel.

Figure 1-11 shows some possible designs for a composite power/optical-fiber cable.

It is important that the optical fiber not be subject to strain after installation, as this would result in an increased loss due to microbending - assuming the fiber did not break. It is possible to avoid straining the fibers by arranging for the helical lay of the conductor to provide freedom. The cable may then be strained by some amount, known as the strain margin, before the optical fiber tightens in the conductor to the point that it is in contact with the inner wall of its tube. In calculating total strain a number of factors must be considered:

- (1) There is an initial stretching of the power conductor after installation. This is caused by the bedding down of the strands in various layers. A value of 0.05% to 0.1% has been quoted [1-17] for multilayer conductors.
- (2) There will be an elastic (i.e. non-permanent) deformation under normal mechanical loads, in the region 0.1% or 0.2%.
- (3) There is a possibility of a small plastic (i.e. permanent) extension caused by abnormal load on the conductor, perhaps due to heavy ice loading. This might amount to 0.05%.
- (4) The conductor will experience some creep (i.e., flow) during its lifetime, perhaps amounting to 0.1%.
- (5) Thermal expansion, a function of electrical load and ambient temperature, might amount to 0.2%.

It can thus be seen that the optical fiber must have a strain margin of 0.5% or more, depending on the application. (Ice loading and thermal expansion are unlikely to occur together, for example.)

Strain margin can be increased by shortening the lay length of the fiber helix, but it is important that this procedure not result in too small a radius of curvature for the fiber, or macrobending losses will increase. Suitable cables are reportedly available [1-17].

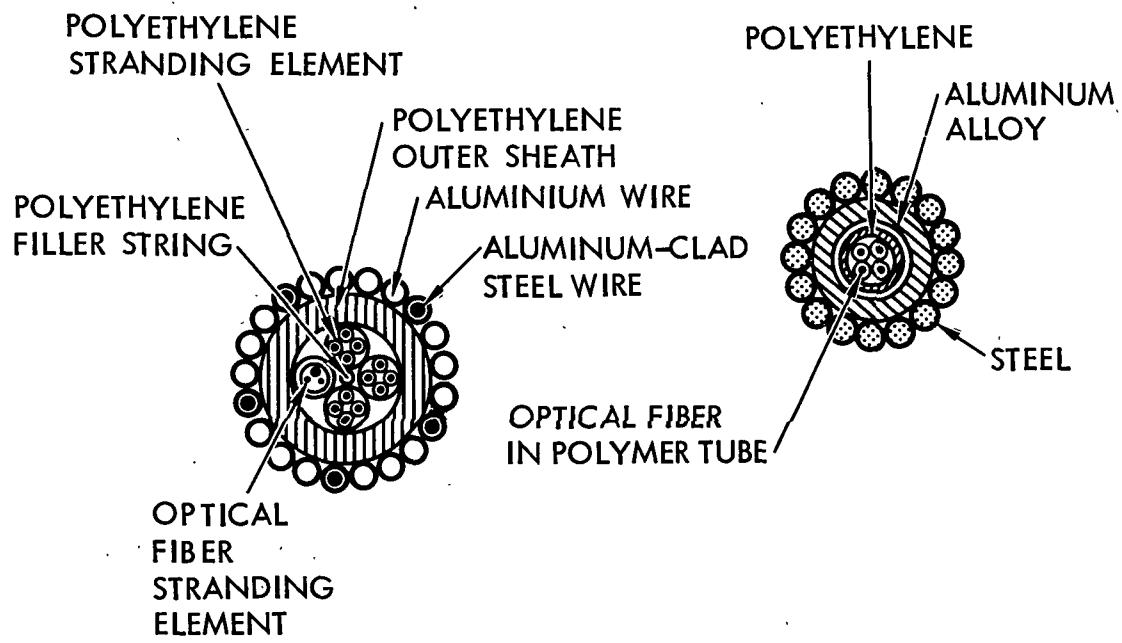


Figure 1-11. Possible designs for composite cable

1.4.3.2 Field Trials. A number of trial installations of optical/electrical composite cables have been made, apparently beginning with an installation in Germany. A 1.8-km link was installed in the shield wire of a 110 kV circuit from Kuppenheim to Rastatt in Baden [1-18], beginning in January 1979. Work on the optical link was apparently completed in April 1979. The error rate was measured as 2 in 10^{12} at 2.048 Mbit/s, and tests at a higher bit rate ((PCM 480 or 34 Mbit/s) resulted in a bit-error rate of 2.3 in 10^{13} over three consecutive days.

At about the same time, work was being done by the Central Electricity Generating Board (CEGB) at their Central Electricity Research Laboratories (CERL) in Leatherhead, England. In July 1979, CERL tested 860 m of a 4-fiber composite, with optical attenuators and regenerators to simulate a longer link. Operation was at 8 Mbit/s and the error rate was 1 in 10^{11} [1-19].

A year later the South Eastern Electricity Board (SEEB) in Hackbridge, England, installed an optical composite on a distribution circuit. In this instance the circuit was a wood-pole 33 kV line operated at 11 kV [1-20]. The optical composite was strung below the phase conductors for 1.2 km, and the fibers were spliced at the end to give a loop of effectively double the length of conductors strung.

In February 1981, Hydro-Quebec Institute of Research (IREQ) installed an optical composite shield-wire on the 735 kV line into Boucherville substation from the IREQ laboratory at Varennes, near Montreal. Two splices were made at towers. Several different fiber housings were used, so that comparative results (unfilled versus gel-filled and high versus low strain margins) could be obtained [1-21].

The only installation made in the United States seems to have been the trial made by Pennsylvania Power & Light Company (PP & L) in April 1981. PP & L installed just over 1 km of optical composite on a de-energized training line, splicing the fiber ends together so as to create a longer optical path.

The Central Electricity Generating Board (CEGB) in England has replaced 21 km of a shield wire on an operating double-circuit 400 kV line. Four gel-filled fiber tubes were used, and the system operates with one regenerator at a rate of 34 Mbit/s. The later installation date (October 1981) meant that hardware developments had been made since the earlier CEGB installation, and this enabled CEGB to use 1300 nm as the optical wavelength, rather than 850 nm. It is reported that the restringing was carried out under single circuit outage conditions using standard tension stringing techniques [1-17].

In Mexico, an experimental link is to be installed near Mexico City by the Instituto de Investigaciones Electricas (IIE). The cable is to be used as a shield wire on a 400 kV line over three spans totalling 1500 m [1-22]. A bit rate of 34 Mbit/s will be used (1983).

1.4.4 CONCLUDING REMARKS

The idea of using a power conductor to contain an optical fiber is at least four years old, and is receiving increasing attention as optical fiber technology advances. It may be reasonably expected that the cost effectiveness of such a system would be higher in the United States than abroad (because of the possibility of leasing data transmission capacity) and yet most of the work on composite cables seems to have been done abroad. In particular, CEGB in England has developed, apparently in conjunction with some of their suppliers, all the hardware necessary to build a reliable composite cable. Such a system should be even more attractive in the near future, as 1300 nm and longer wavelength hardware becomes available at lower costs. At 1300 nm with modern fibers, repeater spacing is likely to exceed the length of any line except at the very highest voltage, so that costs should be lower than all but the most recent field trials.

1.5 REFERENCES

- 1-1 Hondros D. and Debye P., 'Electromagnetische Wellen an Dielektrischen Drahten' Ann. Physik, Vol 32, 1910, pp. 465-470.
- 1-2 Rueter H. and Shreiver D., Schriften des Naturalwissenschaftlichen vereines fuer Schleswig-Holstein, Vol. 16, 1959, p. 2.
- 1-3 Snitzer E. and Hicks J.W., Journal Optical Society Am, Vol. 49, 1959 p. 1128
- 1-4 Kao K.C. and Hockam G.A., 'Dielectric Fiber Surface Waveguides for Optical Frequencies', Proc. IEE Vol 113, 1966, pp 1151-158.
- 1-5 Kapron E.P., Keck D.B., and Maurer R.D., Applied Physics Letters, Vol. 17, 1970, p. 423
- 1-6 Kanada T., Okano Y., Aoyama K-I., and Kitami T., 'Design and Performance of WDM Transmission Systems at 6.3 Mbits/s', IEEE Transactions on Communications, Vol. COM-31, No. 9 September 1983, pp. 1095-1102.
- 1-7 Work done at Heinrich Hertz Insitut fuer Nachrichten Technik, Berlin, reported in Electronic Letters, August 1983 and cited in Communications Commentary, Wireless World, November 1983
- 1-8 Lau K.Y., 'Signal-to-Noise Ratio Calculation for Fiber Optics Link', TDA Progress Report 42-58, Jet Propulsion Laboratory, Pasadena, California, August 15, 1980, pp. 41-45
- 1-9 Conversation with Times Fiber Communications, Inc. sales personnel.
- 1-10 a) Keck D.B, Single-Mode Fibers Outperform Multimode Cable IEEE Spectrum, March 1983, pp. 30-37.
b) Kaplan G., 'Fiber Optics', ICs, and Satellites IEEE Spectrum, January 1983, pp. 38-40.
- 1-11 a) News, Wireless World, March 1983, p. 59.
b) Communications, Wireless World, February 1983, p. 42.
- 1-12 IEEE Microwave Radio Subcommittee and Research Subcommittee of the Power System Communications Committee, 'Fiber Optic Applications in Electrical Substations', Paper No. 83 WM 025-4 presented at IEEE PES 1983 Winter Meeting, New York, NY, January 30-February 4, 1983.
- 1-13 Malewski R. and Nourse G., 'Transient Measurement Techniques in EHV Systems', IEEE Transactions on Power Apparatus and Systems, Vol. PAS-97, No. 3, May/June 1978, pp. 893-902.
- 1-14 Kirkham H., et al., 'AEP-ASEA UHV Station: The Data Systems', WINPWR 78 Abstr. A78 235-4, Trans PAS, Vol. 97, No. 4, July/August 1978, p. 1013.

- 1-15 Yamanoi M., et al., 'Application of Optical Fibre Communication Systems for Electric Power Utilities', CIGRE 1982 Session, Report 35-03.
- 1-16 Fernandes R.A., 'Fiber-Optic Link Breaks Data Logjam', Electrical World, February 1981, pp. 89-93.
- 1-17 Dey P. et al., 'Optical Communication using Overhead Power Transmission Lines', CIGRE 1982 Session, Report 35-01.
- 1-18 Berndorf H., et al., 'Fiber Optic System for Transmission of Information on High Voltage Overhead Power Lines', CIGRE 1980 Session, Report 35-09.
- 1-19 Maddock B.J., et al., 'Optical Fibre Communication Using Overhead Transmission Lines', CIGRE 1980 Session, Report 35-01.
- 1-20 Maddock B.J., et al., 'Optical Fibres in Overhead Power Transmission System for Communication and Control', 29th International Wire and Cable Symposium Proceedings, New Jersey, 1980, pp. 402-409.
- 1-21 Peloquin J. and Missout G., 'Composite Overhead Ground Wires with Fibre Optic', Paper presented at the Canadian Electrical Association Meeting on March 18, 1981.
- 1-22 Pineda D., et al., 'Use of Optical Cables in Power Transmission Lines', IEEE Transactions on Power Apparatus and Systems, Vol. PAS-102, No. 4, April 1983, pp. 812-816.

SECTION TWO

POWER SYSTEM APPLICATIONS

OF

FIBER OPTICS SENSORS

by

Alan T. Johnston and Harold Kirkham

SECTION TWO

POWER SYSTEM APPLICATIONS OF FIBER OPTIC SENSORS

2.1 INTRODUCTION

This section has three purposes. The first one is to review generally the various techniques for sensing with optical fibers, and to review prior work involving the use of optical fibers and optical sensing in power systems. Second, having narrowed the field of study somewhat, we investigate and evaluate techniques that could be useful for measuring electric field in the power system environment. Third, we report some of the experimental work done at the Jet Propulsion Laboratory in 1983 in the area of electric field measurements.

In the remainder of Section 2.1, we mention the main features of the optical fiber technology, and discuss the ways in which light and fibers can be combined and used to make measurements. In Section 2.2, the sensing requirements and constraints of the power system are described. Section 2.3 enters more specifically into techniques and needs for electric field sensing, without particularly emphasizing the role that optical fibers might play. Section 2.4 diverges to some extent in order to describe the types of optical elements available for use in a fiber system. Section 2.5 concentrates on comparing the principles, performance, and characteristics of a number of passive optical E-field sensing techniques which directly influence the light intensity in a fiber channel. Section 2.6 is a similar discussion of techniques using fiber optic readout of an electronic sensor, and Section 2.7 summarizes our conclusions. Over 80 references are listed in Section 2.8.

2.1.1 Optical Fiber Technology

If light enters a transparent rod sufficiently close to an axial direction, it becomes trapped, and the rod acts essentially as an optical waveguide. If, in addition, the transparent rod is encased in another transparent material in which light propagates faster, the waveguide is isolated from the external world and can be packaged or supported without significantly affecting its light transmission. The technology of optical-fiber data transmission is based on this simple idea. The construction of various kinds of optical fiber cables and their applications are described in Section One of this report.

By modulating the light wave propagating in a fiber, the wave can be made to convey information. It is this application of optical fibers which has primarily motivated interest in the field, and the technology has now developed to the point where fibers can be used to convey information at extremely high bandwidths (up to several Ghz) over extremely long distances (over 100 km) without the use of intermediate repeaters and at a sufficiently low cost to be competitive with the use of metallic conductors. A rather extensive review of this technology as applied to power systems has been published in Reference 2-1.

As carriers of information, optical fibers have many advantages over metallic conductors:

Their high bandwidth makes it possible to multiplex many channels onto one fiber -- their channel capacity is extremely high. This is particularly important for telephone trunking applications, which have been the first wide-scale uses of optical fibers for carrying information.

Because the guided light in the fiber is not coupled to its surroundings, its information content is substantially impervious to external influence. This means that a fiber can be used in a situation where there is strong electromagnetic interference without degradation of the information carried by it.

Fibers are conventionally made of silica glass, so they are chemically resistant and do not react even in quite corrosive environments.

The fiber and its protective cabling can be an excellent electrical insulator. Certain applications can take advantage of the fact that electrical stress can be applied to the fiber longitudinally, and very high voltage can be readily sustained.

Because the losses in the fiber are usually relatively small and quite constant, it is almost impossible to tap off enough power from the fiber to receive the information contained therein without this loss of power being detectable at the appropriate receiving end of the system. Consequently, secure data links can be made using optical fibers.

2.1.2 Fibers as Sensors

Many of these characteristics of optical fibers are also useful for extracting information from remote sensors. The simplest approach to sensor readout, which we will call direct fiber optic sensing, results when the sensing element itself modulates a light beam. For example, if light passing through a small sample of a special transparent material is somehow changed by the presence of a magnetic field, the combination of the glass fiber and the transparent material effectively forms a magnetic field sensor, and the combination could be calibrated as a current sensor. There has been much interest in developing sensors of this kind, and it now seems that a number of crystalline transparent materials are available to produce changes in light due to an electric field or magnetic field [2-2], thus enabling measurement of voltage or current in electric circuits.

It is also possible to use the fiber itself as a sensor. Although glass fibers are normally considered to be insensitive to external influences, their sensitivity is not identically zero, so that advantage can be taken in a suitably designed sensor of their susceptibility to, for example, acoustic pressures. A considerable investment has been made by the U.S. Naval Research Laboratory in the development of hydrophones using acoustically sensitized fibers, and it has been shown that the overall sensor can be shaped

to achieve special frequency or spatial responses with extremely high sensitivities [2-3].

In another form of sensor system, which we term fiber optic readout, the fiber merely acts as a carrier of information which is generated elsewhere. The sensing element itself can be quite complicated and require power at the sensor location. In this case, it may be possible to furnish this power over an optical fiber to maintain the many advantages of optical isolation. This aspect of sensor design is discussed more fully in a Section Four of this report.

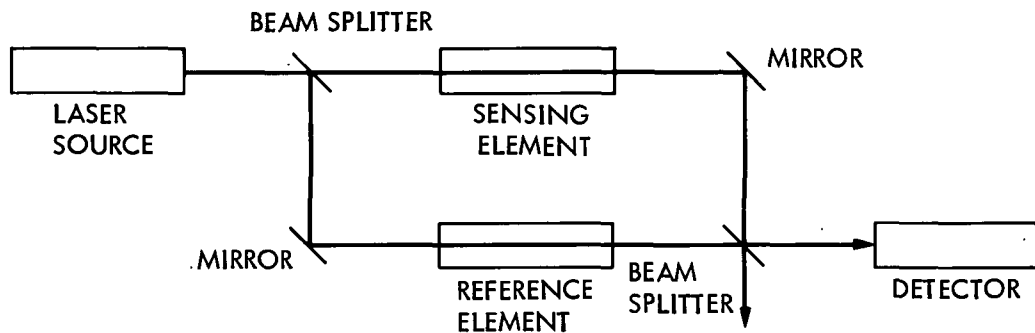
2.1.3 General Sensor Types

There are at least four ways that light can be used for measurement. It is possible for the sensing element to change the phase, polarization, intensity, or spectrum of the light. Clearly the measurement system will be radically different depending on which of these techniques is applied.

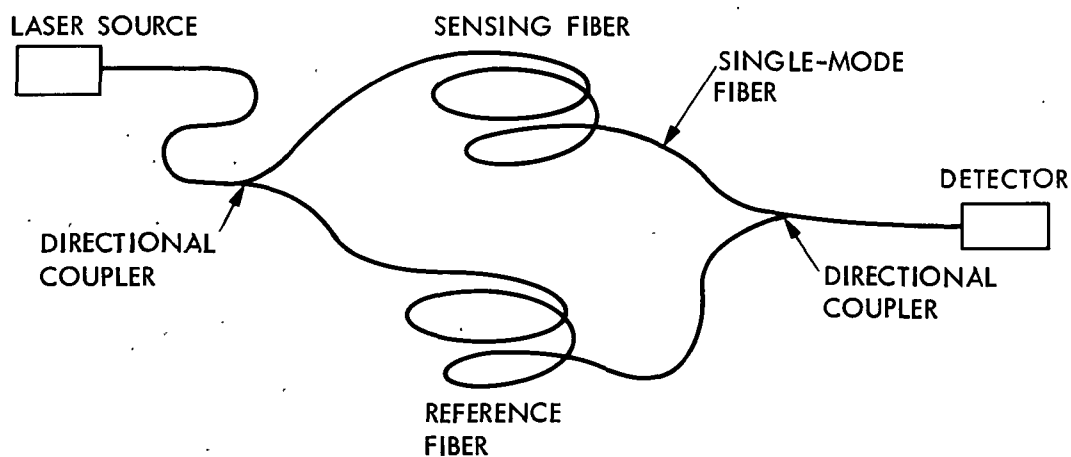
For measurements using phase variations, an interferometer forms the basis of the sensing element. Figure 2-1 shows representative sensing optics, that is, a Mach-Zender type interferometer, set up in two forms, one with conventional optics and another using a fiber-optic configuration.

The interferometer works as follows: sufficiently coherent light is split by means of a partially reflecting mirror or fiber coupler and sent into two paths, one including the sensing element, the other one used as a reference. The two beams are then recombined with another mirror or coupler. The amplitude of the recombined beam depends on the relative phase of the reference and the measurement beams. Usually, the reference path contains optical elements carefully matched to those in the sensing arm in order to compensate for unwanted effects such as that of temperature variation. It is necessary to shield the reference arm of the interferometer from the measurement parameters to which the sensing arm is exposed, or to arrange for an inverted response.

The degree of coherence required in the source depends greatly on the way the interferometer is set up. In fact, if the two legs can be made so there is never more than one light-wavelength difference in length between them, white light can be used. In general, the spectral width of the source, expressed as a fraction, must be small compared to the path difference in wavelengths. A well collimated light source is also required, such that phase variations across the aperture are small compared to a wavelength. In a fiber interferometer, this normally means that single-mode components must be used. In a multimode fiber, bends and imperfections exchange energy between modes, thereby destroying the interference (reducing the fringe visibility).



a. A CONVENTIONAL OPTICAL INTERFEROMETER



b. AN EQUIVALENT OPTICAL FIBER INTERFEROMETER

Figure 2-1. Interferometer sensor configurations

In any interferometer, two light waves here described by amplitudes E_s and E_r , are superposed to form an output beam E:

$$E = E_s e^{j(\omega t + \phi)} + E_r e^{j\omega t} \quad (2.1.1)$$

which can be shown to result in a term in the output light intensity which depends sinusoidally on the phase difference:

$$I = I_o \cos^2 \frac{\phi}{2} \quad (2.1.2)$$

and:

$$I_o = \text{const} (4E_s E_r) \quad (2.1.3)$$

There is also a term in the output intensity, of magnitude $\text{const} (E_s - E_r)^2$, which contains no useful information. In a practical sense, the fiber form of the interferometer, Figure 2-1b, is an exceedingly sensitive device, even more so than a conventional interferometer, (Figure 2-1a) because a very long sensing leg can readily be implemented. However, there are drawbacks which stem from the extreme sensitivity and the requirement for single-mode propagation. Single-mode fiber components, especially couplers, are more difficult to implement than multimode. Great care must also be exercised to stabilize and control the single-mode diode-laser source. Additionally, some form of d.c. feedback stabilization of the reference arm is almost certain to be required to eliminate thermal or other drift. An interferometer sensor should be thought of as more of a sensitive instrument requiring skilled care and monitoring than as a simple, robust, and long-lived field instrument.

A special case of interferometry, called polarimetry, involves the use of polarized light, and is useful in sensors based on the electro-optic (Pockels) or magneto-optic (Faraday) effect.

The polarization state of a light beam specifies the behavior of the transverse orientation of the electric vector in the electromagnetic field which describes the light. Light in which the electric field vector has random orientation is said to be unpolarized, while light having the electric field vector aligned in a fixed direction is termed linearly polarized.

Most crystalline materials have an index of refraction which is dependent on the plane of polarization of the light within the crystal. Such materials are said to be birefringent, a term which means that there are two indices of refraction for a given propagation direction. For a material to be useful as a sensor, the index difference, which is called birefringence, must be dependent on some external factor, such as an electric or magnetic field.

A specific configuration for an electro-optic field sensor is described in more detail in a subsequent section (see Figure 2-7). A magneto-optic sensor would have a somewhat different optical configuration, but the basic principle is very similar.

A polarimetric sensor is closely analogous to the interferometer of Figure 2-1a. The two interferometer legs are spatially coincident within the same crystal and carry orthogonally polarized beams of light. Since light beams are electromagnetic rays, these two beams can be superposed in the crystalline material without interacting with each other. The incident light is polarized, and the role of the first beam splitter is assumed by the crystal itself, since any crystal resolves incident light into its two orthogonally polarized components.

The second beam splitter in Figure 2-1a is replaced by a second polarizing element, conventionally called an analyzer. The analyzer selects a given component of each polarization, usually at 45° to each, and adds them together as phased EM fields. Therefore, the output is given by exactly the same expression (Equation 2.1.2) as in the case of an interferometer. Here, the phase ϕ means the phase difference (retardation) between the two polarizations, which is dependent on the external electric field (as distinguished from the light-wave E-field) in the electro-optic medium.

As a practical measurement instrument, a polarimeter is different from an interferometer in that it is usually short, and both beams are coincident in the same medium, greatly reducing the demands on source coherence and the stability of both source and optics.

A sensor based on intensity measurement is very simple, consisting only of a stable light source (which could be stabilized by means of feedback), and a device capable of measuring the output of the sensing element on the assumption that the input of light to the sensing element is constant. In simplest form this measurement can even be accomplished with a ready-made optical power meter, some versions of which provide a ratioing measurement using a reference detector.

Examples of this technique are a microbend fiber displacement transducer, illustrated in Figure 2-2, or the fiber electrometer described in Section 2.5.4. In the microbend transducer, carefully shaped corrugated anvils are arranged to press on a section of fiber, creating a periodic series of 'S' bends in the fiber. Light escapes from the fiber core at each bend and is lost. The magnitude of the loss can be made extremely sensitive to the amount of bending and thus displacement.

In an optical sensor based on a spectral measurement, a material is used in which some spectral feature such as an absorption line or band edge is perturbed by the parameter being measured. This material is placed in the region of interest, while light is led to the sample and back to a monitoring instrument by fibers.

Examples of phenomena which could be used in this way are the Stark effect (see Section 2.5.5 below), or the shift of a band edge or perturbation of a fluorescent transition by temperature [2-4]. The Stark effect involves a splitting of a spectral line into a number of components under the influence of an electric field. The amount of splitting—that is, the spectral shift of one of the component lines—depends on the electric field. The detection instrument would be basically a spectrometer, set up, for example, to monitor

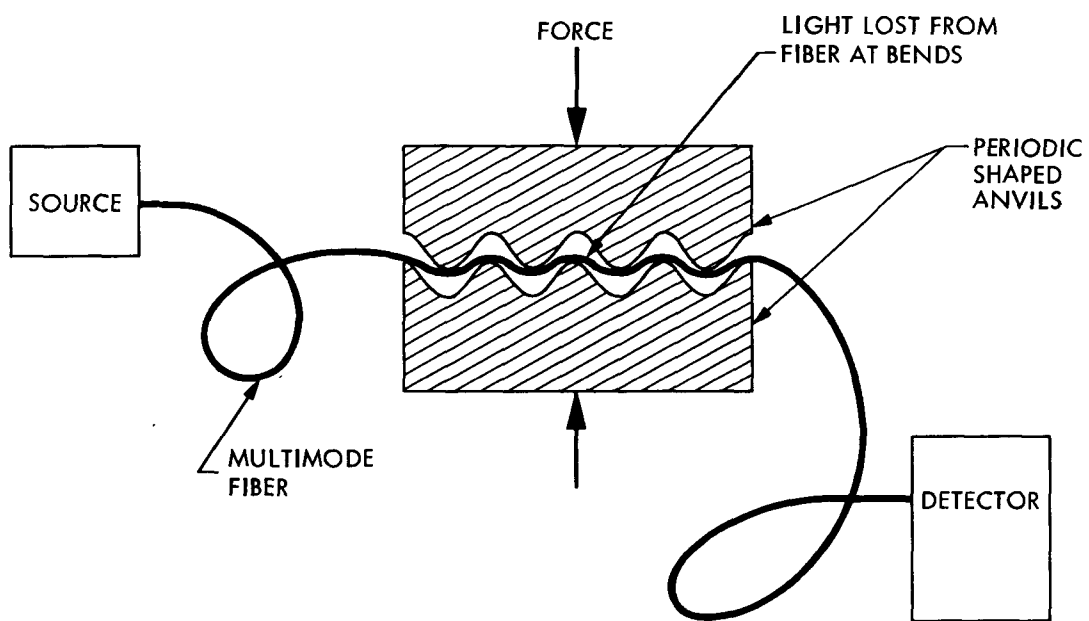


Figure 2-2. An example of an optical sensor based on intensity, the fiber-optic microbend transducer

the sample transmission at two or more carefully positioned wavelengths. Externally, then, the sensor is similar to the intensity-measuring type illustrated in Figure 2-2, except that the detector is capable of simultaneously measuring the intensity in more than one narrow wavelength band and, of course, the sensing element proper is different. The wavelengths can be positioned on the sides of a spectral line or band edge near the point of maximum slope in order to detect a wavelength shift effectively, or they can be set on the centers of different lines in certain cases where the relative strength of two spectral lines contains the desired information.

2.1.4 Distributed vs Point Sensing

Unlike a compact device, an optical fiber can be used either for distributed sensing or point sensing. An optical fiber can be inherently sensitive, or it can be sensitized to certain parameters such as temperature or pressure along its entire length.

The light output observed at one end of the fiber can therefore represent changes in environment along the entire length of the fiber. The measurement can be averaged over the length of the fiber, as in a hydrophone, or alternatively a measurement as a function of position along the fiber can be made. The latter depends on a technique called optical time domain reflectometry, or OTDR. Conventional OTDR can give a display of loss or discontinuities along the length of the fiber. In a much more sophisticated form of OTDR, more complex measurements can be made [2-5]. Alternatively, a temperature extreme occurring at any point along the fiber is detectable [2-6].

Considerable development work is still to be done in order to obtain sensitized fibers and instrumentation that would permit such measurements to be made in a practical way over tens of kilometers distance.

2.2 POWER-SYSTEM SENSORS

All of the quantities necessary for the safe and economical operation of a power system can be adequately measured with the present-day technology. After all, the power industry has been in existence for practically a century and during that time methods have been devised to measure all of the parameters required with considerable accuracy.

2.2.1 General Criteria for a Power System Sensor

Indeed, in the normal operation of a power system, electrical measurements are made in abundance. Voltage, current, power, power factor, and reactive power readings are routinely sent in great number from all over the power system to the energy control center. Another, usually independent, set of measurements is routinely made for the protection and relaying system.

It follows, then, that in order to have any impact, a new method of measurement using fiber optics must fulfill one of the following three criteria.

First, the new method of measurement may do something much more cheaply than it has been done before. Since there are a large number of measurements routinely made in the power system, economy is of paramount importance and even a slight decrease in the cost of a measurement could produce significant savings throughout an entire system.

Second, the new method of measurement may do something much better than it has been done before. For most power system applications it is difficult to see just how this could take place. For example, electrical measurements are routinely made with an accuracy of better than half of a percent. However 'better' does not apply only to the absolute accuracy of the measurement, and it may be possible to improve a measurement, for example, by producing a voltmeter which is more reliable or an ammeter which has wider dynamic range.

Third, the new method of measurement may do something that has not been done before and for which there does exist a need. For example, if it should prove possible to sense remotely the temperature of a transmission line conductor, it may be possible to update in real time a transmission line ampacity table in the energy management center. This might enable the transmission line to be operated closer to its thermal power limit and therefore lead to modified ways of operating the power system.

2.2.2 Measurement Quantities

It is pertinent at this point to ask what quantities might usefully be measured in a power system using fiber optics. The range of quantities is surprisingly small, although the number of total measurements is large. The measurements are usually of current, voltage, power, and temperature. Initially, it is rather hard to see applications for fiber optics, but it would be premature to reach such a conclusion.

In fact, the measurements of electrical quantities in a power system usually involve intermediate parameters, most often magnetic fields. Thus, the measurement of current is customarily made by causing the current to produce a magnetic field which is then measured. Perhaps this is because of the historical development of measurements by means of moving-coil instruments. Similarly, measurement of voltage is frequently a measurement of a current produced by that voltage applied to a known impedance, and the current is in turn measured in a conventional, magnetic way. As a result, when one looks at the way in which the electrical parameters of a power system are actually measured, it appears that there is a very limited repertoire of measurements actually being made. Further, measurements have been standardized to have a 120 V output if they are voltage measurements and 5 Amps if they are current measurements, so that for power systems a range of voltage transformers and current transformers has been produced using these standards.

Most power system measurements, therefore, are based on knowing the effective transfer ratios of the voltage and the current transformers involved. Voltage transformers, possibly including capacitive voltage dividers, are applied usually between the phase conductor and ground. Current transformers usually surround a bus, a transformer bushing or may be associated with circuit breakers. To substitute for any of these applications, a fiber-optic sensor would have to demonstrate that it is cheaper than the conventional method.

This is not as farfetched as it might seem. It has been found that current transformers can be economically incorporated into the solid insulation of a transformer bushing, so that the insulation required by the need to bring the transformer lead out through the tank serves the dual purpose of isolating the current transformer secondary winding as well. It may be possible to add at this location either a fiber optics current sensor or a fiber optics voltage sensor (or both) and do so economically. However, it should be borne in mind that the present technology of using a capacitive-type voltage divider in the bushing insulation is a fairly satisfactory way of measuring the voltage. To the extent that the solid insulation changes its parameters with temperature, the method could suffer from ratio drift which might also be experienced by a fiber optic sensor at the same location.

2.2.3 Voltage Measurement

The measurement of voltage has its own problems. Voltage is a measure of the line integral of the electric field between two points. The potential or voltage is independent of the path over which the integration is carried out. In spite of this, there is apparently no equipment available which performs this integration and truly measures the voltage between any two points. How then is voltage measured? There are surely a large number of 'voltmeters' available. First, it should be understood that if a pair of wires leading from a voltmeter are attached to the points between which the voltage is to be measured, then that voltage or potential difference is caused to exist at the terminals of the voltmeter. The attachment of the two wires from the voltmeter will significantly change the electric field at the point of attachment, but if the voltmeter is of high quality, there is only an insignificant current in its leads, so that for all intents and purposes the same voltage is caused to exist across the known impedance in the voltmeter.

Here it gives rise to an electric current and the electric current is, in turn, measured.

The potential of most power system components is much too high for a straightforward measurement of this sort. Instead some kind of voltage division is customarily carried out before the measurement is made.

If the voltage divider function is implemented by means of a transformer, then again we have a situation in which the electric field distribution on the conductor whose potential is to be measured can be radically changed by the addition of the transformer connection. However, since the transformer functions by establishing a magnetic field (because of the current flowing in the primary) rather than an electric field, the distortion of the electric field is usually considered to be irrelevant.

If the voltage division function is performed by capacitors rather than a transformer, then again the electric field is significantly disturbed by the presence of the capacitors. In effect, the potential difference sets up a field across the dielectric medium of the capacitor. In the case of a capacitor stack using oil-filled capacitors, there may be many elements in series. In the case of a gas capacitor, there is usually only one capacitor element and the entire potential to be measured is applied across it. The current measured is proportional to the voltage since the field geometry is fixed. Strict precautions are necessary to operate a gas capacitor with accuracy. These precautions include locating the capacitor at a sufficient distance from other metallic objects so as not to disturb the dielectric (gas) within the capacitor. Thus, it can be seen that electrostatic types of voltage dividers (capacitors) function by constraining the electric field to exist within a known region of space with constant, known geometry and a known dielectric.

Similarly, it follows that the electric field is entirely known in the region between the conductor emerging from a transformer tank and the tank itself. This region contains also the dielectric bushing used to hold the conductor in place and to shed rain from the emerging conductor. Because the dimensions are usually quite small at this point, the field can be quite high. Similarly, in a voltage divider consisting of capacitors in series, the entire voltage is sustained across only a few elements of the solid dielectric of the capacitors. Within each capacitor the field is quite high.

Because the field is high and is controlled by the design of the capacitor or bushings, either of these would be a reasonable place to measure the electric field optically and thereby produce an optically based metering of voltage. However, if one is forced to go to the expense of providing a capacitive voltage divider solely for a voltage measurement, there is little to be saved by making an optical field measurement. One might just as well go the conventional route of using a potential transformer at the bottom of the capacitor stack. On the other hand, in locations where the primary purpose is to support a bus or to penetrate a transformer tank, and the field is known and can be calculated from geometrical considerations or can be calibrated by comparison with another device (such as a gas capacitor or a coupling capacitor voltage transformer), then it may be reasonable to insert an

optically based field measurement in order to produce the equivalent of a voltage reading. Transformer bushings, circuit breaker bushings, and so on are possible applications of this kind of measurement.

However, because the field is so intense, even small changes in the dielectric constant will result in field enhancement. It may be that a driving factor behind the feasibility of the approach would be the difference in dielectric constant between the fiber measuring sensor and the ceramic bushing. It seems very likely that the dielectric constants of the two materials will not be terribly dissimilar.

In conclusion, it seems that that voltage can be measured by applying Ohm's laws in one of its various guises, and causing a current to pass in direct proportion to the voltage or by performing field shaping and measuring the field with an E-field sensor.

Voltage itself apparently cannot be measured — unless it is possible to produce a fiber whose output represents the line integral of the axial (in fiber geometry) component of the field. Just what property of the fiber might be exploited to perform this is by no means clear.

Since voltage measurements are widely performed and, in addition, rely on a voltage transformer or other costly device, we are justified in devoting some effort to developing E-field sensors. Possible ways of measuring electric field without disturbing it are discussed in the next section.

2.3 E-FIELD MEASUREMENT

2.3.1 Background

There are a number of parameters which can be used as guidelines in comparing and evaluating the various options for measuring electric fields. Thus, for example, it would be useful to know the range of possible values of the electric field, the limits to the size of the sensor, and so on.

The commonly used value for the dielectric strength of air is 30 kV per centimeter. In other words, with an air insulator a greater field than this cannot be sustained without ionization and breakdown. In solid dielectrics a higher gradient can readily be withstood, but as a rough guide it is reasonable to assume that an upper limit to the gradient to be measured is in the order of 100 kV per centimeter.

It is difficult to establish a lower limit for the field strength which might be measured, but an estimate can be had from considering the range of values of the electric field which are of interest in some of the biological work presently under way. In some work, 'screening studies' use fields in the order of the 100 kV/m. In other work the attempt is being made to replicate the effect on biological specimens of long-term exposure to very low-value electric fields, 60 cycle or dc. These represent the fields that might be experienced by farm animals or wild animals in the vicinity of a transmission line. The maximum value of the field under any operating transmission line in the United States is presently about 10 kV per meter. This represents the field exactly under the line at midspan — for the most part, even on lines of the highest voltage in use, the field is lower than this. Biological effects are considered possible as a result of exposure to fields lower than 1 kV per meter [2-7]. A figure of 100 V/m might therefore be used as a lower extreme of the range for any proposed E-field sensor.

In fact, of course, biological effects may or may not occur in an undisturbed field whose value can be calculated or measured to be 1 kV per meter, but when the biological specimen is inserted into the field, field enhancement occurs because the biological specimen is (at least partly) conducting. The disturbed field at its surface can be much greater than 1 kV per meter. For our purposes the point is not whether biological effects occur, but rather to be aware that biological specimens of large or small size cause changes in the electric field into which they are inserted. It certainly would be advantageous if the E-field sensor developed were able to measure the changed field without causing further changes.

Existing methods of measuring electric field rely on the measurement of the displacement current in a capacitor with metal electrodes. This capacitor causes considerable changes in the field, and it is necessary to calibrate such E-field sensors in fields whose dimensions are similar (usually very large) to the field that is being measured. Thus, if the field to be measured is the electric field due to a transmission line, which is considered to be many meters away, then the device must be calibrated in a uniform electric field generated by electrodes many meters in dimensions. It is further necessary to use such a measuring instrument only in a field similar to the

one in which it was calibrated and then only at the height above ground for which the calibration was performed. The ideal E-field sensor for biological work, on the other hand, would have a dielectric constant of unity, contain no metal parts, and be physically small. In this way it could be used to measure the field close to or far from the surface of the biological specimen, and would enable measurement of the field at the surface and including the field enhancement effect due to the conducting nature of the biological specimen.

For biological measurements then, the ideal sensor should be physically small and contain very little in the way of conducting components, have a dielectric constant close to unity and be capable of measuring fields in the region 1-10 kV per meter.

For voltage measurements using a device located in a ceramic or plastic bushing, the ideal sensor would again be physically small, would have a dielectric constant close to that of the medium in which it was to be inserted (which could be above 100), would contain no metal parts at all, would contain little if any in the way of internal voids or spaces, and should be capable of measuring fields perhaps in the region of 10-100 kV per centimeter.

At this point it seems unreasonable to expect a single instrument to cover the range from 100 V/m to 100 kV/cm, although this may be possible.

There is a surprisingly large number of ways in which electric field can be measured optically. As was mentioned in Section 2.1, the field may influence the phase, the intensity, the polarization, or the spectrum of the light or it may affect a transducer so that the measurement is actually made of an intermediate parameter such as motion, or displacement.

2.3.2 General Considerations for E-Field Measurement

2.3.2.1 Sensor Principles. There are three distinct principles upon which an electric-field sensor, optical or non-optical, can be based:

- (a) Electrostatic induction.
- (b) Electrostatic force.
- (c) An electric-field-dependent physical effect.

In a sensor based on electrostatic induction, electronic means are provided to detect and measure the charge induced on a conductor by the electric field in which it is immersed. Various forms of field mill [2-8] and commercial products [2-9] are representative of this approach. The induced charge $q = \epsilon_0 EA$ is linear with field, where ϵ_0 is the vacuum permittivity, and A is the area of conductor exposed to field E. In an alternating field, the rate of change of the charge represents a current which can be led to the input of a sensitive electrometer amplifier. On the other hand, steady-state charge induced by a constant field is not easily measurable and, therefore, some method of moving or vibrating the conductor is necessary, creating an oscillating current that can be readily amplified and measured.

The second sensor type, the electrostatic force balance, measures the force exerted on a conductor (or dielectric) by the electric field. Various forms of fused silica electrometers [2-10] and a special force balance used in an insulator evaluation [2-11] are examples. The force $F = \epsilon_0 AE^2$ is inherently quadratic in field.

The third method for field sensing involves a measurable physical effect that depends on an external electric field. Examples are the electro-optic effect, the piezoelectric effect in crystals [2-12], and the Stark effect in a gas or in an atomic species in an ion beam. All these effects have been used as the basis for sensing field, and are further discussed in the following sections.

Although it is difficult to say that there are no exceptions (for example, where does the deflection of an electron beam in a vacuum fit in?), we feel that the important sensing techniques will utilize one of the three principles listed above.

2.3.2.2 AC Field Sensors. The obvious way to measure an alternating electric field is to insert into it a parallel plate capacitor and measure the open circuit voltage between the plates. When the plates are normal to the undisturbed electric field (the plates, being conductors, will always be normal to the field, but may disturb it), the voltage will be a maximum and the field will be accurately measured. Provided the undisturbed field is uniform over a region larger than the capacitor plates, the plates will not affect the equipotential lines (planes) and the field is simply the open circuit voltage divided by the separation of the plates.

Of course, it is assumed that the open circuit voltage can be measured. An ordinary voltmeter would present too low an impedance. Some kind of ultra-high impedance isolating amplifier must be used, otherwise the capacitor would not be truly open circuit. The plates of the capacitor could be regarded, in circuit analysis terms, as a high-impedance source. If a voltage source is to be measured without perturbation, the measuring system should present an impedance that is large compared to the source.

The rather stringent requirements of such an amplifier can be met with a suitable operational amplifier, with careful design. Modern FET-input amplifiers with matched FETs in the input stage can provide input resistances of several G Ω , and bias currents of only a few pA. However, at 60 Hz a 1-pF capacitor has an impedance of about 2.6 G Ω . A small parallel-plate capacitor with dimensions in the order of centimeters might therefore have a series impedance of this order, requiring a voltmeter input impedance in the order of 10^{11} or 10^{12} Ω .

Such an input impedance is readily achieved by bootstrapping. In a normal voltage follower amplifier, the output and the inverting input terminal are effectively bootstrapped to the non-inverting input. Since the voltage on these terminals is nominally identical, no current will flow through the shunt impedances between them. The voltage follower therefore has an input admittance which consists chiefly of the shunt admittance to the power supplies. The effect of this admittance can be reduced to insignificance by bootstrapping the power supply terminals, as shown in Figure 2-3.

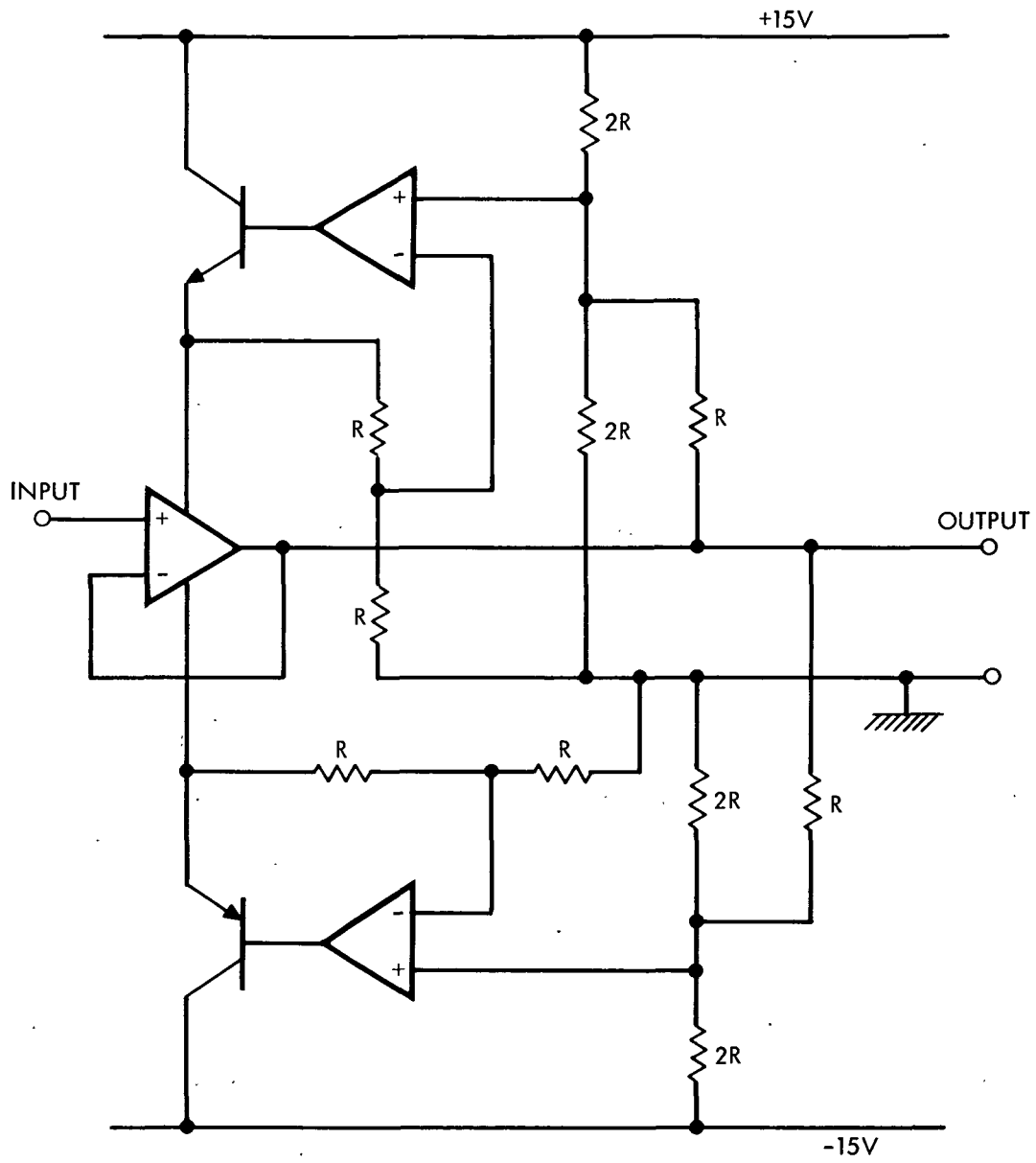


Figure 2-3. High-impedance amplifier configuration

As a practical field-measuring system, however, the open-circuit capacitor has serious difficulties which would limit its use in the outdoor power-system environment.

A ready alternative exists in the form of a short-circuit current measurement. Such a measurement has the advantage that the amplifier input impedance could be quite low. Indeed, such a system will work quite adequately, and devices based on this approach have been used successfully to measure electric fields. The current will, of course, depend on the size and separation of the plates of the capacitor, whereas in the open-circuit approach only the source impedance depended on physical size. For plates of spherical design, the field problem is mathematically tractable. An analysis is presented in Reference 2-13, where it is shown that a field of 10 kV/m will produce a current of about 0.3 μ A in a reasonably sized instrument. This current is easily measurable.

The main problem with the short-circuit method is that it distorts the field it is measuring. Because the capacitor plates are conductors, there can be no potential difference across their surfaces. Thus, when a parallel plate capacitor is inserted into an electric field with the plates normal to the undisturbed field, the field is not disturbed. Each plate assumes the potential of the field at that position. However, if we now connect the top and bottom plate together, we introduce an additional constraint into the system, namely that the two plates should have the same potential. The field inside the plates decreases and the field around the device increases.

In one version of the method, due to Don Deno at Project UHV in Pittsfield, Massachusetts, the instrument is physically large, with a large moving-coil type meter on one face to permit an operator to read the field value from a meter or two away. (Closer proximity of the investigator would disturb the field, so that remote reading is essential.) As a result, the meter disturbs quite a large region of field, and it can only be used to measure fields that are uniform (before the measurement) over large regions. Because the meter is rectangular, its calibration factor cannot be calculated as it can in the spherical case, and the instrument is normally calibrated by inserting it into a large uniform field of known intensity.

There seems to be nothing particularly wrong with this approach. The main problems with the device mentioned above are that it is large, and cannot be used to measure fields which are uniform over only a small region, or are close to another disturbing body, and there is no remote readout. The problems go hand in hand - it would be very difficult for an investigator to read a small meter of this type, as it must necessarily be remote from him.

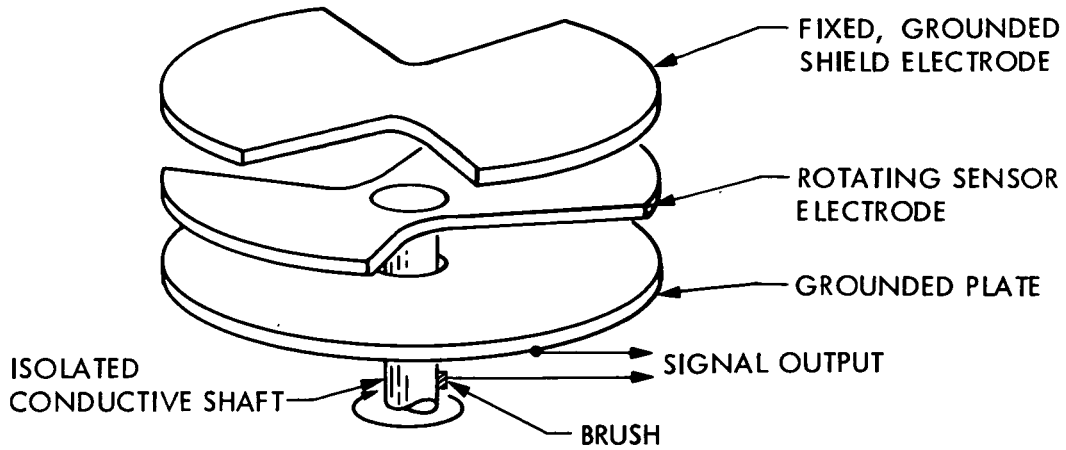
It might be possible to scale the device down, and solve the problem of reading the current by sending a current signal down an optical fiber to a location closer to the investigator. The current might be expected to decrease as the square of the linear dimensions of the probe, so that a few nA should be available from a capacitor only a centimeter or so across. A current of this magnitude should not be particularly difficult to measure electronically. It is thought that it should be rather straightforward to produce a small, remote-reading field meter based on this principle.

2.3.2.3 DC Field Sensors. One of the most widely applied methods of measuring unchanging electric fields (such as those due to a dc line) is the field mill. In this device a vane rotates under a grounded shield electrode of similar shape, and is therefore alternately shielded from or exposed to the field. Figure 2-4 shows two possible arrangements, one in which the sensor vane rotates and an equivalent alternative in which the grounded shield rotates.

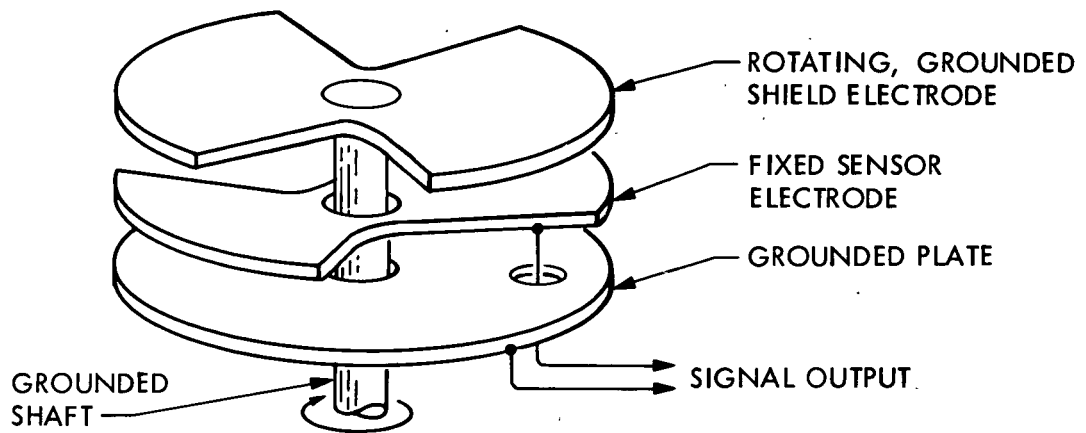
In either case, an alternating current linearly related in magnitude to the electric field can be extracted from the vane. The fact that the output is ac accounts for the widespread use of the method, as the effects of charge accumulation on the instrument are overcome. If we assume (for the sake of analytic simplicity) that the original field was uniform and is undisturbed by the presence of the field mill (that is to say, there are no fringing effects), then the flux density in the undisturbed field $D = \epsilon_0 E$ is equal to the surface charge density on the metal of the electrodes. The charge is given by the density times the area, $q = \epsilon_0 EA$, so that when the rotating vane is completely exposed to the field, it acquires a surface charge proportional to its total area and the field. As it rotates and becomes gradually more shielded, part of this charge must leak away through the resistance of the measuring circuit, until no surface charge remains when the vane is completely shielded. The process reverses as the vane reemerges from the other side of the shield.

Clearly, for a fixed field, the variation in surface charge is the same as the variation in exposed area. The rate of change of surface charge gives the current in the resistor. The rotating vane can be shaped to produce a number of waveshapes, such as triangle waves or sine waves. It is difficult to analyze this in detail, however, because in practice there is always some fringing, and the effective exposed area is not quite the same as the projected area.

Instruments of this type have been in use for over 50 years [2-8] and are commercially available. A number of these devices were recently compared in a field test [2-9].



a) WITH ROTATING SENSOR ELECTRODE



b) WITH FIXED SENSOR ELECTRODE

Figure 2-4. Rotating-vane field mill

2.3.2.4 AC vs DC E-Field Sensors. Since a dc electric field will not penetrate for long any real dielectric, unlike the analogous case in magnetostatics, it is important to realize that a dc E-field sensor will be a basically different device than an ac sensor. An ac device can be permanently enclosed in a dielectric shield — for example, a glass or plastic envelope — if this envelope is kept sufficiently clean. The sensor inside, whatever it may be, can therefore be protected from dirt and moisture. The result is a durable, practical, no-moving-parts device. In the dc case, however, a dielectric shell is precluded and, in addition, the sensor itself is likely to involve a fragile vibrating plate or rotating vane. This sensing element must unavoidably be exposed to the environment when the device is in use, a serious practical restriction. An alternative is to provide a means for rotating the sensing element, along with a protective dielectric cover, in effect chopping the unknown dc field. Charge deposited on the dielectric cover would not be detected, since the cover would rotate with the sensor. Experiments involving a rotating sensor of this type were not found in our survey of the literature. Further investigation of this possibility could prove fruitful.

2.3.2.5 Feedback Sensors. Although we find no reference to the use of feedback in E-field sensors, it has been used in the past in accelerometers, torque meters, [2-14] and gyros, where electromagnetic force from a conductor placed in a magnetic field is used as the feedback input to balance the force to be measured. The precise and linear force relationship provided by the feedback mechanism takes the place of the pickoff displacement sensor in providing the quantitative input-output relation. The same principle could perhaps be applied to an E-field sensor, and is another idea that we feel deserves further study.

2.3.2.6 Self-Charging and Ion Current. The volume surrounding a transmission line in which a significant field exists is also traversed by an ion current. Typical ion current and field have been determined at ground level under an HVDC line [2-15]. A simple calculation shows that the ion current on a field-mill electrode at ground level is likely to be a significant error source since this current will add to the output current of the mill. In addition, the ion current intercepted by an isolated E-field sensor located above ground will rapidly charge it to a potential different from the ambient potential at that location before the sensor was placed there. The potential reached by the sensor will be self-limiting, but its magnitude is unknown. The collected charge will create an electrostatic field which will be superimposed on the ambient field. Any response by the sensor to this field, such as a simple gold-leaf electroscope would exhibit, must be minimized.

A third consequence of ion current is that it can perturb the ambient field which we desire to measure. The perturbation would be calculable from Poisson's equation if the space charge associated with the ion current were known, but both the ion current and the space charge associated with it may vary.

An idea of the magnitude of the perturbation of the electric field under a transmission line due to space charge can be obtained from a mathematical analysis based on the appropriate solution of Poisson's equation. The field in the presence of a space charge is described by Poisson's equation:

$$\text{div grad } V = \nabla^2 V = \frac{-\rho}{\epsilon_0} \quad (2.3.1)$$

where ρ is the space charge density, and ϵ_0 the permittivity of space.

This equation can be solved without particular difficulty by applying boundary conditions in a system of rectangular coordinates. Unfortunately, such a geometry is unconvincing as a model of a transmission line. An argument can be made, however, for the use of cylindrical coordinates, which might be expected to yield a solution of only slightly greater complexity.

This choice of coordinate system can be used to model with great precision the field inside a conductor test cage, a device widely used to evaluate the corona performance of a proposed transmission line design [2-16]. If suitable dimensions are chosen for the cage, the electric field gradient at the surface of the conductor and in its vicinity can be made as high as it would be on a transmission line, but with considerably less voltage. In this case, the gradient at the cage wall is higher than the gradient would be at the ground under a transmission line. In our application, a larger cage is modeled so that the ground gradient is also reasonably well modeled.

In cylindrical coordinates, Poisson's equation is written

$$\nabla^2 V = \frac{\partial^2 V}{\partial r^2} + \frac{1}{r} \frac{\partial V}{\partial r} + \frac{1}{r^2} \frac{\partial^2 V}{\partial \theta^2} + \frac{\partial^2 V}{\partial z^2} = \frac{-\rho}{\epsilon_0} \quad (2.3.2)$$

Since we can assume axial and circumferential symmetry, the last two terms vanish, leaving the complete differential equation

$$\nabla^2 V = \frac{d^2 V}{dr^2} + \frac{1}{r} \frac{dV}{dr} = \frac{-\rho}{\epsilon_0} \quad (2.3.3)$$

We assume, further, that the space charge is made up solely of positively charged ions, and neglect electron density because of the much higher electron drift velocity. While an individual ion is subject to an acceleration because of the field, the fact that it is in the atmosphere, rather than free space, means that there will be many collisions with the molecules that constitute the air. The ensemble effect is that of viscous drag. The motion of the ions is therefore assumed to be described by a constant mobility μ , which we take

to be of the order of $1 \text{ cm}^2/\text{V s}$ [2-17]. The current density per unit length, J , is given by

$$J = \rho v \quad (2.3.4)$$

where v is the ion drift velocity, given by

$$v = \mu E \quad (2.3.5)$$

Considerations of symmetry lead to the conclusion that the current density falls as the reciprocal of the radius, or

$$J = \frac{I}{2\pi r} \quad (2.3.6)$$

where I is the ion current per unit length and r is the radius. It follows that

$$J = \rho \mu E = \frac{I}{2\pi r} \quad (2.3.7)$$

whence

$$\frac{d^2 V}{dr^2} + \frac{1}{r} \frac{dV}{dr} = \frac{-I}{2\pi \mu E \epsilon_0 r} \quad (2.3.8)$$

This second order equation in V can be written as a first order equation in E

$$\frac{dE}{dr} + \frac{E}{r} = \frac{-I}{2\pi \mu E \epsilon_0 r} \quad (2.3.9)$$

After some effort, this can be solved to yield

$$E^2 = \frac{I}{2\pi \mu \epsilon_0} + \frac{b}{r^2} \quad (2.3.10)$$

where b is a constant. (Rather than clutter this explanation with mathematical manipulations, details of how this equation was derived are given in Appendix A.)

It can readily be seen that, in the absence of a space charge, Equation (2.3.10) reduces to the familiar $1/r$ form for the field. The addition of the ion current term, however, modifies this simple field distribution,

intensifying the ground level field and reducing the gradient near the conductor.

Equation (2.3.10) was integrated and a numerical solution was obtained (details are, again, in Appendix A) for the case of a cage 10 m in radius with a conductor of 10 cm diameter at its center. A potential of 500 kV was applied, and various representative values of ion current [2-15] were assumed. The results are shown in Figure 2-5.

It can be seen in Figure 2-5 that even small ion currents can have significant impact on the electric field, particularly at the ground. A current as small as 1 μ A can evidently cause a 60% increase in the field intensity. Previous authors have noted problems with repeatability of E-field measurement, by several percent in recent HVDC tests [2-9], and even by greater than an order of magnitude in textile charging experiments [2-18]. We feel that ion current and self charging of the sensor will be the limiting factors in the accuracy of E-field mapping in power systems, and should receive careful attention in the sensor design. In particular, it appears difficult to avoid a direct E-field sensor response to ion current, regardless of the sensing principle. An attempt to minimize the perturbation, or to compensate accurately for it by a detailed understanding of ion-current effects, appears to be needed.

2.3.2.7 Desired Sensor Characteristics. Some consideration was given to developing a set of requirements or desirable parameters for an E-field sensor and the results are summarized in Table 2-1. The various sensor concepts described in the following section can be compared by reference to the tabulated requirements.

Table 2-1. Desired Characteristics and Parameters of an E-Field Sensor

-
- o Minimum disturbance of unknown field
 - small size
 - dielectric materials
 - o Enclosed, cleanable, durable
 - o No response to self charging
 - o Negligible perturbation by ion current
 - o DC response for HVDC measurement
 - o Fiber (all-dielectric) or free-space optical transmission for readout
 - o Linear response
 - o Parameter values
 - accuracy 1%
 - repeatability 0.1%
 - dimensions 1 cm³ or less
 - full-scale field in the range 10³ V/m to 3 MV/m
(Value selected depends on application).
 - response time 1 ms
-

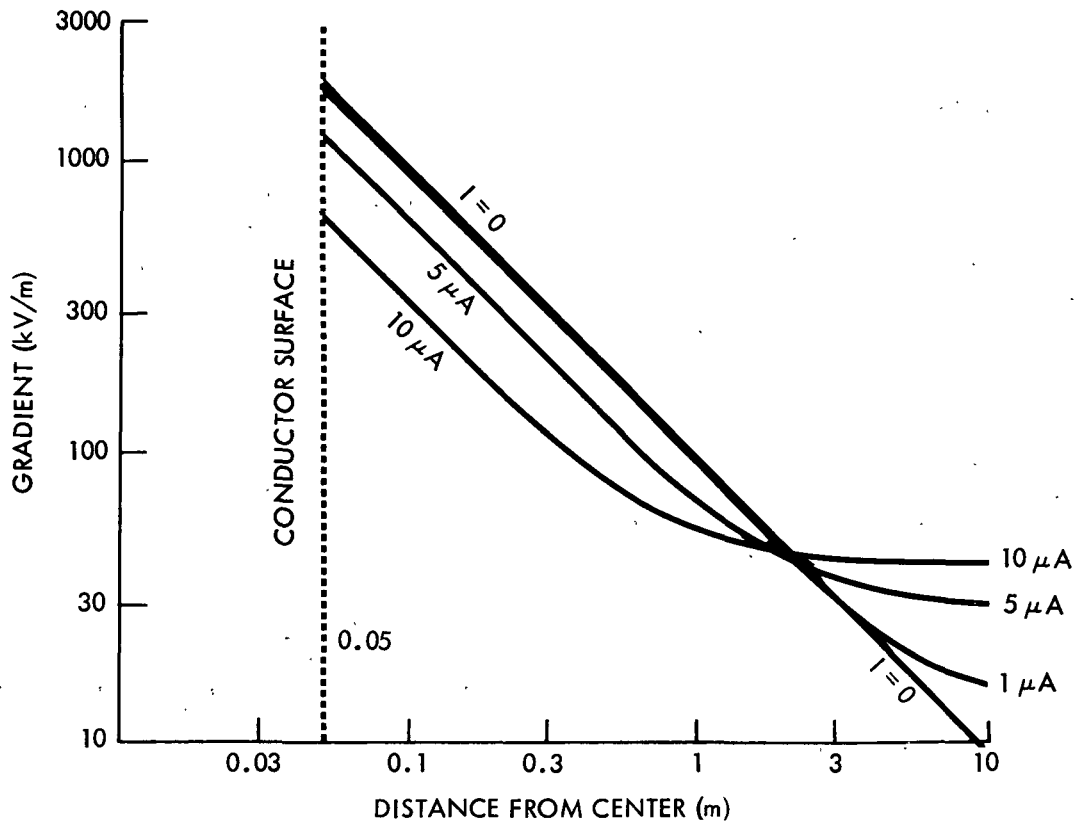


Figure 2-5a. Electric field gradient as a function of radius for various values of ion current, cylindrical geometry

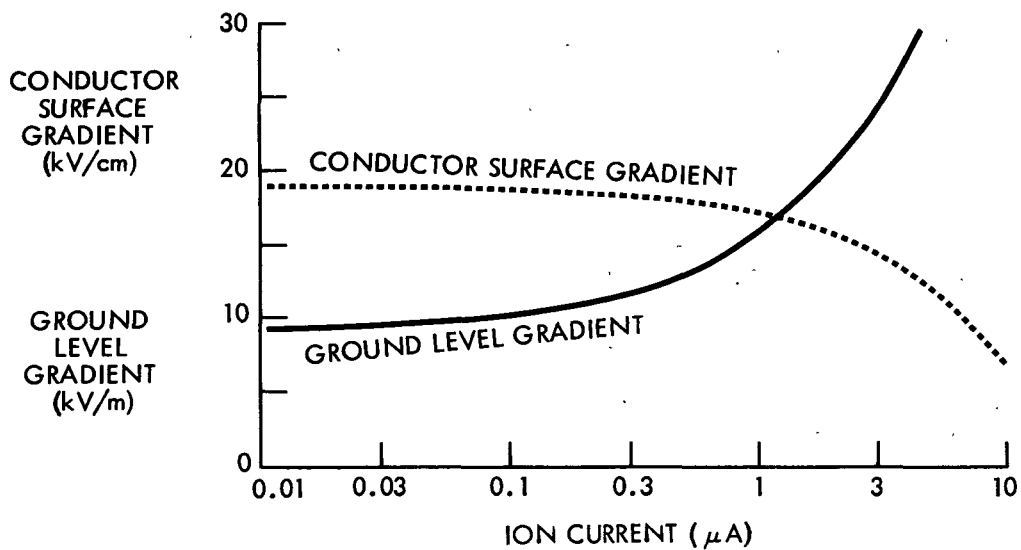


Figure 2-5b. Electric field gradient at the conductor surface and at the ground as a function of ion current.

2.4 OPTICAL BUILDING BLOCKS

In this section we describe several optical elements which are used with optical fibers, and which are somewhat different than conventional optics. These are the components that can be drawn on, along with the optical fibers themselves, in order to build the sensors that we are interested in.

2.4.1 Input and Output Coupling Considerations

A multimode fiber guides light encompassing a distribution of propagation directions within its core. Even if a perfectly collimated light beam could be launched in a multimode fiber, its angular distribution would soon broaden because of bends and imperfections in the fiber. The angular range of propagation directions is characterized by the numerical aperture (NA) of the fiber, defined as $NA = \sin\theta_{\max}$. The angle θ_{\max} is the greatest angle that can exist between a ray and the axis of the fiber for light which is guided within the fiber core. Note that θ_{\max} is measured in air outside the fiber. Typical fibers have an NA between 0.2 and 0.3. A consequence is that a sufficiently collimated large beam of light collected by a lens of matching NA (NA = 0.2 corresponds to $f/2.5$, a rather fast lens) can be coupled with residual loss approaching the reflection loss at the fiber-air interface. Similarly, the light emerging from a fiber requires a lens with matching NA to be recollimated without loss.

A single-mode fiber, on the other hand, although it can be properly understood only in terms of the wave description of light, can be thought of as propagating only the axial light ray. A spatially coherent light beam, such as provided by a well-behaved laser, must be collected by a diffraction-limited lens for efficient coupling. The required NA of the lens is determined by diffraction (wave optics) considerations only, and relative alignment of laser, lens, and fiber is significantly more critical than in the multimode case. As a result, single-mode systems also require fairly fast lenses for efficient coupling.

Diode lasers, by far the most practical source, are sensitive to their own light when reflected back by a discontinuity. A reflected intensity of less than 0.1% can cause mode-hopping effects which would be detrimental to the operation of a fiber interferometer sensor. Work aimed at improving the capability to control these effects is still an active research area [2-19].

2.4.2 Lenses

Conventional simple lenses of appropriate size (micro lenses) can be used for coupling, and can be obtained or fabricated down to the order of 1 mm focal length. However, much more attention has been given to graded index lenses (also called selfoc lenses) [2-20]. A graded index lens is a glass rod, typically 1-2 mm in diameter with index of refraction varying radially as r^2 , exactly as a graded index fiber core does. When cut to the correct length, (typically a few mm) such a rod functions as a lens. Simple optics can be fabricated without air spaces, which makes it possible to couple from fiber core to elements like wave plates, beam splitters, and birefringent optics using a monolithic cemented assembly with overall length of a few millimeters.

2.4.3 Couplers

Multimode couplers can be made with reasonable ease from fiber by a fusion technique [2-21], resulting in a small, passive package. These are called tapered fused fiber couplers, and can be obtained commercially. The basic form of the coupler is made from two fibers, yielding four ports. It can have any desired splitting ratio, and if it is symmetrical (a 3 dB coupler), it can have of the order of 1 dB excess loss, and less than -50 dB coupling into the reverse direction. Figure 2-6a is a sketch of such a coupler. The multimode coupler is useful for signal splitting or recombining, but is not suitable for use in a fiber interferometer except under very special circumstances. The reason is that multimode fibers and couplers compatible with them can propagate light at a significant angle from the axial direction. The optical path of the inclined ray will differ from the axial ray enough to destroy interference effects after traveling a very short distance (the order of 1 mm).

An analogous single-mode device is feasible, but is more difficult to make and in some forms is cumbersome to use. A single-mode four-port (two-fiber) coupler is analogous to a beam splitter in an interferometer, and indeed is the basic building block of a fiber interferometer. Fused couplers similar to the multimode form shown in Figure 2-6a have been successfully fabricated. A sketch of a type of coupler developed at Stanford [2-22] is shown in Figure 2-6b. At present, these couplers tend to be laboratory devices. Similar couplers can also be made on planar substrates by integrated optics techniques, but these devices require coupling from fiber to planar waveguide and back again, at present a lossy (>5 dB) technique.

2.4.4 Polarizers

Polarizing elements incorporated into the structure of a conventional circular fiber do not exist. However, a graded-index lens pair with a polaroid sheet between can provide the function in a cemented integrated block and similar devices have been built by butt-coupling through a polaroid film with no lenses. (Note that this type of device is not conventionally termed integrated optics.) An alternative has been demonstrated in planar integrated optics waveguides [2-23] and is, at least in principle, also applicable to fibers. This approach requires a birefringent crystal to be cut in such a way that the larger index is greater than the index of the fiber core, and the smaller index is lower than that of the core. The crystal is mounted in contact with the fiber core, which requires careful lapping of the fiber. Light whose plane of polarization in the fiber core is associated with the high crystal index is not guided at the core-crystal interface, and is therefore dumped into the crystal and lost. Light polarized in the perpendicular plane can propagate undisturbed in the fiber core, since the core-crystal interface reflects back to the core. Recently, a new in-fiber polarizer has been described [2-24] using a specially fabricated section of fiber which is capable of propagating only one polarization mode. Techniques for splicing such a fiber into circular cross section fiber have not yet been explored.

It should be remembered that the state of polarization is not normally preserved in a fiber. Typically, less than a meter of length will result in large changes in the polarization because of very small residual asymmetry in the fiber. It appears to be impossible to completely remove the polarization effects, but a number of experiments suggest that if a sufficiently birefringent fiber can be fabricated, then the two polarization modes are decoupled, and energy launched in one polarization will remain polarized in that plane.

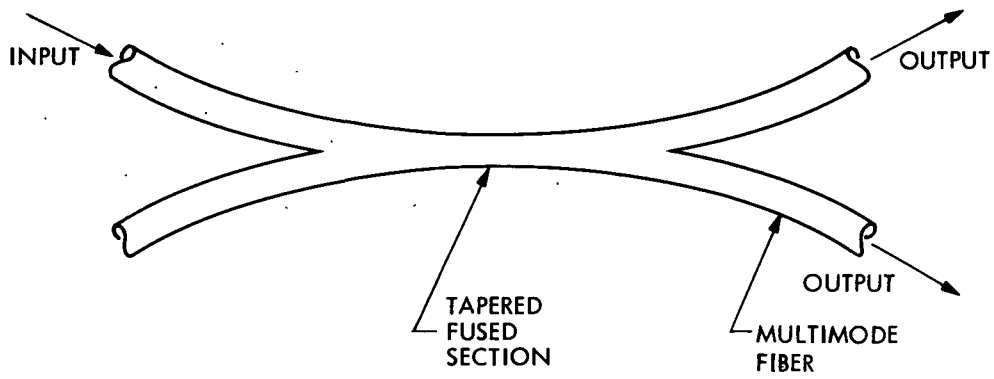


Figure 2-6a. Four-port fused tapered multimode fiber coupler

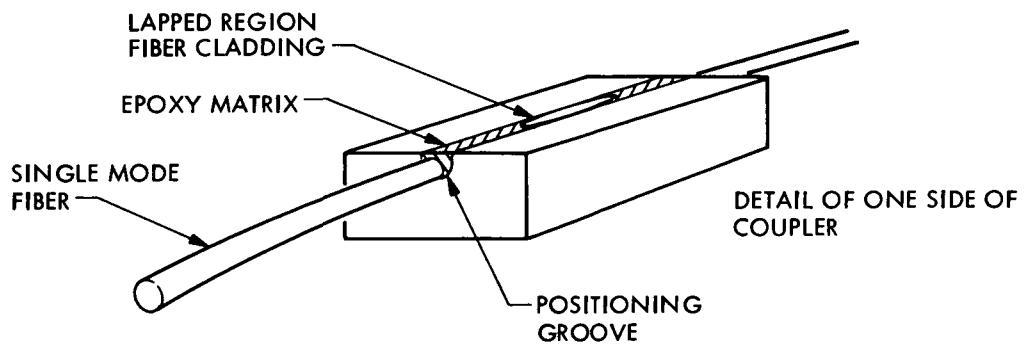
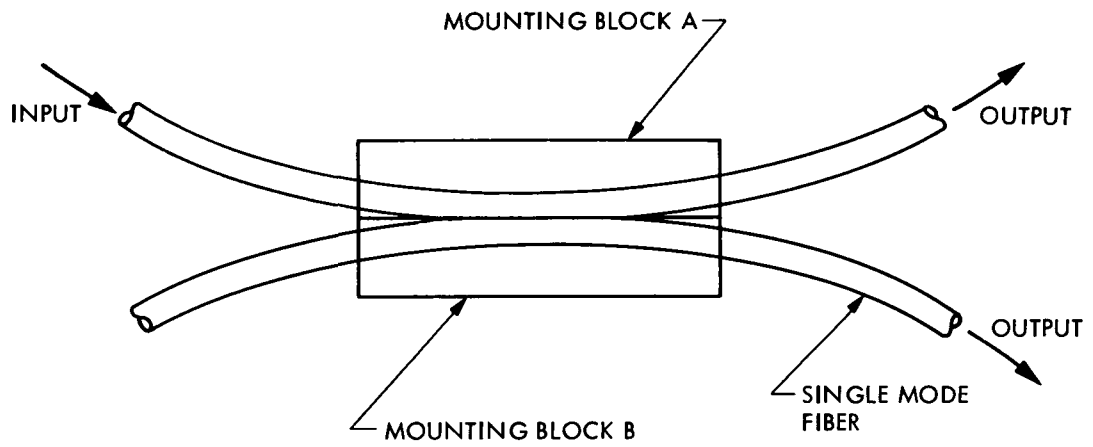


Figure 2-6b. Stanford single-mode four-port fiber coupler

2.4.5 Isolator

An isolator — that is, a component which transmits light in one direction only — is an important component to control feedback to a diode laser source. Isolators in a number of forms have been demonstrated [2-25]. The most straightforward form at present is a cemented hybrid device using bulk polarizing optics and graded index lenses.

2.4.6 Connectors and Splices

Many different implementations of fiber connectors are commercially available [2-26]. With few exceptions, connectors are designed to position two fiber ends close together and in precise alignment, sometimes using the same outer mechanical hardware that is used in copper coax or multiple pin connectors. Typical loss that should be expected per connector is about 2 dB, so the number of connectors in series in any channel must be kept to an absolute minimum.

Field splicing techniques are also available [2-26], the difference between a connector and splice being that the connector can be separated and rejoined repeatedly, while a splice is a permanent connection. The most readily available tools are designed for making a fusion splice, which can be reliably done with less than 0.1 dB loss. Alternate techniques based on optical cementing of the fibers after aligning them in a precision bore tube or other fixture are also available.

2.4.7 Integrated Optics

Simple guided wave optical systems, involving a few (say, less than 10) waveguide components such as couplers, modulators (an electrically variable coupler), lenses, and filters can be connected with optical waveguides and fabricated on planar substrates by means of photolithographic techniques very similar to those used in electronic microcircuit fabrication. Devices of this type are conventionally referred to as integrated optics [2-27]. Most work to date has been in LiNbO_3 , a ferroelectric, piezoelectric, high dielectric constant material. Recently, interest in III-V semiconductor material systems based on GaAs appears to be increasing. Indeed, a semiconductor laser is itself a single, planar integrated optics component. Electronic components can be monolithically integrated with the optical elements using the III-V materials system, but not in LiNbO_3 . Applications of integrated optics that have been demonstrated in the laboratory in rudimentary form are, for example, spectrum analysis, correlation, and wavelength multiplexing. This technology will need perhaps three to five years more before emerging from the research laboratory. Although an analogy with the transition in electronics from transistors to VLSI should not be taken literally, it is still a useful guide and suggests that the integrated optics technology may have an important impact in the future.

2.4.8 Sources and Detectors

Last, but not least, we mention the essential elements of almost any fiber system, the sources and detectors. Two types of sources are available, semiconductor lasers and LEDs, available at either the 0.8 or 1.3 μm wavelength [2-28]. Lasers require more complex driving circuitry and can be made single mode (monochromatic and spatially coherent), while an LED corresponds more closely to a diffuse source.

There are several devices that could be used to convert an optical signal to electrical form. Photoconductive detectors have inferior noise performance (except when the input power is high), pyro-electric detectors can only be made fast at the expense of sensitivity, and phototransistors are generally slow and insensitive, though they do provide gain. Gain can also be obtained from avalanche photodiodes, but with some noise problems [2-29]. The PIN diode [2-28] would almost certainly be the detector of choice in any power system sensor. Lasers are typically capable of coupling 1-20 mW into a fiber, and can be modulated in the optimum case from dc to several GHz. PIN detectors can be made with a similar range of bandwidth, if required. The optical power margin achievable for use in a fiber sensor is perhaps two orders of magnitude at the highest bandwidths ($> 1\text{GHz}$) and rises at lower bandwidths, since heavier noise filtering in the receiver is then permissible, to perhaps five orders of magnitude at bandwidths in the order of tens of kHz.

2.5 DIRECT FIBER OPTIC SENSING OF E-FIELD

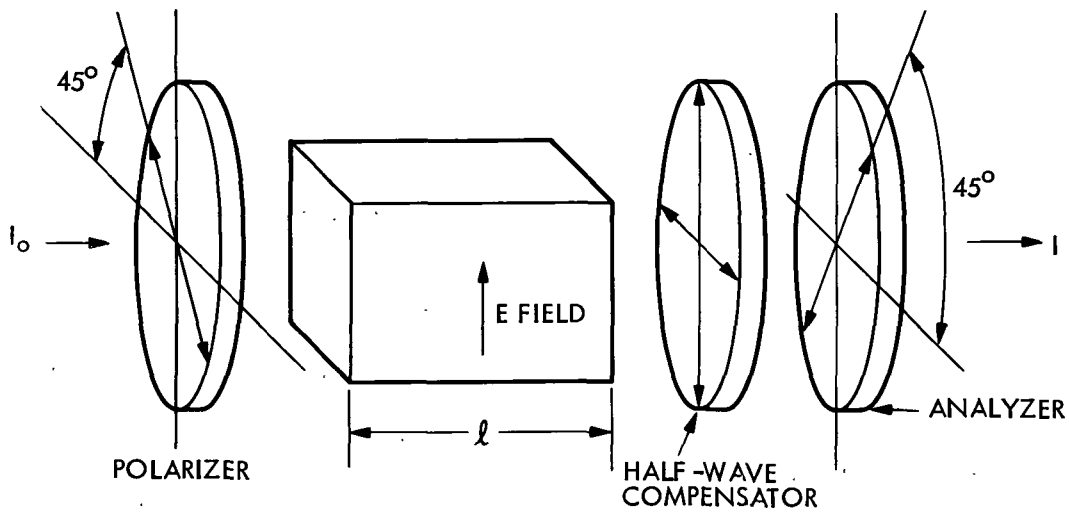
In this section, a number of methods of measuring E-field directly using fiber optics are reviewed. These sensors modify light guided by an optical fiber to the sensor and then back to a readout instrument. Some, namely the electro-optic effect, piezoelectric fiber coatings, and the fused silica electrometer are clearly useful approaches. The relative advantages of several others, including an all-dielectric force balance, membrane force balance, Stark effect, and fluorescent excitation are less clear at this point, but brief discussions are given. We do not intend to make a final judgment here on relative merit. Many of these ideas have not been thoroughly explored, and further work may yield new perspectives.

2.5.1 Linear Electro-Optic Effect Sensors

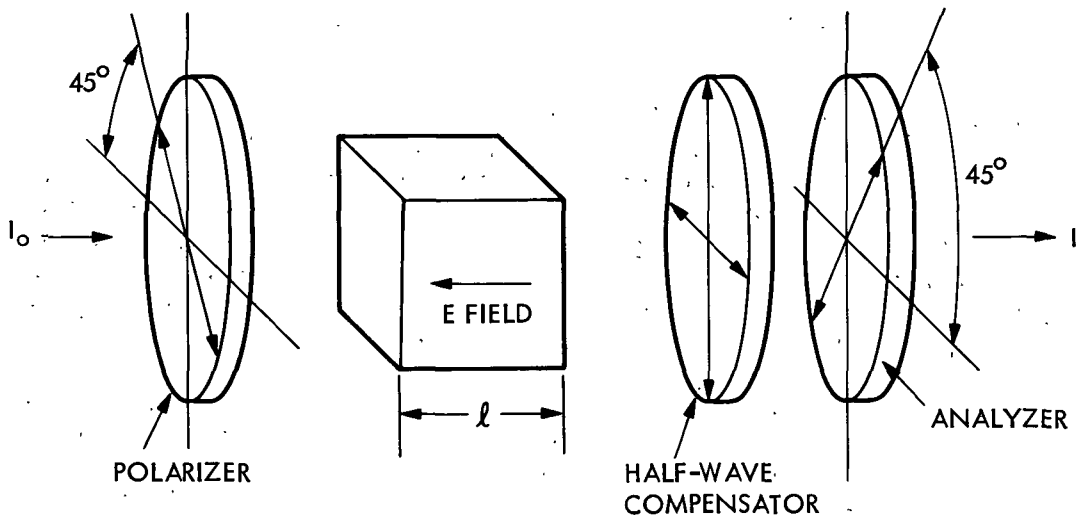
Sensors based on the linear electro-optic effect (Pockels effect) take advantage of a perturbation of the refractive index of specially selected materials caused by an external electric field. The change in index depends linearly on field in non-centro-symmetric crystalline materials. The index change is typically very small, of the order of 10^{-4} or 10^{-5} , but can produce a useful optical response through interference effects. Electro-optic devices have been widely studied because of their applicability to light modulation for communication purposes. The general principles are treated in a book by Yariv [2-30]. A general discussion covering electro-optic sensing techniques in power systems is given by Hebner et al. [2-31] with an extensive bibliography.

The useful materials, as a class, typically have a high dielectric constant, are mechanically soft, not exceptionally durable or stable, and are highly piezoelectric, polar, and ferroelectric. Some are very good dielectrics, however. Because a linear electro-optic material must be crystalline, one should not expect an electro-optic fiber to be announced any time in the near future (although growth of short crystalline unclad fibers is probably not impossible). Instead, the sensor element is shaped from bulk crystalline material, with fiber for optical input and output.

The magnitude of the response is dependent on the relative orientation of the field vector, light propagation direction, and crystal axes. Two special geometries are possible, one with the electric field perpendicular to the direction of propagation of the light, the other with field and light propagation parallel. Figure 2-7 illustrates the elements of a transverse and a longitudinal sensing element. The preferred geometry is determined by the material selected, but some crystals can be used in either the transverse or longitudinal configuration. The purpose of the compensator element is to adjust the zero field transmission of the sensor to the desired point. A transmission of 50% would typically be selected because it results in the largest small-signal response and the best linearity.



a. TRANSVERSE GEOMETRY



b. LONGITUDINAL GEOMETRY

Figure 2-7. The elements of an electro-optic field sensor,
 (a) for transverse geometry
 (b) for longitudinal geometry

The readout could be done interferometrically, but it is more practical to use interference between the two orthogonal polarizations in the same crystal as discussed in Section 2.1. Incoherent light from a multimode fiber can be used for input and output. A polarizer at the input sets up the two coherent polarization modes that are required and the half-wave compensator and output polarizer (analyzer) yields an output intensity dependent on the induced optical phase change within the sensing crystal.

The output light intensity is given by the relation

$$I = I_0 \cos^2 \frac{\phi - \phi_0}{2} \quad (2.5.1)$$

where ϕ is a field-induced optical phase difference (retardation) given by equation (2.5.2) below, and ϕ_0 is a fixed phase difference built into the optics. The quantity ϕ_0 is made up of two parts, (1) the unperturbed retardation of the electro optic crystal, and (2) the retardation of the compensator. I_0 is the intensity of the input beam after polarization.

Rather than giving the optical phase in terms of the conventional material-oriented electro-optic r_{ij} matrix, we will use the more user-oriented half-wave voltage V_π . The half-wave voltage produces an optical phase shift of π , hence the subscript, which in turn results in 100% modulation, corresponding to the full-scale range of a sensor. The half-wave voltage depends on both the material and the modulator geometry — that is, the field direction and light direction with respect to the crystal axes. The optical phase ϕ in equation (2.5.1) is given by

$$\phi = \pi \frac{V}{V_\pi} \quad (2.5.2)$$

for longitudinal geometry, and

$$\phi = \pi \frac{l}{l_0} \frac{d_0}{d} \frac{V}{V_\pi} \quad (2.5.3)$$

for transverse geometry, where l is the light path within the crystal, l_0 is a reference crystal length, which we assume to be 1 cm, and V is the voltage applied across the crystal, d is the crystal dimension between electrodes, and d_0 is a reference dimension, taken as 1 cm. The parameter V_π is useful for visualizing sensor response to a voltage applied to an electroded crystal. Values of V_π and several other important parameters are shown for the most common electro-optic materials in Table 2-2 [2-32]. Note that V_π depends on orientation even within the transverse field or longitudinal field case. V_π is given only for a conventionally used orientation.

Since we are specifically interested in electric-field sensing, it is instructive to rewrite Equations (2.5.2) and (2.5.3) in terms of a half-wave electric field, E :

$$\theta = \pi \left[\frac{L}{d_0} \frac{E}{E_\pi} \right] \quad (2.5.4)$$

The applied field E is understood to be the intensity of a uniform electric field in which the crystal is immersed.

Equation (2.5.4) is valid for either transverse or longitudinal geometry, and $E_\pi = V_\pi K/d_0$. K is the applicable dielectric constant and d_0 is the reference crystal dimension in the field direction for either geometry. The modulator width perpendicular to both field and light directions is assumed large in order to define E_π . Values of E_π are given in Table 2-2 and are useful for estimating the magnitude of response from a bare crystal exposed to the field. Depolarizing fields decrease as the width of the sample decreases, so the value of E_π given is an upper limit.

Table 2-2. Properties of Linear Electro-Optic Materials

Material	V_π kV	E_π kV/cm	Geometry	Optical Index	Dielectric Constant	Wavelength μm
Lithium Niobate LiNbO_3	4.0	336	Transverse	2.2	84	0.63
Lithium Tantalate LiTaO_3	2.7	116	Transverse	2.2	43	0.63
ADP	7.67	92	Longitudinal	1.52	12	0.63
KDP	19.0	399	Longitudinal	1.51	21	0.63
KD*P	6.9	345	Longitudinal	1.52	50	0.63
GaAs	13.3	152	Transverse	3.3	11.5	1.0
Quartz	161	692	Transverse	1.54	4.3	0.55

A practical difficulty arises because the constant phase θ_0 in Equation (2.5.1) contains the natural birefringence of the sensing crystal, which is typically is strongly temperature-dependent.

A number of experiments have already been implemented in the field using Pockels-effect sensors as electric-field measuring devices for transmission systems. Erickson at Bonneville Power Administration, his collaborators at the Oregon Graduate Center, [2-34] and Sasano [2-35] describe experiments in

which a Pockels crystal is mounted near the high-voltage conductor and read out by a free space laser beam. They report accuracy of the order of 1% and a best sensitivity of less than 1 V/cm. Additionally, a large bandwidth in the sensing channel is easily achieved, making it possible to directly determine the direction of propagation of a fault transient using two sensors separated by an appropriate distance. Rogers [2-36] also analyzes techniques for voltage measurement using the electro-optic effect in quartz.

A limitation to direct electric-field measurement, as opposed to a voltage measurement where electrodes are fixed directly to the sensing element, is low-frequency relaxation of the field within the crystal due to the non-zero conductivity of the sensing material. Temperature-dependent relaxation times of milliseconds to seconds are reported by Massey et al. [2-34] in KD*P. The response of a sensor to a step function input will decay to zero with this time constant.

Field sensors based on the Pockels effect have been investigated by a number of laboratories and they appear to perform well as ac sensors, although probably not with great (0.1% or better) accuracy. We feel that this sensor type is well understood, and will not treat it further here.

2.5.2 Kerr Effect

Electric field measurement using the quadratic electro-optic effect or Kerr effect is essentially identical to the technique based on the Pockels effect discussed in the last section. The differences are internal and do not change the configuration of the sensor.

First, the sensing medium is centro symmetric or isotropic, and usually is a liquid. The transverse field geometry shown in Figure 2-7a must be used. Using a symmetry argument, the field component parallel to the light propagation direction cannot be detected.

Second, the response given by Equation (2.5.3) is modified. For the Kerr cell, instead of Equation (2.5.2) we use

$$\theta = \pi \frac{L}{L_0} \frac{d_o^2}{d^2} \frac{V^2}{V_\pi^2} \quad (2.5.5)$$

where L is the modulator dimension in the light-propagation direction, and d is the dimension in the field direction.

Using arguments similar to those given above for the linear electro-optic case, one can derive expressions in terms of the electric field external to the medium.

$$\theta = \pi \frac{L}{L_0} \frac{E^2}{E_\pi^2} \quad (2.5.6)$$

where E_π is again the half-wave field external to the medium. The half-wave voltage and field can be derived from the conventionally-defined Kerr constant

B [2-32] as $E_{\pi}^2 = K^2/2l_0 B$, and $V_{\pi}^2 = d_0^2/2Bl_0$. The fixed retardation θ_0 found in Equation (2.5.1) will be zero for a Kerr material because it is isotropic, unless an optical retarding element is deliberately introduced in order to bias the sensing element into the quasilinear range near $I/I_0 = 1/2$ (see Equation (2.5.1)).

Nitrobenzene is the classical choice for a Kerr liquid, although it is not a particularly desirable substance to work with. Half-wave voltage and field are given in Table 2-3 for several Kerr materials where l_0, d_0 are assumed to be 1 cm and the cell width is assumed to be large.

Table 2-3 Properties of Several Kerr Materials

Material	V_{π} kV	E_{π} kV/cm	Resistivity Ω -cm	Optical Index $\lambda=0.55$	Dielectric Constant	Wavelength μ
Nitrobenzene	6.2	233	5.5×10^7	1.55	36.0	0.55
Benzonitrile	10.3	270	3×10^6	1.53	26.3	0.55
Acrylonitrile	12.5	406	4.9×10^5	1.39	32.5	0.55
O Dichlorobenzene	16.5	123	2.6×10^9	1.55	7.5	0.55
CS ₂	59.9	155	-	1.62	2.6	0.59
MBAB	6.6	-	-	-	-	0.55

An interesting possibility to consider is that the Kerr medium might be directly introduced into a hollow fiber, forming a liquid core. If the optical loss were low enough, a large increase in cell length could be obtained. A hollow fiber is quite simple to draw, starting with a hollow preform. Previous experiments with liquid-filled fibers for other purposes, however, had to contend with expansion cells on each end to permit filling the fiber without introducing bubbles. From Table 2-3 we can estimate that the half-wave field for a one-meter-long fiber filled with CS₂ would be 15 kV/cm and, if filled (somewhat exotically) with the liquid crystal material MBAB (p-[(methoxybenzylidene) amino] benzonitrile) [2-37], it would be 577 V/m at an optimum temperature near its transition, 119°C.

At present, we feel that a Kerr sensor is not likely to be superior to one based on the Pockels effect because the magnitude of the Kerr effect is small in well-behaved liquids such as CS₂, while the strongly nonlinear liquid crystals are sensitive to the environment. We have not attempted at this point to identify materials for fiber tube and Kerr liquid with the required indices for guiding with low loss. Our purpose is only to suggest a possibility. The idea of a long in-fiber Kerr sensor may be an interesting

one, but it should be remembered that a transverse electric field is required. The longitudinal field type of fiber sensor capable of measuring the line integral of field directly does not appear to be feasible with a Kerr liquid.

2.5.3 Piezoelectric Jacketed Fiber

Recent work at NRL [2-38] and at the 3M Corporation [2-39] has shown that it is possible to jacket an optical fiber with a polymer having piezoelectric properties. The piezoelectric response of the polymer to an external electric field applies a stress to the fiber which can be read out through the stress-optic response in the fiber using conventional interferometric technique. The polymer coating must be poled at an elevated temperature with a large electric field in order to create the ordering necessary for a piezoelectric response. This poling can be accomplished transverse to the fiber axis, thus creating a transverse electric field fiber sensor. The polymer employed is polyvinylidene fluoride.

The configuration of an electric field sensor using this concept is shown in Figure 2-8. Optimum performance would require a Mach Zender interferometer to be built using single mode fiber, in which case fiber lengths up to the order of 1 km can be used. However, a different approach may have some potential. If the two legs of the interferometer are sufficiently short, and can be adjusted closely enough to the same length, that is, within a wavelength or so, then incoherent illumination and multimode fibers may suffice. A second possibility is to use the same fiber for both arms of the interferometer, that is, to sense polarimetrically as in Figure 2-7a. Further investigation would be necessary to determine whether these possibilities are practical.

The output of the device would be of the form

$$I = I_0 \sin^2 \frac{\theta - \theta_0}{2} \quad (2.5.7)$$

typical of interference. Again, I and I_0 are the transmitted and incident light intensities, θ is the induced optical phase change, and θ_0 is a fixed retardation built into the interferometer. The quantity θ depends linearly on applied field. Values of $d\theta/dE$ in the order of 2×10^{-5} radians per volt per meter of fiber have been reported [2-39]. If we (rather arbitrarily) say that a θ of 10^{-2} rad is easily detectable, we conclude that a sensitivity to field of the order of 1 V/cm is achievable with a 1-m-fiber length.

The sensor response is frequency dependent because of mechanical resonance in the fiber-jacket system. These resonances are in the MHz range.

Stability of the jacket properties over long periods or temperature extremes are not known at this time, nor is the low-frequency roll-off expected from residual conductivity in the coating known. Nevertheless, this technique appears to have promise because of the small size and simplicity of the sensing element, and merits further investigation.

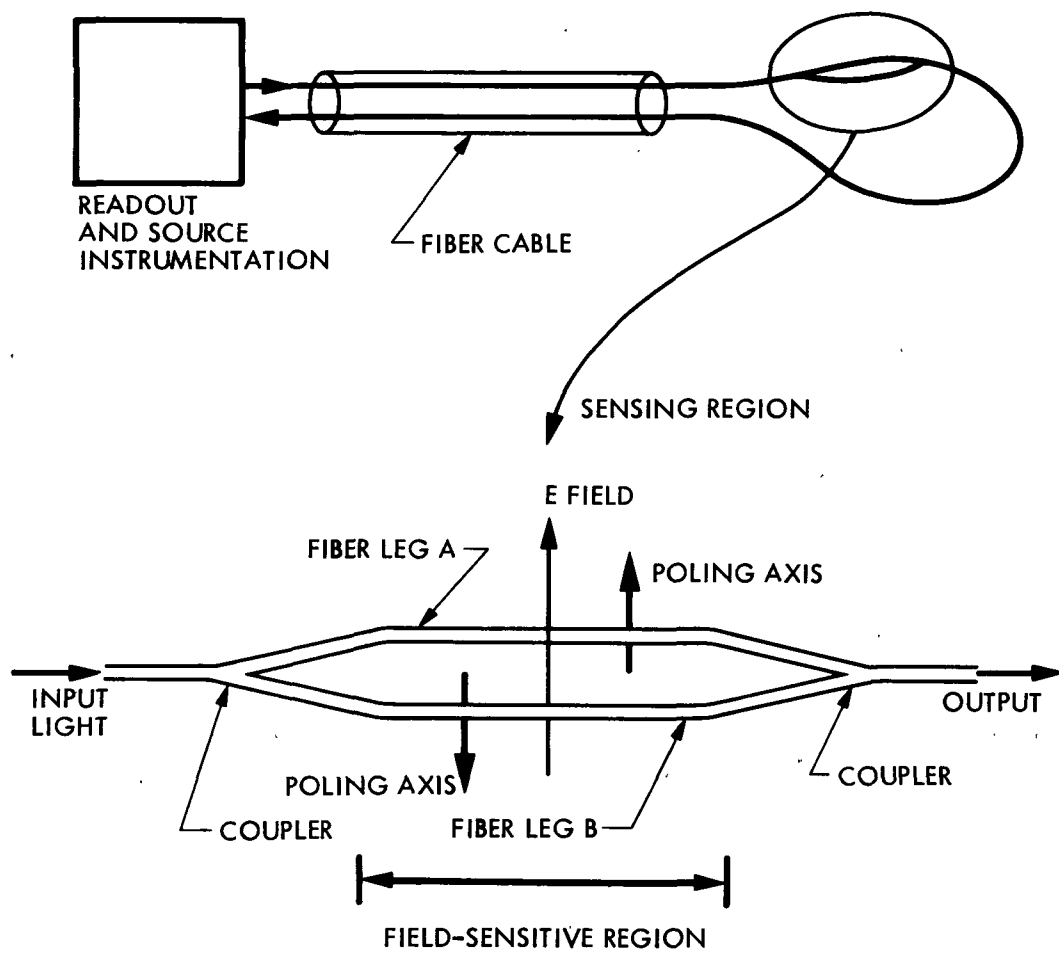


Figure 2-8. An electric field sensor based on piezoelectric-jacketed fibers

2.5.4 Fused Silica Electrometer

Techniques for detection of electric charge and thus electric field using an electroscopes fabricated from fused silica fibers have been known for many years. The possibility of combining optical fibers, also fabricated from fused silica, into a fiber electroscopes structure in order to make possible remote optical readout, has not been explored previously. The classical electrometer techniques have been discussed by Neher [2-40]. More recently, experimental work using fiber electroscopes was reported by Neher [2-41] and by Russell and co-workers [2-42]. An electroscopes is essentially a delicate force balance capable of measuring the electrostatic force associated with the charge induced on the sensor fibers. Many forms have been conceived, and the most sensitive can measure potential differences of less than one volt.

Initial ideas for implementing a fused silica electrometer integral with a fiber readout have been investigated as part of this task, and will be reported in greater detail at a later time. One such concept is shown in Figure 2-9. Suitable lengths of conductively coated fiber are mounted parallel and close together, with one end free so that a field will tend to force them apart, much as the leaves in a gold-leaf electrometer. Suitable optical coupling returns light emitted from the end of one of the fibers into the free end of the other, and the alignment is adjusted to return a maximum in the undeflected fiber position. When the cantilevered fibers deflect under electrostatic force, the optical coupling is degraded, resulting in a field-dependent transmission for the sensing device. It is necessary to enclose the fibers between a pair of electrodes in order to decouple the fibers from ground potential. This decreases sensitivity to self-charging.

We have obtained a preliminary optical transfer curve for such a sensor, measured as a function of a dc voltage directly applied between the electrodes, in Figure 2-10.

It is clearly possible to make such a device very small, of the order of 1 cm in overall size and, if carefully constructed, it would be durable and permanently stable. Initial study of the design parameters which could be varied indicates that an optimized instrument with a field sensitivity of a few volts per cm should be possible.

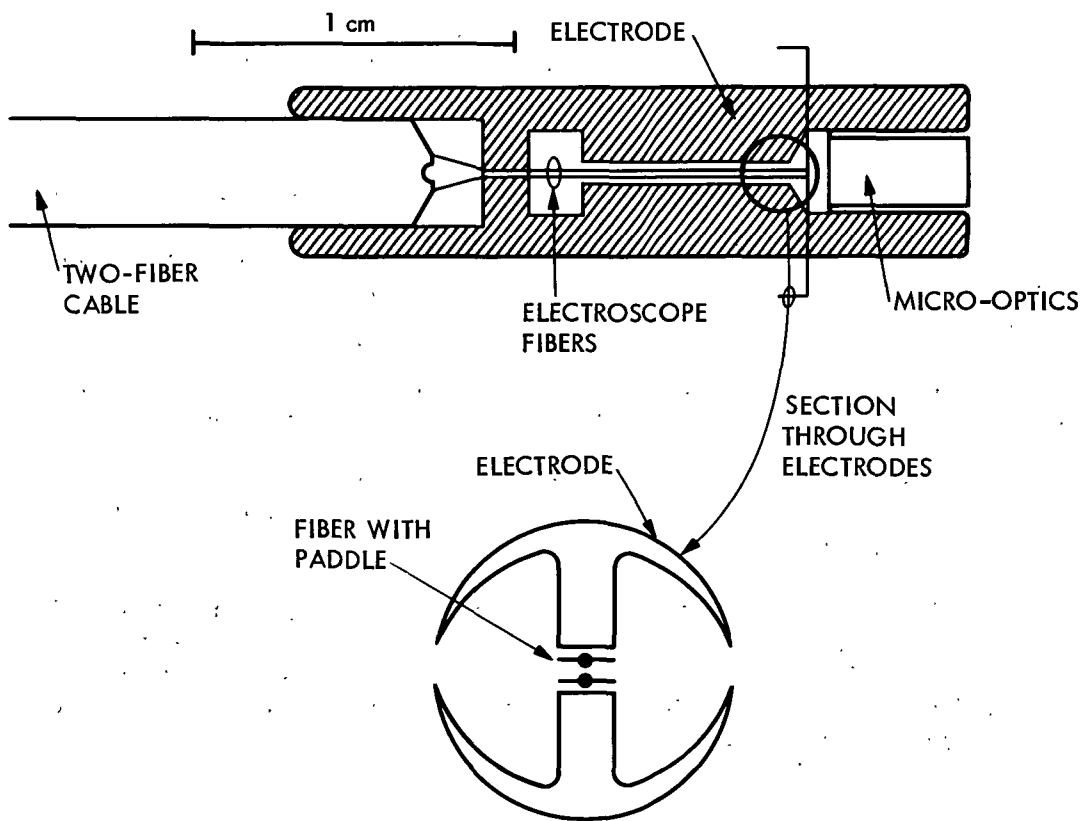


Figure 2-9. A concept for implementing a fused silica fiber electroscopes with integral optical fiber readout

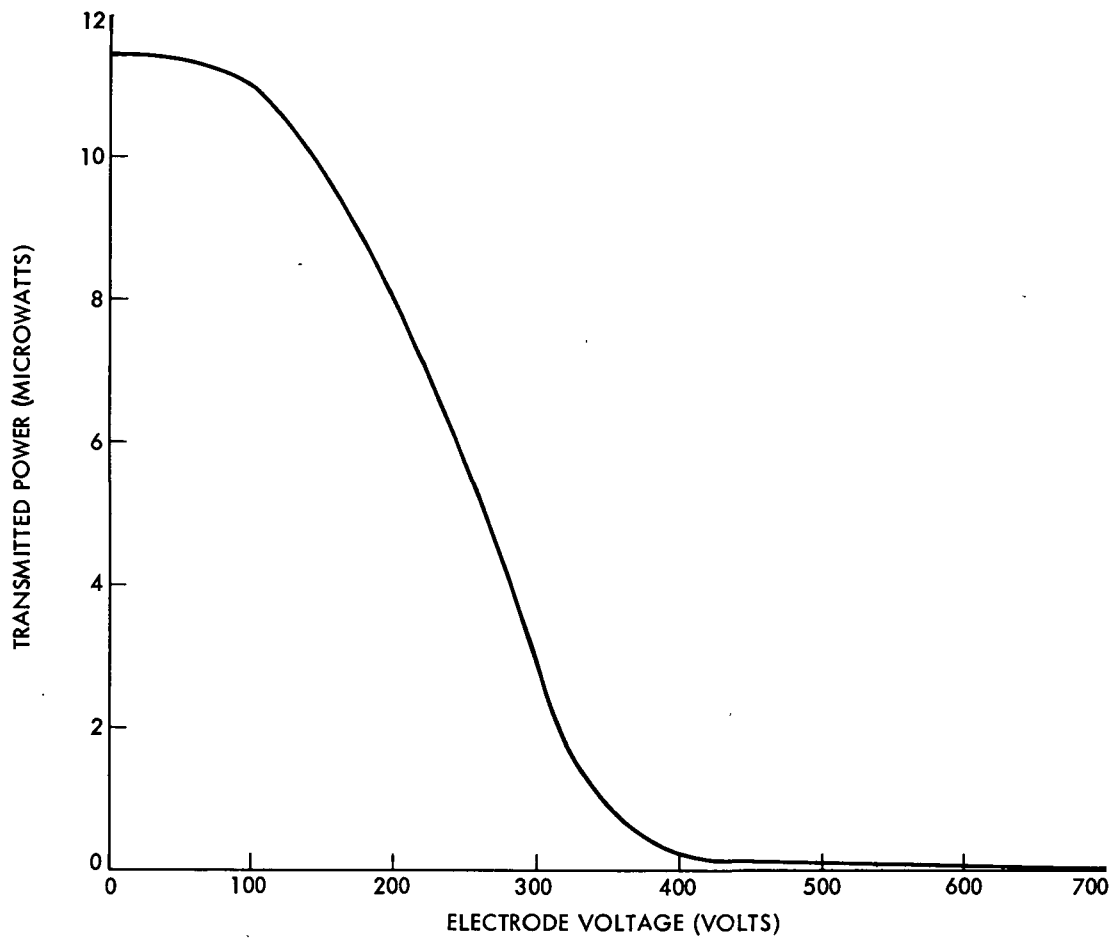


Figure 2-10. Transmitted light intensity for fiber electrometer as a function of directly applied voltage

2.5.5 Other Optical Techniques

In our judgment, the techniques described above are the most promising, but they are by no means the only possibilities. Some other techniques are described below.

2.5.5.1 Membrane Force Balance. If a parallel plate capacitor is made from two thin conductively coated membranes, as shown in Figure 2-11, the membranes will be deflected apart if placed in a field normal to the membranes. The two films are electrically connected in order to drain off the compensating charge from the inner surfaces.

The amount of relative deflection of the membranes can be measured interferometrically, using, for example, a single fiber and graded index lens, as shown in the figure. Other readout geometries could be devised to move the optical elements away from the space near the membranes.

The deflection of the membrane in a field E can be roughly estimated using information given by Dimeff and Lane [2-43] as

$$a = \frac{0.146 \epsilon V E^2}{8\sigma f^2} \quad (2.5.8)$$

where a is the desired deflection, in meters, σ is the area density of the membrane (assumed to be .02 kg/m²), and f is the undamped fundamental frequency of the membrane (assumed 10 Hz). With these numbers, the membrane deflection in a field of 1 V/cm is of the order of a tenth of a fringe, a small but easily detectable deflection. If the membranes are mounted in such a way that they are open and exposed to the field, no relaxation can occur at low frequency. Although undoubtedly fragile, the device would retain full sensitivity to dc. Its response would be quadratic in electrical field, a characteristic of the induced electrostatic force, and unfortunately it would respond to self-charging.

On balance, it appears that the drawbacks of this concept outweigh the advantages. A clear advantage is dc response, but the need for an interferometer readout, the unknown stability of the membrane tension, the response to self-charging and an expected lack of durability are all disadvantages. We will not discuss this concept further.

2.5.5.2 All-Dielectric Force Balance. A field sensor can be constructed solely from dielectric materials, thus eliminating the risk of breakdown at the sharp edges of electrodes in very high fields. One such concept involves taking advantage of the internal polarization induced by the unknown field in a dielectric in order to generate a measurable force. An example of a sensor configuration is shown in Figure 2-12. A dielectric plate is mounted on a torsion suspension so that it can rotate. A cleaved mica sheet of suitable size may serve as the plate, and suitable passive optical means, not shown, could read out the deflection. The component of applied field normal to the

plate E_{on} would yield an electric displacement D_n in the plate equal to that outside, so

$$E_n = (1/K)E_{on} \quad (2.5.9)$$

where E_n is the normal component of field in the plate and K is its dielectric constant. Conversely, the component of field parallel to the plate E_{op} will be equal inside and outside.

$$E_p = E_{op} \quad (2.5.10)$$

Since energy density in an electric field is

$$W = \frac{1}{2} K \epsilon_o E^2 = \frac{1}{2} K \epsilon_o (E_n^2 + E_p^2) \quad (2.5.11)$$

and identifying E_{on} and E_{op} as components of an applied uniform external field, with angle θ between field and the plane of the plate, we obtain

$$W = \frac{1}{2} K \epsilon_o E_o^2 \left(\frac{1}{K} \sin^2 \theta + \cos^2 \theta \right) \quad (2.5.12)$$

The torque is therefore

$$T = V \frac{dW}{d\theta} = \epsilon_o V E_o^2 (K-1) \frac{\sin 2\theta}{2} \quad (2.5.13)$$

V is the total volume of the dielectric plate.

Therefore the torque is a maximum when the field is at 45° to the plate, and is again proportional to E^2 . An electrostatic force balance could be based on this concept, but it would be delicate, and would remain inherently nonlinear. These characteristics may not be a significant penalty in an application involving very high fields where breakdown becomes extremely critical at any point where field intensification occurs.

A more robust geometry would need to be devised to yield a practical sensing device. Further investigation is not contemplated at this time. This concept is felt to be important only for the specialized type of application where very high fields are involved.

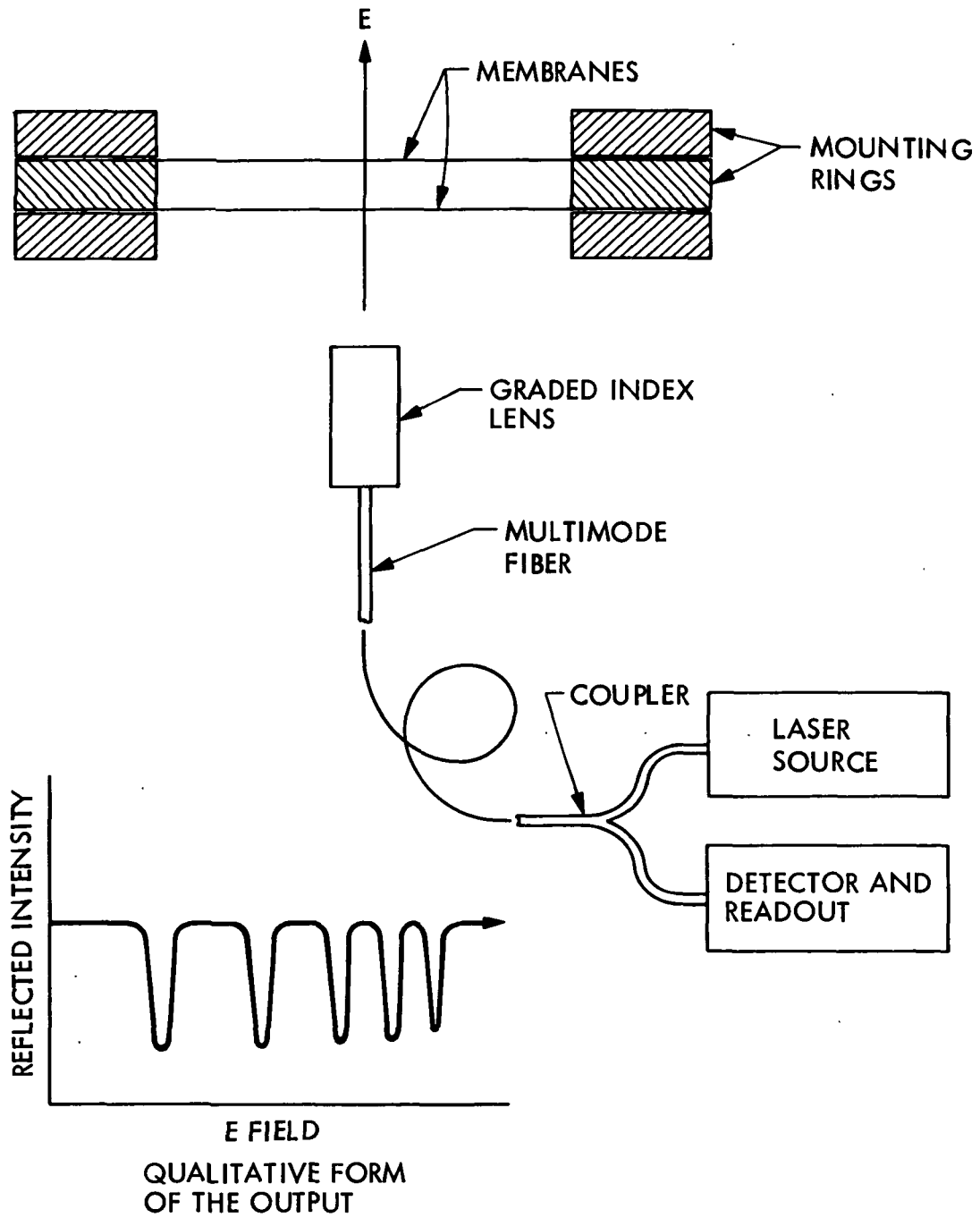


Figure 2-11. A concept for field sensing using deflection of thin membranes;

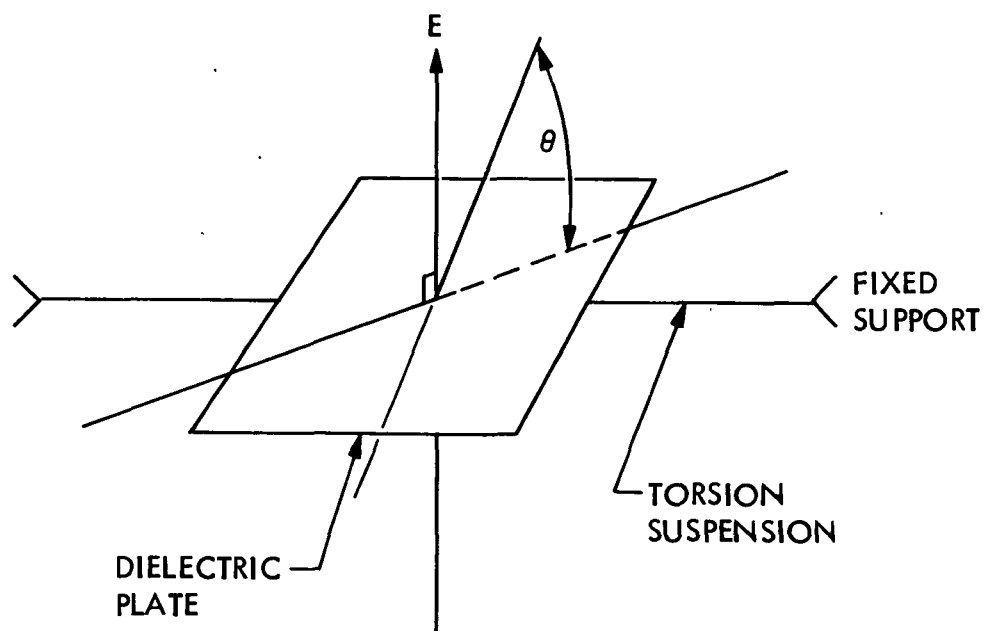


Figure 2-12. An all-dielectric torsion balance for field measurements

2.5.5.3 Stark Effect. The use of the Stark effect at visible light wavelength in an ion beam to measure an electric field has been described by Rebhan et al. [2-44]. The ion-beam technique was used as a plasma diagnostic tool, where electric field fluctuations occurring in a plasma in the microwave frequency domain were of interest. The Stark spectral shift in the visible region is very small, but a field of 400 V/cm could be detected. Unfortunately, this technique appears to be too complex to be of interest as a power-system sensor.

The Stark effect on microwave frequency transitions in a gas is treated by Townes and Schawlow [2-45]. The relative Stark shift on a spectral line at microwave frequencies is proportionately greater, and it is possible in principle to guide microwaves on dielectric (an oversized fiber) waveguides [2-46]. However, a sensor based on Stark effect still looks like it would require a complex development effort to evaluate it, and will not be treated further.

2.5.5.4 Gas Breakdown. Some years ago it was observed that a fluorescent light bulb would emit light when it was held in the air, near a transmission line. One opponent of high-voltage lines used this as evidence of some kind of 'leakage' of electricity from the line [2-47]. In fact, it seems likely that the light is due to the normal fluorescence of the coating of the tube, stimulated in the normal way by excited mercury ions in the gas in the bulb. The ions are excited by the electric field.

In a demonstration of this effect at the Jet Propulsion Laboratory in 1983, the central portion of an ordinary 40-W light was stressed by a 60-Hz field. In a darkened room, light was visible in fields as low as about 1 kV/m. The demonstration showed that an essentially non-metallic sensor could be made. Unfortunately our subsequent efforts to pinch off a section of the tube by melting the glass did not meet with success. The work will continue in 1984.

Another gaseous non-directional sensor using the breakdown of neon gas has been reported, but this method appears to require fields greater than about 10 kV/m [2-48].

2.6 ELECTRONIC SENSING TECHNIQUES WITH FIBER READOUT

An alternative to direct optical readout is the use of a miniaturized electronic sensor to measure the ambient E-field and an optical fiber link to transfer the data from the sensor down to a readout position at ground potential. The concept is illustrated schematically in Figure 2-13. The electronic sensor could be implemented in a number of ways, the common denominator being some form of electrical signal output. Power for the sensing element can be from a self-contained battery or might be transferred to it optically, as described in Section 4 of this report. Assuming that the output signal is analog, it can be encoded and transmitted in pulse form to a receiver decoder circuit at the observing position. Results from power system experiments based on this general concept have been reported [2-49].

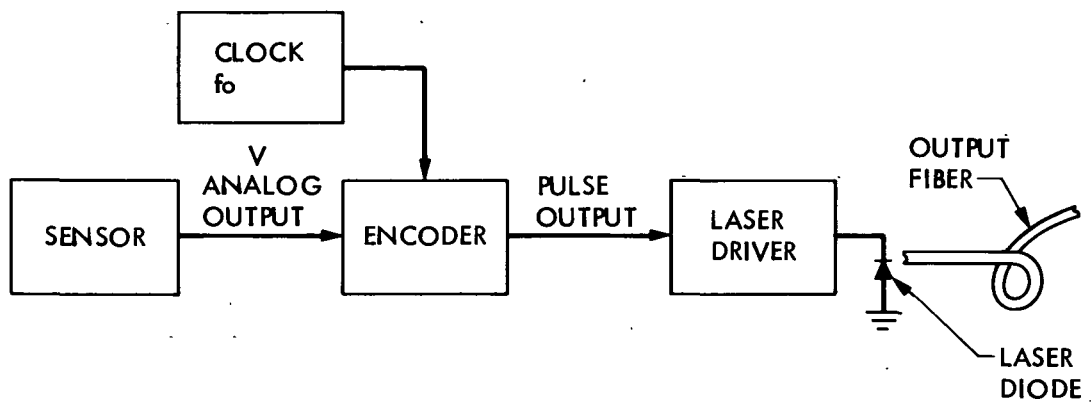
2.6.1 The Influence of Microelectronics--Microtransducer Technology

Although the use of an electronic sensor with optical-fiber readout is not new, the full potential of today's microcircuit technology has not yet been applied. Particularly in the area of electric field measurement, where it is important to disturb the field as little as possible by the measuring device, the potential for miniaturization of the sensing device appears very attractive. Several features of today's microcircuit technology could have an impact:

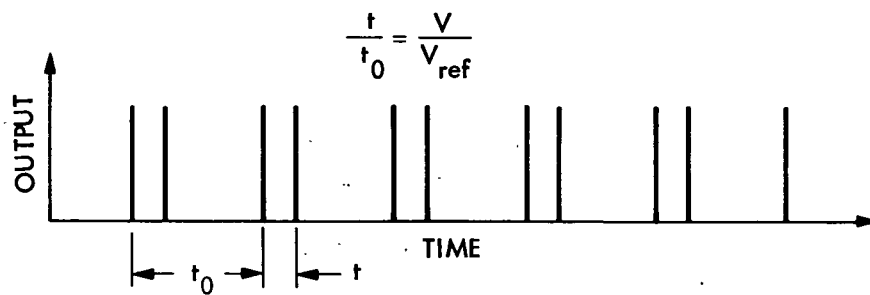
2.6.1.1 Miniaturization. Any electronic complexity likely to be required in the sensing device can be placed on one silicon chip, so that overall device size can easily be much less than 1 cm^3 . Electronic wristwatches provide an example familiar to everyone of the type of self-contained miniaturization that can be achieved.

2.6.1.2 Low-Power Circuits. CMOS (Complementary Metal Oxide Silicon) circuitry can handle frequencies up to the order of 2 Mhz, and may be powered by a tiny battery for periods of the order of a year. By careful design and the use, for example, of pulse-position modulation, the fiber optic transmitter can also be made compatible with typical CMOS power levels.

2.6.1.3 Custom Integration. Techniques are being developed for practical and cost-effective implementation of LSI or VLSI (Large or Very Large Scale Integration) in small quantities, from 10 to 100 units [2-50]. It is no longer necessary to build millions of units in order to take advantage of microcircuitry.



a) FUNCTIONAL BLOCK DIAGRAM



b) OUTPUT PULSE FORMAT; PULSE POSITION MODULATION

Figure 2-13. Functional diagram of a representative electronic sensor-fiber readout field measurement system

2.6.1.4 Mechanical Device Fabrication. Recent reviews [2-51] discuss a new dimension to microcircuit fabrication techniques, namely, the adaptation of the highly reproducible and precise photolithography and etching processes to fabrication of mechanical devices. The sensing electrodes and associated structures of a field sensor could perhaps be implemented in this way.

The process of bringing these capabilities together to bear fully on the problem of sensing in power systems is a considerable challenge, but the potential seems obvious. Two possible sensor implementations, an electrometer amplifier and a vibrating membrane, will be outlined below in order to stimulate further thought in this direction.

2.6.2 Power Considerations For Microcircuit Fiber Transmitter

The fiber optic encoder-transmitter block shown in Figure 2-13 could be a major element of the sensor package in terms of its battery-power requirements [2-52]. To demonstrate that the power drain is not necessarily excessive, a possible implementation will be described. An encoding chip could be based on a current source whose magnitude is proportional to the sensor output, arranged to charge a capacitor to a reference voltage, thus creating a time interval proportional to the sensor output. With appropriate clocking and logic, a pulse-position encoder can thus be created. The second element, the laser driver, generates a very short current pulse with timing set up by the encoder. Using an unbiased single-mode laser as the transmitter in order to achieve maximum coupling efficiency into the readout fiber, and assuming the following numbers:

Peak coupled light power in pulse	10 mw
Pulse width	~100 ps
Pulse peak current	50 ma. into ~50Ω
Pulses transmitted per sample	2
Sampling frequency	10^3 sec^{-1}

one can derive that the required average power drawn from the source (battery) specifically for the laser would be considerably less than 1 μwatt. We conclude that laser drive power need not dominate, and therefore past experience with CMOS logic circuits should be a valid guide to the battery requirements of a combined sensor and fiber optic transmitter.

2.6.3 Electrometer Amplifier E-Field Sensor

As pointed out in Section 2.3, an electrometer amplifier is simply a special-purpose high-input impedance amplifier designed to measure small electric current or charge. Vacuum-tube instruments of this type have been available for many years, and can reach a threshold of approximately 10^{-15} A with optimum design [2-53]. Vibrating reed or other forms of electrometers with modulated input capacitance are well developed and are capable of detecting a few electronic charge units [2-54], which corresponds to a current in the range of 10^{-18} A, depending on the response time of the instrument (typically 0.1 sec.) The vibrating reed instrument has good long-term stability. However, neither of these instrument types has been packaged in the desired 1-cm cube, nor does it appear likely to ever be done. More recently,

specialized CMOS circuits have been built that are capable of detecting 10^{-14} A with a drift of approximately 10^{-15} A/hr [2-55]. Current sensitivity of 10^{-13} A has been reported with a somewhat different approach by Smith [2-56].

The electrostatically induced current I in a parallel plate capacitor placed normal to a uniform and sinusoidally varying field E is given by

$$I = 2\pi f \epsilon_0 A E \quad (2.6.1)$$

where f is the frequency of the external ac field, ϵ_0 is the free-space permittivity, and A is the area of the plate. If the sensing plate is assumed to be 1 cm^2 in area and $f = 60 \text{ hz}$, then the peak induced current is 10^{-11} A for a peak field strength of 1 V/cm .

Therefore, an ac field of the order of 1 V/cm or greater can easily be measured with a CMOS-based electrometer circuit. A truly miniaturized E-field sensor based on such a concept has not been attempted, and it is felt that further investigation of this concept is worthwhile.

2.6.4 The Electret

2.6.4.1 Background. Electret transducers are becoming quite common, several million electret microphones being sold every year. Our potential application as an E-field sensor is somewhat different, and it is worthwhile to review the topic before proceeding with a discussion of an electret field sensor.

An electret is basically an insulating material with a trapped charge. It seems logical that such a device could be made into a sensor for electric field — after all, the very definition of electric-field strength has to do with mechanical forces on a point charge inserted into the field. The term 'electret' was first suggested by Oliver Heaviside in 1892 to denote the electrostatic analog of a magnet, that is to say, a dielectric solid with a permanent electric moment [2-57]. It was about a quarter of a century before an electret was actually made, by the Japanese physicist Mototaro Eguchi [2-58]. Eguchi made electrets by allowing a mixture of wax and resin to cool in a strong electric field. The frozen mixture exhibited internal electric polarization even after the field was removed. The direction of the internal charge was such that the end originally facing the anode was negative and the end facing the cathode positive. This type of charge was later named 'heterocharge' [2-59]. In many electrets, the heterocharge gradually decays and a charge of opposite polarity ('homocharge') remains.

In 1937 another kind of electret was discovered, the effect being due to the simultaneous application of an electric field and light [2-60]. To differentiate this kind of electret from Eguchi's, the term 'thermoelectret' is sometimes used to denote an electret formed by the field-and-heat process, and 'photoelectret' denotes the field-and-light process.

Other methods of preparing electrets have subsequently been discovered, for example, electron bombardment using non-penetrating electron beams [2-61], application of an electric field during the period in which the solvent is evaporating from a dissolved dielectric, and application of a field during dielectric polymerization [2-62].

Although work still must be done to elucidate all the mechanism responsible for the behavior of electrets, very stable electrets can now routinely be made. (See the 'Report on the Electret Conference' in reference [2-61] for discussion of remaining theoretical problems.) Many practical devices use foil electrets (usually Teflon or polytetrafluoroethylene) metallized on one side. The remainder of this discussion will assume the use of such an electret.

To see how such a device might be used to measure electric field, consider the electret in Figure 2-14 which shows an electret microphone. A sound wave arriving at the microphone will cause a difference to exist in the air pressure on either side of the diaphragm. Just how this pressure difference is related to the incoming wave depends on the design of the air passages connecting the front and back of the diaphragm, and will determine the frequency response, the directional pattern, and the noise-canceling properties of the microphone.

Since the metallization on the front surface of the electret forms a capacitor in which the other plate is the microphone back plate, the motion of the diaphragm modulates the capacitance. Since the electret fixes the charge on the capacitor, it follows that the voltage between the plates must vary in response to the sound wave. The voltage may be sensed with a high-impedance amplifier. Typically an FET buffer-amplifier is installed in the electret microphone, and an output at lower impedance is used.

The output voltage will depend on the electret charge and the change in capacitance. For a given sound wave, the change in capacitance will depend upon the size of the diaphragm and the stiffness of the dielectric.

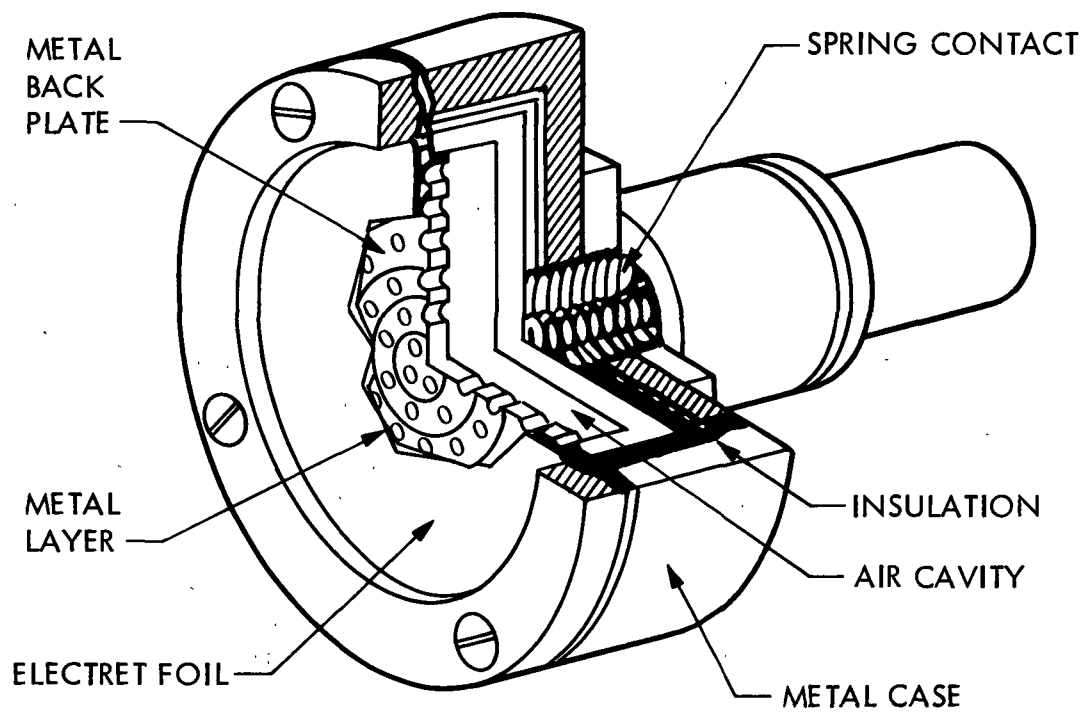


Figure 2-14. Cutaway view of electret microphone

2.6.4.2 Use as an E Field Meter. The entire device can also be made to operate 'in reverse'. If a voltage is applied between the backplate and the metallization, the diaphragm will move, the steady-state position being determined by the stiffness of the foil and the charge on the electret, as well as its capacitance. This movement could be measured and used as an indication of the field strength or applied voltage. To gain an impression of the amount of motion that may be expected, published data may be used. Warren et al. [2-63] indicate that the center of a circular electret made of polythene 38 μm thick, $\epsilon = 2.2$, over a 140 μm air gap was 700×10^{-6} inch (18 μm) with an applied voltage of 500 V. The membrane radius was 0.833 cm and its tension was 0.63×10^5 dyn/cm. If we assume the field in the air gap is solely that due to the applied voltage, the intensity is of the order of 3.5 MV/m, or, in more familiar field units, 35 kV/cm. This is a very high value of field intensity — above the value for the breakdown strength of air.

2.6.4.3 Suitability of Electret as Field Measuring Device. Electrets have found wide application as high-quality microphones. The availability of low-cost suitable dielectrics and field-effect transistors has made possible the use of devices of such inherently high impedance. As microphones, electrets have two important advantages: they are extremely low mass and they provide high output voltage. The first factor means that they can be made to have excellent frequency-response characteristics. The second factor means that a simple source-follower amplifier can be used to provide a high-level low-impedance signal source, capable of driving long cables.

The large signal-voltage output from a electret microphone is a clue to the fact that, as an electrical-to-mechanical transducer, the device requires a high voltage. A sensitive microphone makes an insensitive field meter.

A sensor using an electret to measure electric-field strength might be constructed somewhat similarly to a microphone. The material strengths and the electret charge density largely fix the dimensions. If this were the case, the field to be measured would have to be intensified considerably for the measurement, and this would necessarily distort the field. Assuming that the distorted region can be kept physically small enough, there remains only the problem of measuring (optically) the small membrane movements produced. This should be relatively straightforward — it was shown in Section 2.5 that there are ways to measure deflections on the order of the diameter of an optical fiber without resorting to interferometry.

Alternative implementations may offer some improvements. First, it might be possible to use the fiber as a structural material on which to mount an electret. The electret could then be rectangular (or any other shape) and might be cantilevered from a single point of suspension, rather than fixed all around the edge.

2.6.5 Vibrating Plate Electrometer

It would appear that a parallel-plate capacitor in which the plates are mechanically vibrated would function as an electric field sensor with dc response. Devices based on this concept are commercially available [2-9]. Somewhat surprisingly, a brief analysis indicates that such a device would not work.

Suppose that the plate is located flush with the ground, but isolated from it, in an electric field of strength E . The charge on the upper surface of the plate is then simply

$$Q_1 = \epsilon_0 EA \quad (2.6.2)$$

where A is the area of the plate. If the plate is separated from the ground by some small distance d (in practice the ground under the plate is the device housing), the charge on the lower surface of the plate is given by

$$Q_2 = \epsilon_0 \frac{V}{d} A \quad (2.6.3)$$

where V is the voltage on the plate. The spacing d may be assumed to vary sinusoidally $d = d_0 + d_1 \cos \omega t$. If the plate is connected to an amplifier with finite input resistance R , the two charges Q_1 and Q_2 need not be equal and opposite. A current can flow in the external circuit, given by

$$i = \frac{d}{dt}(Q_1 + Q_2) = \frac{V}{R} \quad (2.6.4)$$

Substituting

$$\frac{d}{dt}(\epsilon_0 EA) + \frac{d}{dt}\left(\frac{\epsilon_0 VA}{d}\right) = \frac{V}{R} \quad (2.6.5)$$

Since the first term is not time-dependent, (2.6.5) reduces to

$$\epsilon_0 A \frac{d}{dt} \left(\frac{V}{d}\right) = \frac{V}{R} \quad (2.6.6)$$

Note that the external field E does not appear in Equation (2.6.6), except implicitly as an initial condition if E is applied as a step function at time $t = 0$. The voltage V appears to decay exponentially to zero, so that eventually the device output becomes zero.

In other words, the charge on the inside of the device eventually vanishes, so that the vibration of the plate does not modulate the voltage between the plate and its housing. This voltage is zero.

Clearly, the analysis is too simple for, as we mentioned earlier, devices based on this principle are available. In fact, two simplifying assumptions were made. First, it was assumed that there were no fringing effects. This can only be true for a fixed geometry — as soon as the plate moves, the local field will be disturbed. To put it another way, the upper surface of the plate must have a capacitance to the housing of the device, and since there is a charge on the upper surface, modulating that capacitance will result in a current flow (displacement current). Second, it was assumed that the external field E was constant. In fact, as the plate moves, the capacitance between the plate and the high-voltage line (or the other plate of the external capacitor) will be modulated. Since the separation of the plates of this external capacitor is many meters and the plate vibrates only a millimeter or so, the capacitance will not change much, and the displacement current will be small. The fringing effects may predominate, but it would be extremely difficult to calculate their magnitude.

2.6.6 Other Electronic Field Sensor Concepts

A unique approach for electric-field sensing has been described by Lorne and Harrison [2-64]. This concept involves the use of a low-energy ion beam which is exposed to the unknown field. Presumably, an electron beam could also be used. A sensitivity of 3.5 V/cm was reported for the ion beam device, which depended on deflection of a thermal cesium ion beam by the unknown field. Unfortunately, both the size (25 cm long) and power requirement (5 W) of this device rule it out for our application, and it is not clear to what extent these numbers can be decreased. An electron beam requires an energy-consuming cathode for its generation, and therefore suffers a similar disadvantage.

2.7 SUMMARY AND CONCLUSIONS

In Section Two we have examined the use of optical fibers for sensing in power-system applications. Many of the well-known features of fiber optics are of value in extracting information from sensors, and, in particular, their lack of coupling with ambient electromagnetic fields is important.

In addition, the optical fibers themselves can be tailored to be sensitive sensing elements for certain parameters, including pressure, temperature, and electric and magnetic field. In the high-voltage environment around transmission lines or substations, the dielectric fiber cable can be an extremely important tool for reading out devices placed at high potential away from the ground plane.

In the past ten years, a great deal of research and development effort has been directed toward the use of fiber optics for data transmission, and the field is now well on its way toward being the billion-dollar-a-year industry that has been forecast. Research and development continues, of course, tending recently to emphasize single-mode, long-wavelength (1.3 μm or 1.5 μm) techniques. As a result of this effort, a wide range of optical components analogous to the familiar lenses, mirrors, and beam splitters has been developed for use in fiber systems. There is nearly a one-to-one correspondence between bulk optical components and functionally equivalent ones for fiber systems. Some valid analogies also exist between the optical-waveguide (fiber optics) world, and the microwave waveguide world. For example, an optical coupler, though functionally equivalent to an optical beam splitter, looks much more like a microwave directional coupler. Commercial availability of these components varies, with multimode connectors, couplers, and sources being widely available, while single-mode couplers and connectors are just now becoming available. Single-mode long-wavelength sources, though they can be obtained commercially, are still an active area of research.

It is recognized that techniques for sensing the important power-system parameters already exist, and that these measurements are made routinely in all systems. Therefore, new approaches, using optics or not, must be cheaper or better than the instrumentation they replace, or they must enable a new and useful measurement which could not previously be made.

We have focused our attention on electric-field sensing, which is of interest in three different areas:

1) Monitoring of Biological Effects

Electric-field measurement is needed in experiments involving investigation of possible biological effects in the neighborhood of high-voltage transmission lines. Measurement of field with minimum distortion of the field is important.

2) Field Mapping

Field mapping in three dimensions—for example, in a substation—is a difficult experimental problem to which optical-fiber techniques

may be able to make a significant contribution because of their dielectric properties.

3) Voltage Measurement

Voltage measurement, especially in areas of high field, also benefit from techniques which can completely avoid the use of metal conductors.

Prior work has been reviewed in this section, but we have also sought to identify new approaches and have examined a number of sensor concepts in enough detail to compare them to anticipated requirements. Electro-optic and magneto-optic techniques using bulk sensing crystals and either free-space optical or optical-fiber readout have been adequately explored, and they do work. The application addressed has been that of providing an optical equivalent of a voltage transformer (VT) and current transformer (CT). We have provided a fairly comprehensive bibliography of this work but our analysis has concentrated on only a few of the new concepts.

At this point, our investigation has identified four concepts which are felt to be promising. Preliminary experimental work has been done at JPL on the first two.

1) Optical-Fiber Electroscope

This concept involves the adaptation of classical electroscope techniques for optical-fiber readout. A feasibility breadboard was built in our laboratory to test the concept and some preliminary experiments were done. The concept is simple and, clearly, a very small monolithic robust device can be built, although specialized techniques are necessary.

The significant development area required to turn it into a producible device is related to fabrication techniques. Evaluation of accuracy and performance has not yet been done. The concept is capable of adequate sensitivity, the ultimate limit seen as being due to sensitivity to acceleration or vibration. The desired full-scale range would be permanently built into the sensing device. Scaling of its sensitivity over a wide range would be accomplished by providing a number of sensing heads.

2) Gas Breakdown

In the low-pressure environment inside the glass tube of a fluorescent light, mercury ions can be accelerated by an externally applied electric field to sufficient velocity to cause some ionization. The excited mercury ions release photons of ultraviolet light, which is converted to visible wavelengths by the coating on the tube. The effect has been observed in fields as low as 1 kV/m.

To make a practical field meter using this concept, it will be necessary to produce a container entirely free of metal parts. It will also probably be fruitful to investigate the question of gas pressures inside the container, and whether it would be more efficient to measure the U.V. directly or to convert to visible first.

3) Piezoelectric Fiber Coating

Techniques have been reported in the literature for coating a fiber with a piezoelectric polymer, thereby making it sensitive to electric field. This idea is attractive because the sensing element proper is only a short section of specially prepared fiber or, more likely, two parallel fibers, perhaps the simplest possible sensing element mechanically, and also the smallest, at least in two of its three dimensions. The estimated sensitivity can be very high using sensing-fiber lengths of a meter or more. Nothing is known at this time about the short- and long-term stability and hysteresis properties of the coating material.

4) Electrometer with Fiber Readout

Existing microelectronics technology makes it possible to construct a very small capacitive pickup and electrometer amplifier having considerably better than the required sensitivity. The electronics required for a fiber-optic readout can in principle also be incorporated in the miniaturized package. The complete device need not require excessive power. The development required to yield a field-deployable instrument would be primarily directed at packaging the electronics, and would involve in an intimate way the modern microelectronics technology.

One of the current areas of interest is related to HVDC transmission lines, which implies a need to measure dc fields. It should be recognized that a dc sensor is almost certainly going to be a fundamentally different device than an ac sensor. An ac sensor needs to have no moving parts, and can in principle be enclosed in a protective dielectric shell to make an easily handled package. A corresponding dc sensing element must be fully exposed, and almost certainly will contain a chopping or modulating element in addition. Field use of such a device when exposed to the weather will therefore require adherence to careful procedures and constraints. Development of a non-fragile field-packaged and miniaturized dc sensor concept would be a valuable contribution.

We feel that the presence of ion current, which in turn can result in space charge and self-charging of the sensor, are fundamental issues which can have an important effect on the accuracy of electric-field measurement. It is important to take these factors into account, both in the design of the sensor and in its use in order to obtain accurate measurements. It is also important to recognize that a net space charge, if present, can modify the field according to Poisson's equation. The magnitude of the space-charge field and self-charging of the sensor are not known. A simple analysis shows that ion current can be a large error source.

We feel that future work should focus on developing a sensor design capable of the desired size, robustness, and accuracy. In addition, analytical and, as far as possible, experimental work aimed at understanding the effects of space charge and ion current should be included as part of the sensor development in order to minimize error from these effects.

2.8 REFERENCES

- 2-1 IEEE Microwave Radio Subcommittee and the Research Subcommittee of the Power-System Communications Committee, 'Fiber-Optic Applications in Electrical Substations,' Paper No. 83 WM 025-4 presented at the IEEE PES 1983 Winter Meeting, New York, New York, January 30-February 4, 1983,
- 2-2 a) Malewski R., 'High-Voltage Current Transformers with Optical-Signal Transmission,' Opt. Eng. Vol. 20 (1), p. 54 (1981).
- b) Papp A. and Harms H., 'Magneto-optical Current Transformer,' Appl. Opt. Vol. 19 (22), p. 3729 (1980).
- c) Rogers A. J., 'Optical Technique for Measurement of Current at High Voltage,' Proc. IEEE Vol. 120 (2), p. 261 (1973).
- d) T. Yoshino T. and Y. Ohno, 'Highly Sensitive All-Optical Method for Measuring Magnetic Fields,' Fiber and Integrated Optics Vol. 3 (4), p. 391 (1981).
- 2-3 a) Giallorenzi T. G., Bucaro J. A., Dandridge A., Sigel G. H. Jr., Cole, H., Rashleigh S. C., and Priest R. G., 'Optical-Fiber-Sensor Technology,' IEEE J. Quant. Electr. Vol. QE-18 (4), p. 626 (1982).
- b) Giallorenzi T. G., 'Fiber-Optic Sensors,' Optics and Laser Technology, pp. 73-78 (1981).
- 2-4 a) McCormack J. S., 'Remote Optical Measurement of Temperature Using Luminescent Materials,' Elect. Lett. Vol. 1 (3), p. 630 (1981).
- b) Gottlieb M., Brandt G. B., and Butler J., 'Measurement of Temperature with Optical Fibers,' Instru. Soc. Am., p. 457-466 (1979).
- 2-5 Rogers A. J., 'Polarization-Optical Time Domain Reflectometry: A Technique for the Measurement of Field Distributions,' Appl. Opt. Vol. 20 (86), p. 1060 (1981).
- 2-6 Fox R., 'Measurement of Peak Temperature Along an Optical Fiber,' Appl. Opt. Vol. 22, 967 (1983).
- 2-7 a) Proceedings of the 18th Annual Hanford Life Sciences Symposium at Richland, WA, October 16-18, 1978.
- b) 'Electrostatic and Electromagnetic Effects of Ultra High Voltage Transmission Lines', EPRI EL-802, 1978.
- 2-8 a) Gunn R., 'Principles of a New Portable Electrometer', Phys. Rev Vol. 40, pp. 307-12, April 15, 1932.
- b) Evans J. E. and Velkoff H. R., 'The Design, Test and Evaluation of a Miniaturized Electric Field Meter,' Interim Technical Report #13,

Contract DA-31-124-ARO-D-246, U.S. Army Research Office, Durham, NC,
Ohio State Research Foundation, July 1972.

- c) Gathman Stuart G. and Anderson Robert V., 'Improved Field Meter for Electrostatic Measurements', Rev. Sci. Instr. Vol. 36, p. 1490 (1965).
 - d) Paul J. C., 'Design and Construction of Rotating Voltmeter for the Measurement of High D.C. Voltage,' J. Phys. E: Scientific Instruments Vol. 3 p. 321 (1970).
 - e) Hammond D. P., 'A Rotating Vane Electrometer of High Sensitivity,' J. Phys E: Sci. Instr. Vol. 4, p. 97 (1971).
 - f) Mapleson W. W. and Whitlock W. S., 'Apparatus for the Accurate and Continuous Measurement of the Earth's Electric Field', Journal of Atmospheric and Terrestrial Physics, Vol. 7, pp. 61-72 (1955).
- 2-9 Comber M., Kotter R., and McNight R., 'Experimental Evaluation of Instruments for Measuring DC Transmission-Line Electric Fields and Ion Currents,' IEEE Trans. Pwr. Appar. and Syst. Vol. PAS-102, p. 3549 (1983).
- 2-10 Neher H. V., 'Electrometers and Electroscopes,' Procedures in Experimental Physics, John Strong, Ed. (Prentice Hall, 1938).
- 2-11 Train D. and Dube, R., 'Measurements of Voltage Distribution on Suspension Insulators for HVDC Transmission Lines,' paper presented at IEEE PES 1983 Winter Meeting, New York, New York, January 30-February 4, 1983.
- 2-12 Nye J. F., 'Physical Properties of Crystals,' Clarendon Press, 1957.
- 2-13 Transmission Line Reference Book, 345 kV and Above, Electric Power Research Institute, Palo Alto, CA, 1975.
- 2-14 Humphrey F. B. and Johnston A. R., 'Sensitive Automatic Torque Balance for Thin Magnetic Films,' Rev. Sci. Instr. Vol. 34, p. 348 (1963).
- 2-15 a) Comber M. G. and Johnson G. B., 'HVDC Field and Ion Effects Research at Project UHV: Results of Electric Field and Ion Current Measurements,' IEEE Trans. Power Appar. and Systems Vol. PAS-101 (7), pp. 1998-2006 (1982).
- b) Sendaula M., Hilson D. W., Myers R. C., Akens L. G., Woolery B.J., 'Analysis of Electric and Magnetic Field Measured Near TVA's 500 kV Transmission Lines,' IEEE PES Summer Meeting, Los Angeles, CA, July, 1983 (83SM 463-7).
- c) Maruvada P.S., Dallaire R. D., Heroux P., Rivest N., 'Long Term Statistical Study of the Corona Electric Field and Ion Current Performance of a 900 Kv Bipolar HVDC Transmission Line

Configuration,' IEEE PES Summer Meeting, Los Angeles, CA, July 1983 (83 SM 460-3).

- 2-16 a) Perz M. C., 'Method of Evaluating Corona Noise Generation from Measurements on Short Test Lines', IEEE Transactions on Power Apparatus and Systems, No 59, December 1963, pp. 833-844.
- b) Sforzini M., Cortina R., Sacerdote G., and Piazza R., 'Acoustic Noise Caused by AC Corona and Conductors: Results of an Experimental Investigation in the Anechoic Chamber', IEEE Transactions on Power Apparatus and Systems, Vol PAS 94, March/April 1975, pp. 591-601.
- c) Trinh N. G. and Maruvada R. D., 'A Method of Predicting the Corona Performance of Conductor Bundles Based on Cage Test Results', IEEE Transactions on Power Apparatus and Systems, Vol PAS 96, January/February 1977, pp. 312-325.
- d) Maruvada P. S., Dallaire R. D., Heroux P., and Rivest N., 'Corona Studies for Bipolar HVDC Transmission at Voltages Between ± 600 kV and ± 1200 kV, Part 2: Special Bipolar Line, Bipolar Cage and Bus Studies', IEEE Transactions on Power Apparatus and Systems, Vol PAS 100, No 3, March 1981, pp. 1462-1471.
- 2-17 a) McKnight R. H. and Kotter F. F., 'A Facility to Produce Uniform Space Charge for Evaluating Ion Measuring Instruments', IEEE Transactions on Power Apparatus and Systems, Vol PAS 102, No 7, July 1983, pp. 2349-2356.
- b) Brown S. C. and Allis W. P., 'Motions of Electrons and Ions in Gases', American Institute of Physics Handbook, McGraw-Hill, 1963.
- 2-18 Murasaki N., 'Measurement of Electrification,' Journal of Textile Machinery Society, Japan, April 1963, p. 101.
- 2-19 Lang R. and Kobayashi K., 'External Optical Feedback Effects on Semiconduction Injection Laser Properties', IEEE J. Quantum Elec., Vol. QE16, p. 347 (1980).
- 2-20 a) Marchand E. W., 'Gradient-Index Imaging Optics Today,' Appl. Optics Vol. 21, 983 (1982). See also other articles in March 15, 1982, issue.
- b) Topical Meeting on Gradient-Index Optical Imaging Systems, Technical Digest, Monterey, CA, April, 1984.
- 2-21 a) Kawasaki B. S. and Hill K. O., 'Low-Loss Access Coupler for Multimode Optical Fiber Distribution Networks,' Appl. Opt. Vol. 6, p. 1794 (1977).
- b) Technical Digest, Conference on Optical Fiber Communication, New Orleans, LA, January 1984, Optical Society of America.

- 2-22 Bergh R. A., Dignonnet M. J. F., Lefevre H. C., Newton S. A., and Shaw H. J., 'Single-Mode Fiber-Optic Components,' SPIE Proceedings Vol. 326 p. 137, January 1982.
- 2-23 Findakly T., Chen B., Booker D., 'Single Mode Integrated Optical Polarizers in LiNbO₃ and Glass Waveguides,' Opt. Lett. Vol. 8, p. 641 (1983).
- 2-24 Varnham M. P., Payne D. N., Birch R. D., and Tarbox J., Elect. Lett. Vol. 19, p. 246 (1983).
- 2-25 Shirasaki M. and Asama K., 'Compact Optical Isolator for Fibers Using Birefringent Wedges,' Appl. Optics Vol. 21, p. 4286 (1982).
- 2-26 SPIE Proceedings Vol. 326 (Fiber Optics Technology 82) pp. 37-62, SPIE, Bellingham, WN, January, 1982.
- 2-27 a) Technical Digest, Integrated and Guided Wave Optics, Asilomar, CA, Optical Society of America, January 1982.
- b) Tamir, T. Integrated Optics, Topics in Applied Physics, (Springer-Verlag, 1979), Vol. 7.
- 2-28 Garrett I., 'Receivers for Optical Fibre Communication', Wireless World, April 1982, pp. 62-65.
- 2-29 Kressel H., 'Semiconductor Devices for Optical Communication,' Topics in Applied Physics (Springer-Verlag, 1982), Vol. 39.
- 2-30 Yariv Amnon, Introduction to Optical Electronics (Holt, Reinhart and Winston, 1976).
- 2-31 Hebner R. E., Malewski R. A., and Cassidy E. C., 'Optical Methods of Electrical Measurement at H. V. Levels,' Proceedings of the IEEE Vol. 65 (11), p. 1524 (1977).
- 2-32 Hartfield E. and Thompson B. J., 'Optical Modulators,' Handbook of Optics (Optical Society of America, McGraw-Hill, 1978), pp. 13-17.
- 2-33 Kyuma K., Tai S., and Nunoshita M., 'Development of Fiber-Optic Sensing Systems—A Review,' Optics and Lasers in Engineering, 1982, pp. 155-182.
- 2-34 a) Erickson D. C., 'The Use of Fiber Optics for Communications, Measurements and Control within High-Voltage Substations,' IEEE Trans. Power App. and Syst. Vol. PAS-99 (3), p. 1057 (1980).
- b) Massey G. A., Johnston J. C., and Erickson D. D., 'Laser Sensing of Electric and Magnetic Fields for Power Transmission Applications,' SPIE Vol. 88, Polarized Light, 1976, pp. 91-96.

- c) Massey G. A., Erickson D. D., and Kadlec R. A., 'Electromagnetic Field Components: Their Measurement Using Linear Electro-Optic and Magneto-Optic Effects,' *Appl. Optics* Vol. 14 (11), p. 2712 (1975).
- 2-35 Sasano T., (translated from Japanese by D.G. Ronbushi), 'Laser CT and Laser PD for EHV Power Transmission Lines,' *Electrica Engineering in Japan*, Vol. 93 (5), p. 91 (1973).
- 2-36 Rogers A. J., 'Optical Methods for Measurement of Voltage and Current on Power Systems,' *Optics and Laser Technology*, December 1977, pp. 273-283.
- 2-37 Johnston A. R., 'Kerr Response of Nematic Liquids', *J. Appl. Phys.* Vol. 44, p. 2971 (1973).
- 2-38 Jarzynski J., 'Optical Fibers with Piezoelectric Plastic Jackets Overview of Modulator and Sensor Applications,' *SPIE* Vol. 425, Paper 15, August 1983.
- 2-39 a) Donalds L.J., French W. G., Mitchell W. C., Swinehart R. M., Wei T., 'Electric Field Sensitive Optical Fibre Using Piezoelectric Polymer Coating,' *Electronics Lett*, Vol. 18, p. 327 (1982).
- b) Wei T., Donalds L. J., Onstott J. R., and French W. G., 'Characterization of Piezoelectric Polymer Coating for Fiber Optic Sensor Applications,' Fall Meeting, American Physical Society, San Francisco, CA, November 1983.
- 2-40 Neher H. V., 'Electrometers and Electroscopes,' *Procedures in Experimental Physics*, John Strong, Ed. (Prentice Hall, 1938).
- 2-41 Neher H. V., 'An Automatic Ionization Chamber,' *Rev. Sci. Instr.* Vol. 24, p. 99 (1953).
- 2-42 Russell M. C. B., Leng J., 'An Automatic Quartz-Fibre Electrometer,' *J. Sci. Instru.* Vol. 35, p. 134, (1958).
- 2-43 Dimeff J., and Lane J. W., 'Vibrating Membrane Electrometer with High Conversion Gain,' *Revs. Sci. Instr.* Vol. 35, p. 666 (1964).
- 2-44 Rebhan V., Wiegart N., and Kunze H. , 'Measurement of Fluctuating Electric Fields by Means of High-frequency Stark Effect in a Laser-excited Lithium Beam,' *Phys. Lett.* Vol. 85A, p. 228 (1981).
- 2-45 Townes C. H., and Schawlow A. L., *Microwave Spectroscopy* (McGraw Hill, 1955, Dover 1975).
- 2-46 Cavour Yeh, private communication.
- 2-47 Young L. B., *Power over People*, Oxford University Press, New York, 1973.

- 2-48 Friedmann D. E., Curzon F. L., Feeley M., Young J. F., and Auchinleck G., 'Electric Field Meter Based on the Breakdown of Gases', *Rev. Sci. Instrum.* Vol 53, No 8, August 1982, pp. 1273-1277.
- 2-49 Brown A., and Zinkernagel J., 'Optoelectronic Electricity Meter for High Voltage Lines,' *IEEE Trans. Instr. Meas.* IM-22, p. 394 (1973).
- 2-50 Mead C. A., and Conway L. A., Introduction to VLSI Systems (Addison-Wesley, 1980).
- 2-51 a) Petersen , 'Silicon as a Mechanical Material,' *IEEE Proc.* Vol. 70, p. 420 (1983).
- b) Angell J., Terry S. C., and Barth P. W., 'Silicon Micromechanical Devices,' Scientific American, p. 44 (1983).
- 2-52 Johnston A. R., and Bergman L. A., 'Application of Fiber Optics in Spacecraft,' *Proc. SPIE*, Vol. 224, p. 74, 1980.
- 2-53 a) Dagpunar S. S., 'Electrometer Valves', Mullard Technical Communications, No. 66, p. 194, August, 1963.
- b) Pacak M., 'An Electrometer Circuit', Electronic Engineering Vol. 35, p. 454 (1963).
- 2-54 Williams W.R. and Hawes R. C., 'Vibrating Reed Electrometers', Instruments and Control Systems Vol. 36, p. 112 (1963).
- 2-55 Pacak M., 'Simple MOSFET Electrometer Circuits', Electronic Engineering Vol. 41, p. 24 (1969).
- 2-56 Smith B., 'Infinite Z Junction-FET Electrometer Amplifier', *EEE Circuit Design Engineering* Vol. 14, p. 63 (1966).
- 2-57 Heaviside O., Electrical Papers (MacMillan, Press, London, 1892), p. 488.
- 2-58 a) Eguchi M. , 'Effects of Electric Force on a Permanent Electret,' *Japanese Journal of Physics* Vol. 1, p. 10 (1922).
- b) Eguchi M., 'On the Permanent Electret,' *Phil. Mag.* Vol. 49, p. 178 (1925).
- 2-59 Gemant A., 'Recent Investigations on Electrets,' *Phil. Mag.* Vol. 20, p. 929-952 (1935).
- 2-60 Nadzhakov G. , 'Uber eine Neue Art von Elektreten: Photoelektreten,' *Physik Z.* Vol. 39, p. 226-227 (1938), or 'A New Method of Permanent Polarization of Dielectrics.' *Godishnik Fiz. Mat. Sof. Universitet* Vol. 33, p. 409-420 (1936-1937).
- 2-61 Sessler G. M., and West J. E., *Appl. Phys. Lett.* Vol. 17, p. 507 (1970).

- 2-62 LaTour M., 'Formation Conditions of Thermoelectrets' in Electrets, Charge Storage and Transport in Dielectrics, M. Perlmann, Ed. (The Electrochemical Society, Princeton, NJ, 1973), pp. 436-443.
- 2-63 Warren J. E., Hamilton J. F., and Brzezinski A. M., J. Acous. Soc. Amer. Vol. 52, p. 711 (1972).
- 2-64 Lorne S. G., and Harrison S. R., 'Device for Measuring Electric Fields,' NASA Tech Brief, B72-10148, 1972, NASA CR 73177.

SECTION THREE

**POWER SYSTEM APPLICATIONS
OF
OPTICAL DATA PROCESSING**

by

Harold Kirkham

SECTION THREE

OPTICAL DATA PROCESSING

3.1 INTRODUCTION

The term 'data processing' is normally taken to mean electronic data processing, that is to say, the conversion of information to binary form and the manipulation of the binary data by high-speed electronic computer. It is a fair question to ask, then, what does optical data processing mean? There are three possible answers to the question.

First, optical data processing could mean the processing of information in binary form by a computer using optical elements, for example, optical gates, the optical equivalent of transistors, and so on. While no such computer has yet been built, much of the hardware necessary to construct such a device has at least been fabricated in the laboratory, and there is no inherent reason why a high-speed optical computer of this kind could not be built. This subject will be explored in Section 3.2.

Second, optical data processing could mean the performing of certain fixed operations on the optical signal by means of a specially constructed optical processor. It has been reported in the literature that it is possible to perform a wideband, high-speed Fourier Analysis of a signal by means of an optical device, for example. This subject is also explored in Section 3.2.

Other specific processing devices can be envisioned. However, neither of the two examples of optical data processing listed above is what we had in mind when we defined a task for optical data processing as part of the calendar year 1983 Fiber Optics Task at the Jet Propulsion Laboratory.

The third possible meaning for optical data processing, and the one intended here, is the application to power systems of optically based measurement and control or protection systems, wherein as much of the signal is retained in optical form for as long as possible. It was thought that there may be some economic or engineering advantage to this approach, in which conversion of the signal to an electrical form would take place as late as possible in the signal handling chain.

The work was envisioned as a small review study. Some original ideas would be required to give the concept concreteness. Section 3.3 describes three ideas which fall under the category of optical data processing as far as this task is concerned. They are transformer protection, using optical measurements of parameters which are inherently symmetrical in most power apparatus, transformer fault location using the ultrasonic pulses emitted by partial discharges, and HVDC control pulse generation using optical switching rather than electrical.

Section 3.4 lists the References.

3.2 BACKGROUND

This section provides a background to the subject of optical data processing. To do this, three different kinds of processing are discussed. They are the optical computer or optical analog of the digital computer, the special-purpose optical computer (the example given here is a kind of array processor), and the optical Fourier transform.

By considering these examples in some depth it is hoped to provide an introduction to the kinds of processing that can be done optically, and to identify some of the possibilities and limitations. It is also hoped that the reader will become more familiar with some of the hardware (such as interferometers, linear or non-linear) that might be useful in optical data processing.

3.2.1 Optical Logic

The fundamental component of a digital computer is a switch, capable of two different states of transmission. In an electronic computer these switches are typically transistors, and the signal on the gate (or base) controls the state of the source-drain (or emitter-collector) path. By judicious interconnection of such devices, all the logic functions necessary to implement a programmable computer can be realized, including arithmetic and logic operations and memory.

As it happens, transistors can provide power gain, and so compensate for small losses in the fidelity of the signals (in particular, logic voltage levels are readily restored). If an optical computer is to be made, it must contain some elements capable of restoring levels, or the levels must not be degraded by multiple operations.

A suitable candidate for use as an optical 'transistor' is the Fabry-Perot interferometer, shown in Figure 3-1. The interferometer consists of a layer of transparent material sandwiched between two plane parallel mirrors. The mirrors are partial reflectors - an incoming wave might be 90% reflected and 10% transmitted. Because of the fact that the mirrors are partially reflecting, a standing-wave pattern is built up inside the interferometer. The amplitude of the standing wave is determined by the optical length of the interferometer, which determines whether the interference at the mirrors is constructive or destructive. If the interference is constructive, the transmitted beam is close to the incident beam in intensity. Destructive interference results instead in a large reflected beam, but in most applications the reflected beam is not considered.

To use the interferometer as a switch, all that is needed is to change the phase relationship of the beams (forward and reverse) inside the interferometer. A change in wavelength is one way to accomplish this, or it may be possible to change the refractive index of the transparent material which comprises the 'cavity' between the mirrors.

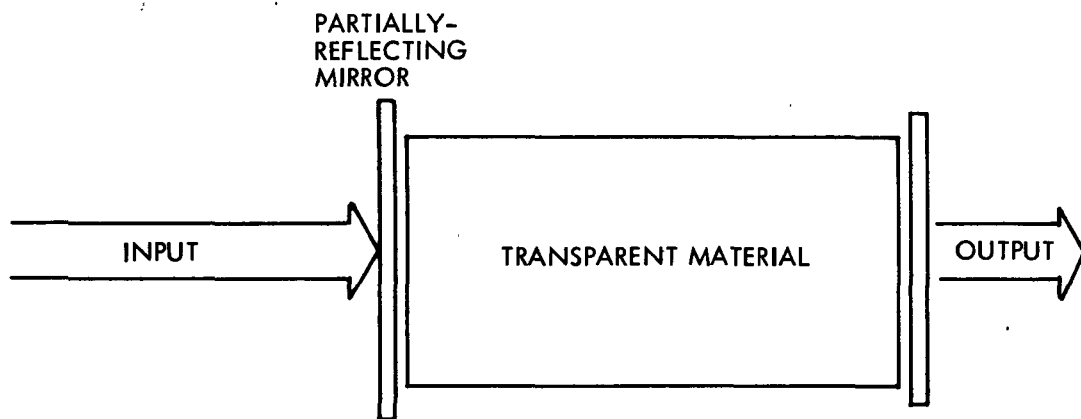


Figure 3-1. Fabry-Perot interferometer

The change in refractive index may be accomplished by using an electro-optic material (one that exhibits the Kerr effect or the Pockels effect, i.e., a change in refractive index with applied electric field) in the cavity, but such an approach would result in an electro-optical computer, not an optical computer.

Certain materials have a nonlinear refractive index. This means that the refractive index is itself a function of the intensity of the light used to measure the index. If the interferometer cavity contains such a material, it is possible to arrange the cavity and the incident beam intensity so that switching occurs for a relatively small change in the intensity of the incident beam. Assume that at low intensities there is destructive interference. If the intensity of the incident beam is gradually increased, there comes a point at which the refractive index approaches the value required for constructive interference. The intensity inside the cavity increases, causing the refractive index of the cavity material to change without further change in the intensity of the incident beam. The interferometer switches to 'transmit'. Further increases in the intensity of the incident beam result in corresponding increases in the transmitted beam, without further dramatic jumps. If the incident beam intensity is now gradually reduced, the reverse process occurs, and the interferometer switches abruptly to 'block'. There is likely to be a hysteresis effect, as shown in Figure 3-2, due to the presence (and self-maintaining effect) of a large standing wave inside the cavity as the incident intensity is reduced. Interferometer transmission then becomes a function of the history of the device.

It can be seen from Figure 3-2 that, with appropriate input conditions, it is possible to construct the optical equivalent of a transistor (and hence of any kind of logic gate) and a memory element. The devices would not be exactly analogous to their transistor equivalents. The 'transistor' analog requires that the input signal and the control signal be applied to the same place, whereas in the transistor they are applied to separate electrodes. The optical memory element requires a minimum value of input power to 'hold' the data. Nevertheless, the nonlinear Fabry-Perot interferometer can be made to function as the optical equivalent of a transistor or a memory element. It is not hard to see how such devices could be interconnected to form an optical digital computer.

Consider, for example, the 'Truth Table' of the simple two-input Fabry-Perot interferometer of Figure 3-3. If the two incident beam intensities are such that neither alone is sufficient to cause the device to transmit, but both together are sufficient, the interferometer is equivalent to an AND gate, with a truth table as shown in Table 3-1.

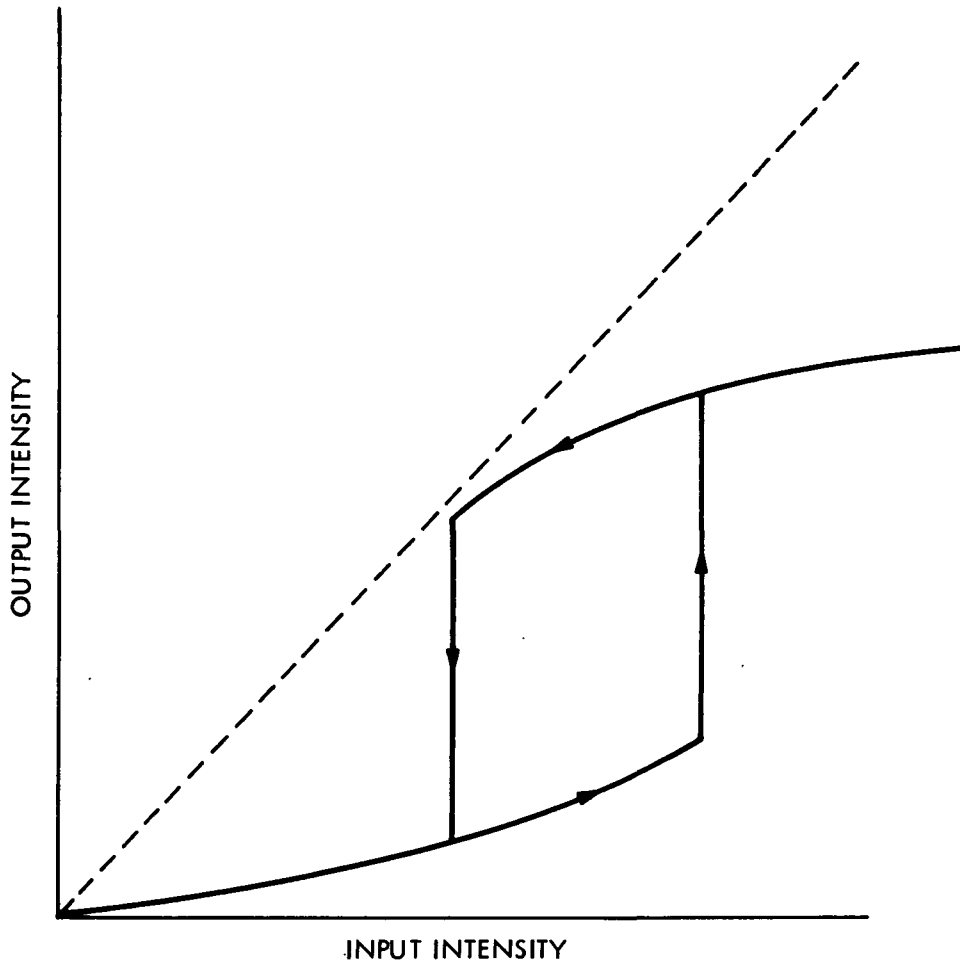


Figure 3-2. Transfer curve of nonlinear Fabry-Perot interferometer

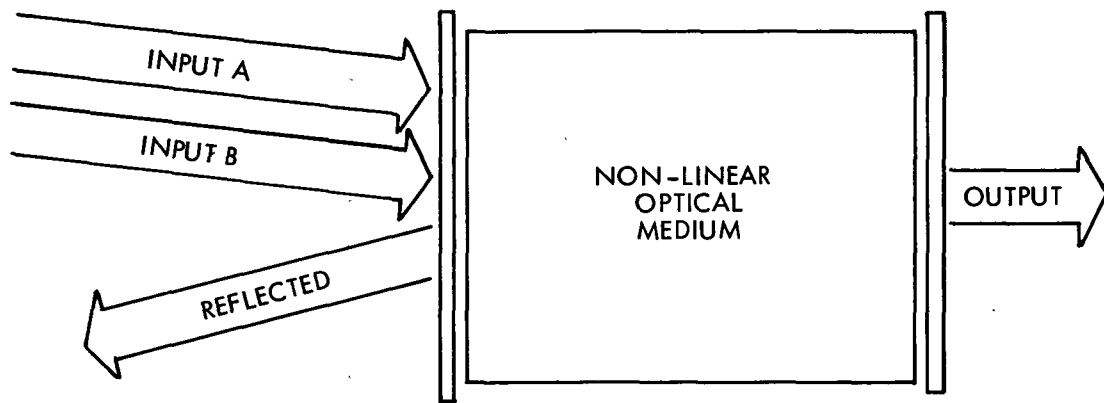


Figure 3-3. Two-input nonlinear Fabry-Perot interferometer

Table 3-1. Truth Table for two input interferometer

Inputs		Outputs	
I_a	I_b	I_t	I_r
H	L	L	H
L	H	L	H
H	H	H	L
L	L	L	L

Table 3-1 shows that the transmitted beam is effectively the AND of the two inputs. Somewhat surprisingly, the reflected beam is effectively the exclusive-OR of the inputs.

To form a memory element, an interferometer with a wide hysteresis loop may be used, and a bias (or holding) input used to move the operating point up to the bottom of the hysteresis 'square'. An additional high input will move the operating point above the switching point for increasing inputs, and the hysteresis will ensure that the output remains high as long as the bias is maintained. The memory is cleared by removing the bias.

A digital computer constructed of elements such as those described has the advantages of speed and low power. Some speed estimates have the optical computer 1000 times faster than the best available present computer [3-1] although not all materials are this fast. It should be clear from the foregoing discussion that a certain critical power density is required to make a nonlinear Fabry-Perot interferometer switch state. It seems that the faster-switching materials require higher power densities to switch [3-2]. Some materials must be maintained at very low temperatures, and it seems that no material has yet been found with the desirable properties of low threshold, high speed, and room temperature operation. In addition, it should be remembered that optical components are necessarily quite long. Dimensions of a few millimeters might be regarded as typical, as compared to a few micrometers for microelectronic logic elements.

A considerable amount of research and engineering work is evidently required before the optical computer becomes practical.

3.2.2 Special-Purpose Optical Computing

The optical digital computer is, of course, like the electronic digital computer, a general purpose machine. The possibility exists, however, to do some particular kinds of information processing optically, or electro-optically, in very efficient ways. Such techniques may be of special interest where the information is in optical form, or is needed in optical form. A few examples will be examined in this section. The number of examples is small because of space limitations — after all, the main purpose of this report is not in this area. There is no intent to imply that other kinds of optical information processing are not possible or even attractive, nor to imply that

special-purpose computing of this kind confers some peculiar disadvantage. Indeed, the field is an expanding one, and there are several exciting possibilities for optical processing of the kind described here.

Suppose the input (for processing) is in the format of a two-dimensional picture. Depending on the resolution of the image, each picture could contain 10^6 pixels. To compare this image electronically with another (say, a pre-set image) would then require the comparison of 10^6 pixels per frame, or perhaps 2.5×10^7 operations per second. This is at the limit of electronic computing.

To see that the same operation can be performed optically with great ease, consider that all that is required is to project the input image onto the appropriate mask and collect the light which is transmitted. The system forms a very simple, very fast correlation device [3-3].

An ingenious method of performing parallel logic operations on binary data has been demonstrated in Japan [3-4]. In this scheme, the two inputs (A and B) are encoded digitally in two dimensions as shown in Table 3-2.

Table 3-2. Coding of binary variables A and B

	0	1
a_{ij}		
b_{ij}		

Each pixel a_{ij} of A is encoded by horizontally dividing its square area as shown. The pixel areas b_{ij} of B are divided vertically.

The coded inputs A and B are then placed in the input plane of an optical array processor. Their image, as illuminated by up to four LEDs, is formed on a screen and viewed through a decoding mask. The arrangement is shown in Figure 3-4.

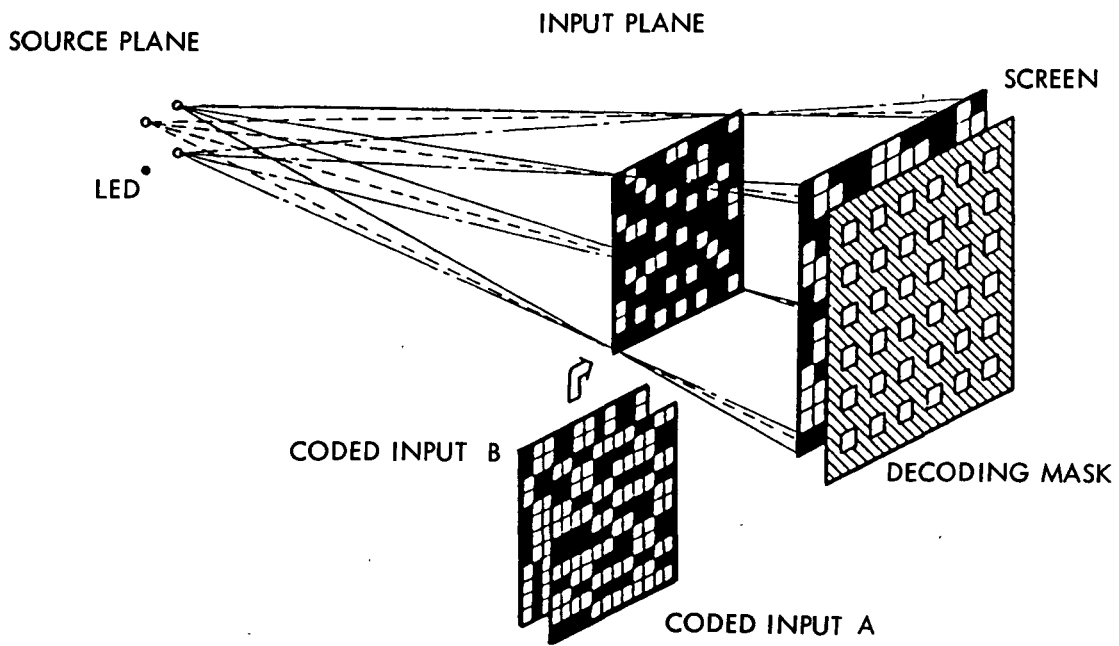


Figure 3-4. Optical logic array processor

In Figure 3-4, the source plane contains four LEDs, α , β , γ , δ . These are illuminated according to the desired logic function. Both A and B inputs, suitably coded, are in the input plane so that they cast shadows on the screen.

Operation of the processor may be understood by considering the typical cell ij . One and only one corner of this cell will be transparent (white), depending on the states of a_{ij} and b_{ij} . This is shown in Table 3-3.

Table 3-3. Overlay of input states a_{ij} and b_{ij}

a_{ij} b_{ij}	0	1
0		
1		

The typical cell ij is illuminated by four LEDs arranged in a square. The geometry is such that the shadow areas of the cell formed from each LED overlap somewhat. The overlapping is such that the total shadow area of the cell can be considered in nine parts, as shown in Figure 3-5.

If the entire cell were transparent (which Table 3-3 shows can never happen), then each of the four LEDs would illuminate a 2×2 area out of the 9×9 total for that cell at the screen. Under this condition, the middle cell of the 9 would be illuminated regardless of which LED was energized. Since only one corner of the cell is transparent (no matter what the binary state of a_{ij} or b_{ij}), each LED will illuminate only one part of the 9×9 image. Which part of the image is lit will depend on which LED is energized (for instance, the bottom right LED could only illuminate the four squares in the top left of the 9×9 region) and which corner of the cell is transparent (which is set by the input states as in Table 3-3). The number of squares in the 9×9 image which are bright will always equal the number of energized LEDs.

So far this seems like a rather complicated logic system. However, with the right mapping between logic function desired and LED(s) illuminated, sixteen logic functions can be distinguished by examining only the central square of the 9×9 image. This is shown in Figure 3-6.

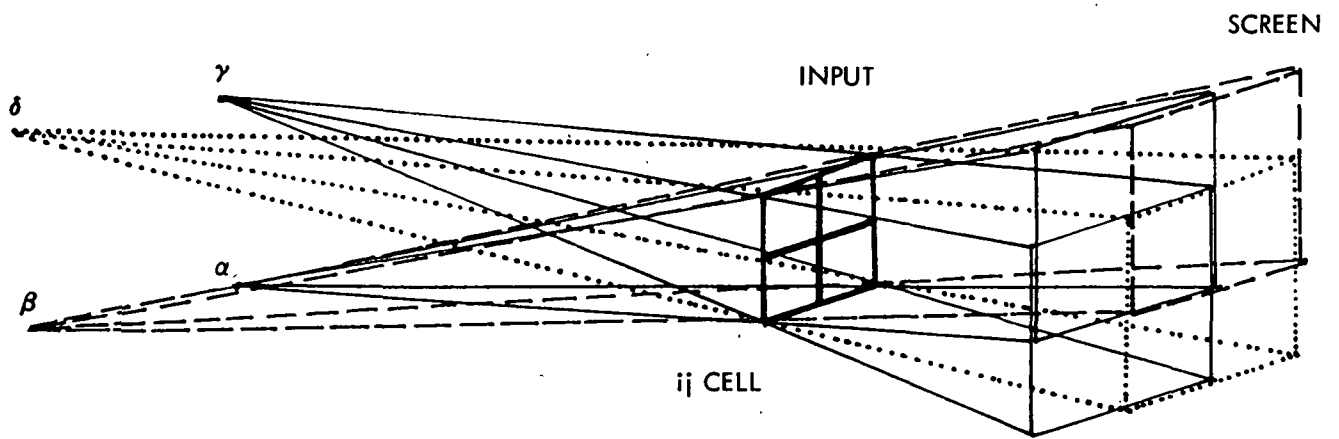


Figure 3-5. Overlapping of projections of the *ij* cell

In a more familiar notation, the light intensity in the central image area can be expressed

$$g_{ij} = \alpha(a_{ij} b_{ij}) + \beta(a_{ij} \bar{b}_{ij}) + \gamma(\bar{a}_{ij} b_{ij}) + \delta(\bar{a}_{ij} \bar{b}_{ij})$$

where α , β , γ , and δ show the LED state and
+ means a logical OR.

The purpose of the decoding mask is now clear. It screens out the eight peripheral squares in the 9 x 9 image so that only the center one is visible.

By illuminating none, some, or all of the LEDs, the logic function implemented can be changed. Sixteen possibilities exist. The similarity between the operation of this processor and the ALU (arithmetic logic unit) in the central processing unit of a computer should be clear. All this processor needs to become a matrix-type ALU is the ability to load data from an input register (which should also be two-dimensional) and the ability to store the result in an output register. However, these operations may not be simple, especially if fully parallel operation is required.

It is not my intention to dwell on the subject of ALU design.

In an experimental demonstration of the technique, the authors of Reference 3-4 performed all sixteen possible logic operations on two distinct images. Their results are reproduced here as Figure 3-7.

The two inputs used in the experiment were 64 x 64 pixels in area, that is to say, each was 4 k bits. Since the bits are processed in parallel, it takes no longer to perform these logic operations on 4 kb than it would on one bit. Larger arrays should be feasible.

There is an implication in the input images that the array processor is intended for image processing, i.e. processing input data which is a map or image of a two-dimensional scene. In fact, there is no reason to restrict application of the technique in this way. The input data could be any data that can be organized into a two-dimensional format. The input might therefore represent one bit of a matrix (or successive slices of a vector) and other processors could be interconnected to represent the other bits in an 8-, 16-, 32-, or 64-bit word.

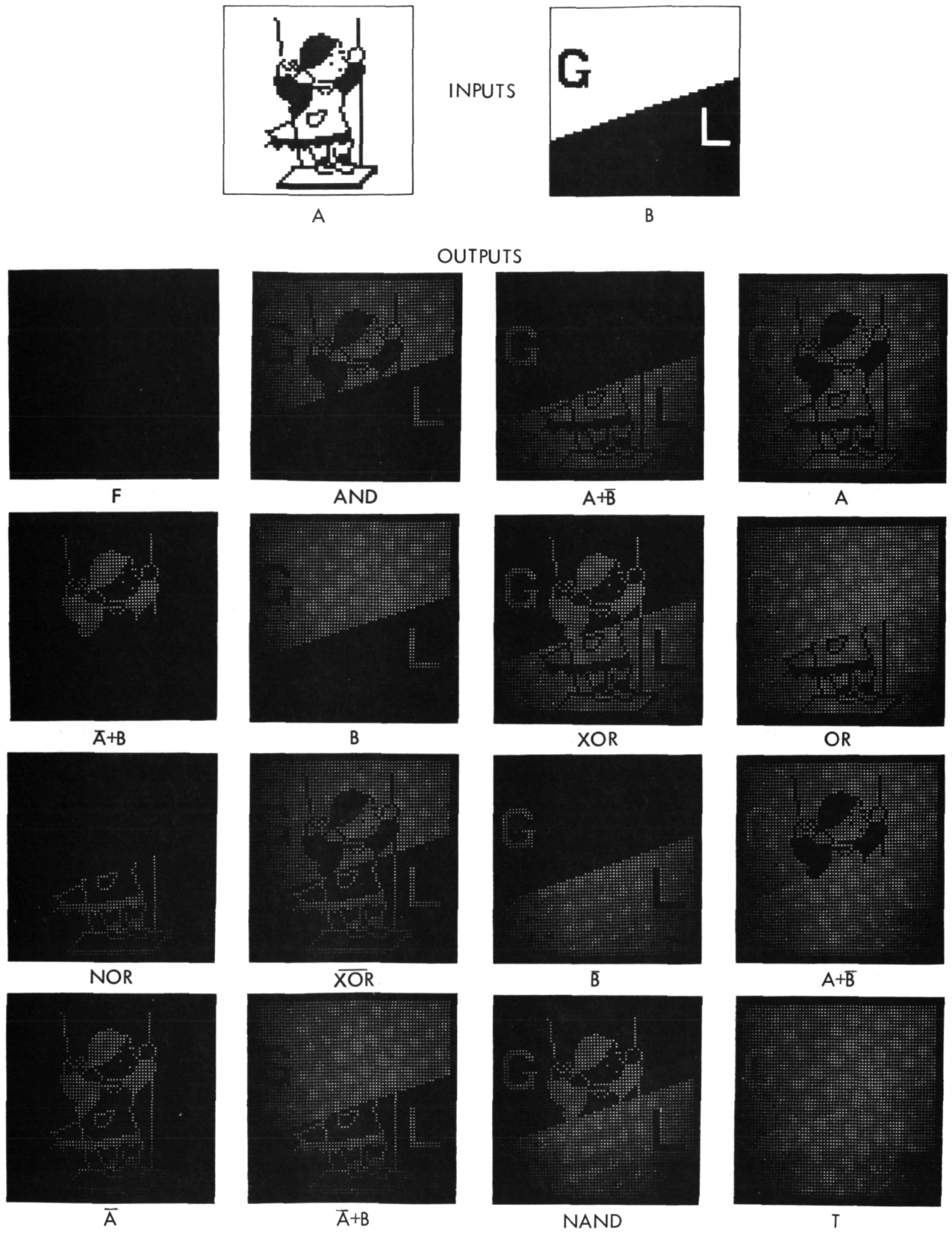


Figure 3-7. Experimental results, 64 x 64 array processor

The inputs to such a processor can be changed rapidly by a 'spatial light modulator'. Such modulators are limiting devices in optical processing. No truly satisfactory modulators are available, but there is promise in the recent advances in display technology. There are now available large, rectangular liquid crystal displays of exactly the type required to perform as input mask in this processor. The displays have been developed as television displays (thin, flat screen) and seem to consist of an $m \times n$ array of separately addressable and controllable elements (pixels). The sample in the author's possession seems to have over a 100 pixels in each line or column, and the pixels, using twisted nematics, change state very rapidly. Clearly, with a highly parallel kind of processing such as this, it would be desirable to maintain the array as an array as long as possible. When it is necessary to revert to ordinary sequential logic, however, a charge-coupled device (bucket brigade) behind the screen might provide a simple way to read out rows or columns of data at will. Such devices have been fabricated in square array form, for example, for use in the space telescope, where they provide high sensitivity (low noise), high resolution, and compatibility with telemetry [3-5].

It is tempting to suppose that very fast matrix operations (such as inversion) are possible using processing of this type, but it would be speculation on the part of the author were such an assertion made. Matrix inversion is a slow process, and has typically been the major bottleneck in solutions of the power system analysis problem on conventional computers. Considerable effort has been expended in an effort to alleviate the problem. At one time diakoptics seemed to offer some promise, and presently computers with special-purpose electronic array processors are being used. Nevertheless, the prospect of being able to handle the entire admittance matrix for a large power system all at once is an attractive one. However, matrix inversion algorithms are never simple, and are rarely (if ever) written in machine code. A power engineer writing a load flow program, for example, would use a high-level language such as FORTRAN and a compiler would produce object code from this. The exact nature of the object code (i.e. machine code) would depend on whether the compiler was written to suit a conventional machine or one with some array processing capability.

Just what the object code might look like for a system such as this is hard to imagine. Is it possible to do matrix operations across the entire matrix together, moving from high-order bits to low? Or are there interactions across the area at any given bit position? What would be the best algorithm—would it be the same as for processing linear arrays? How might a compiler be written?

Clearly, there are many questions left to be answered before two-dimensional optical array processing becomes a routine part of computing. But the technique offers some exciting possibilities and may justify further study.

3.2.3 Fourier Transform

It is impossible to end this discussion of optical data processing without mentioning the optical Fourier transform. It has been known for some time

that a Fourier transform can be obtained optically. It is sometimes given as an example of the power of optical data processing. It is the intention here to clarify what it means to obtain an optical transform. The development presented here is based on Chapters 4 and 5 of 'Introduction to Fourier Optics' [3-6].

The Fourier transform of a function $x(t)$ is defined by

$$X(f) = \int x(t) \exp(-j2\pi ft) dt \quad (3.2.1)$$

Similarly, in rectangular coordinates, the transform G of a function $g(x,y)$ is defined by

$$G = \iint g(x,y) \exp(-j2\pi(f_x x + f_y y)) dx dy \quad (3.2.2)$$

It is this equation which can be modelled optically.

Let a plane object with amplitude transmittance $t_o(x,y)$ be placed immediately in front of a converging lens of focal length f , as shown in Figure 3-8. The object is assumed to be uniformly illuminated by a normally incident, monochromatic plane wave of amplitude A , in which case the disturbance incident on the lens is

$$U_1(x,y) = A t_o(x,y) \quad (3.2.3)$$

The finite extent of the lens aperture can be accounted for by associating with the lens a pupil function $P(x,y)$ defined by

$$P(x,y) = \begin{cases} 1 & \text{inside the lens aperture} \\ 0 & \text{otherwise} \end{cases}$$

Thus the amplitude distribution behind the lens becomes, using (3.2.3)

$$U_1'(x,y) = U_1(x,y) P(x,y) \exp \left[-j \frac{k}{2f} (x^2 + y^2) \right] \quad (3.2.4)$$

The constant phase delay associated with the lens transformation has been omitted since it does not affect the result in any significant way.

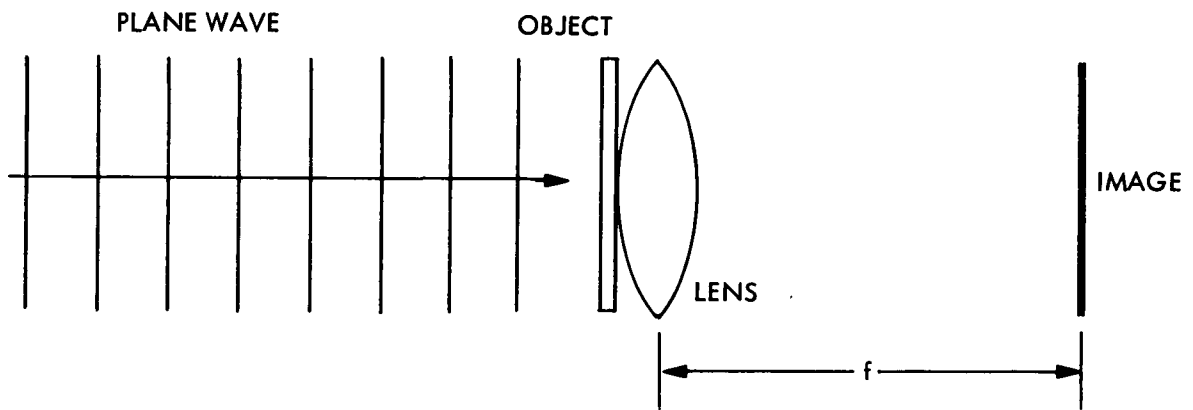


Figure 3-8. Transforming lens/object configuration

To find the distribution $U_f(x_f, y_f)$ of field amplitude across the back focal plane of the lens, the Fresnel diffraction formula

$$U(x_o, y_o) = \frac{\exp(jkz)}{j\lambda z} \exp \left[j \frac{k}{2z} (x_o^2 + y_o^2) \right] \iint U(x_1, y_1) \exp \left[j \frac{k}{2z} (x_1^2 + y_1^2) \right] \exp \left[-j \frac{2\pi}{\lambda z} (x_o x_1 + y_o y_1) \right] dx_1 dy_1 \quad (3.2.5)$$

is applied.

Thus, putting $z = f$,

$$U_f(x_f, y_f) = \frac{\exp \left[j \frac{k}{2f} (x_f^2 + y_f^2) \right]}{j\lambda f} \iint U_1'(x, y) \exp \left[j \frac{k}{2f} (x^2 + y^2) \right] \exp \left[-j \frac{2\pi}{\lambda f} (xx_f + yy_f) \right] dx dy \quad (3.2.6)$$

where a constant phase factor has been dropped. Substituting (3.2.4) in (3.2.6), the quadratic phase factors within the integrand are seen to cancel, leaving

$$U_f(x_f, y_f) = \frac{\exp \left[j \frac{k}{2f} (x_f^2 + y_f^2) \right]}{j\lambda f} \iint U_1'(x, y) P(x, y) \exp \left[-j \frac{2\pi}{\lambda f} (xx_f + yy_f) \right] dx dy \quad (3.2.7)$$

Thus, the field distribution U_f is proportional to the two-dimensional Fourier transform of that portion of the incident field subtended by the lens aperture. When the physical extent of the object is smaller than the lens aperture, the factor $P(x, y)$ may be neglected, yielding

$$U_f(x_f, y_f) = \frac{A \exp \left[j \frac{k}{2f} (x_f^2 + y_f^2) \right]}{j\lambda f} \iint t_o'(x, y) \exp \left[-j \frac{2\pi}{\lambda f} (xx_f + yy_f) \right] dx dy \quad (3.2.8)$$

Evidently the amplitude and phase of the light at coordinates (x_f, y_f) are influenced by the amplitude and phase of the object Fourier component at frequencies $(f_x = x_f/\lambda f, f_y = y_f/\lambda f)$.

3.2.3.1 Perspective. Diffraction is the effect whereby the shadows cast by sharp edges illuminated by point sources (or plane waves) do not have sharp boundaries. Diffraction cannot be understood in terms of a particle model of light and was the effect which required the formulation of a new (wave) theory of light.

Christian Huygens first expressed ideas about wave properties for light in 1678. His ideas were improved by Augustin Jean Fresnel in 1818 by the addition of the principle of interference. A firmer mathematical foundation was provided by the work of Gustav Kirchoff in 1882, though his work was based on some assumptions which have subsequently been shown to be inconsistent with each other. Consequently, Kirchoff's formulation of the Huygens-Fresnel principle must be regarded as an approximation, though a very good one.

There are a number of approximations to the general theory of diffraction patterns by means of reasonable mathematics. Two common ones are referred to as the Fresnel and Fraunhofer approximations. In the formulation of the diffraction equations a term

$$h(x_0, y_0 : x_1, y_1) = \frac{1}{j\lambda} \frac{\exp jkr_{01}}{r_{01}} \cos(n, r_{01}) \quad (3.2.9)$$

appears, relating the intensity inside an aperture to the observed intensity at some distant observation region. Figure 3-9 shows the geometry of interest.

The term $\cos(n, r_{01})$ represents the cosine of the angle between a normal n and the vector r_{01} joining the test point to the observation point. For small angles this cosine is unity, and $r_{01} = z$ so that we can write

$$h(x_0, y_0 : x_1, y_1) = \frac{1}{j\lambda z} \exp(jkr_{01}) \quad (3.2.10)$$

Note that the quantity r_{01} in the exponent cannot be replaced by z without introducing large phase errors, because of the multiplicative wave number $k = 2\pi/\lambda$. In exact terms we have that

$$r_{01} = \sqrt{z^2 + (x_0 - x_1)^2 + (y_0 - y_1)^2} \quad (3.2.11)$$

$$= z \sqrt{1 + \left[\frac{x_0 - x_1}{z}\right]^2 + \left[\frac{y_0 - y_1}{z}\right]^2} \quad (3.2.12)$$

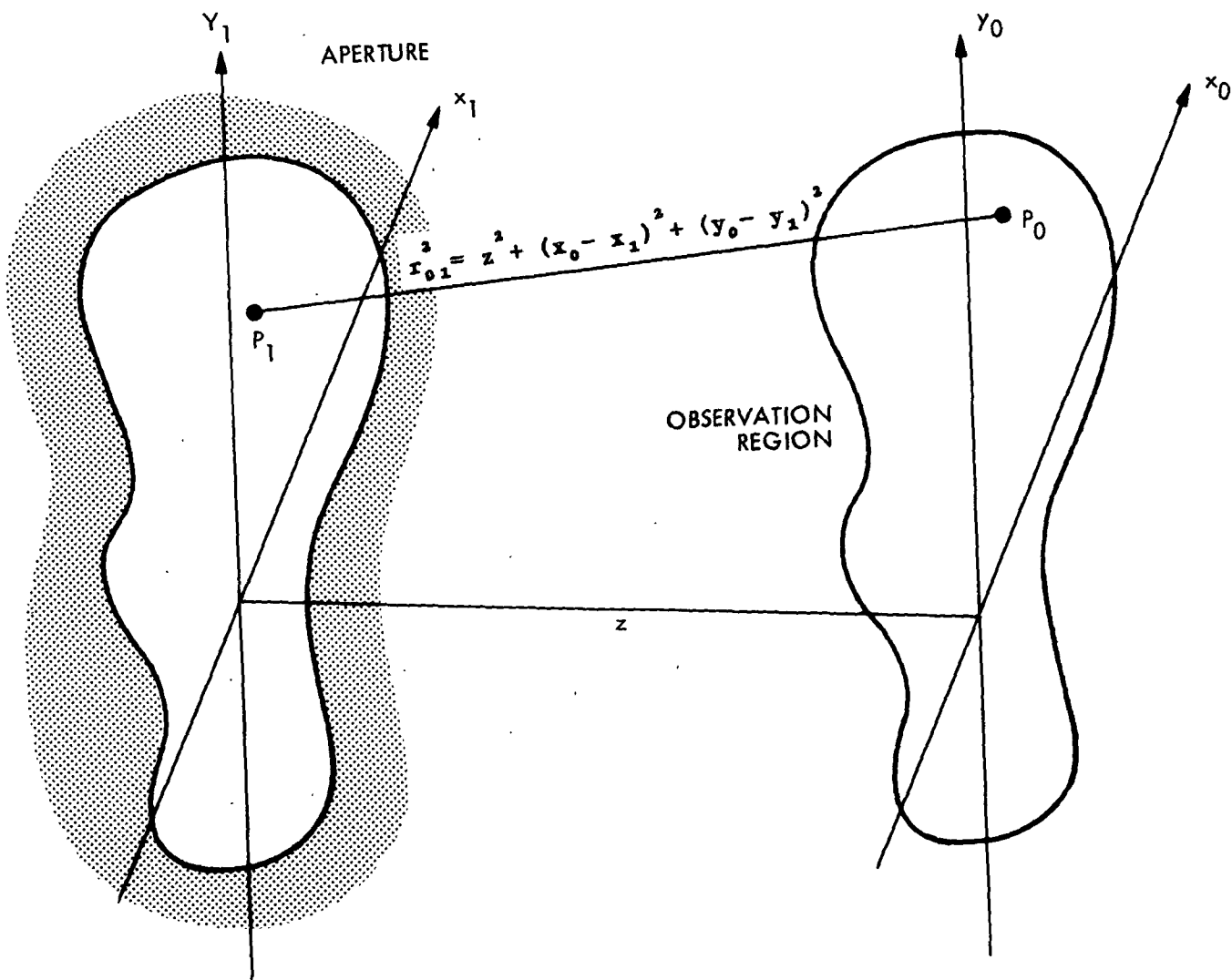


Figure 3-9. Diffraction geometry

The FRESNEL APPROXIMATION consists of expanding the square root by the binomial theorem

$$\sqrt{1+b} = 1 + \frac{1}{2}b - \frac{1}{8}b^2 + \frac{1}{16}b^3 \dots \quad \text{for } |b| < 1 \quad (3.2.13)$$

and retaining only the first two terms. Thus

$$r_{o1} = z \left[1 + \frac{1}{2} \left[\frac{x_0 - x_1}{z} \right]^2 + \frac{1}{2} \left[\frac{y_0 - y_1}{z} \right]^2 \right] \quad (3.2.14)$$

Now, the Fresnel approximation is only valid if the distance z is large. The next highest term in the binomial expansion must contribute negligible phase change. Just what this restriction implies in terms of the relative sizes of the aperture, the observation region, and the distance z is not a simple matter, but it is this approximation which results in the quadratic terms in the diffraction equations developed above, and ultimately the similarity to the Fourier transform. Thus, the region in which Fresnel diffraction is valid is the region in which the diffraction models the Fourier transform, with a multiplying phase factor.

A stronger restriction on z , namely

$$z \gg \frac{k(x_1^2 + y_1^2)_{\max}}{2} \quad (3.2.15)$$

causes the external phase factor to be approximately unity, so that the observed field distribution is the Fourier transform of the aperture distribution alone. This is the Fraunhofer assumption. The very large values for z required by this assumption may be reduced by the use of lenses, so that it is possible to obtain field distributions representing Fourier transforms with some precision.

The similarity between equation (3.2.8) and equation (3.2.2) is obvious, but the relation between the object and the focal plane amplitude distribution U_f is not an exact one, because of the quadratic phase factor before the integral. It can be shown, however, that if the object is moved away from the lens and placed in the front focal plane, the phase curvature disappears. An exact Fourier transform obtains. (It is also possible to obtain a controllable scale factor by placing the object behind the lens).

What exactly do equations like (3.2.8) mean? Just that the light in the focal plane is, in amount and distribution, the two-dimensional Fourier transform of the transmittance of the object. The object diffraction pattern is a representation of the required transform. Figure 3-10 shows an example of an optically obtained Fourier spectrum.

ORIGINAL PAGE IS
OF POOR QUALITY

ORIGINAL PAGE IS
OF POOR QUALITY

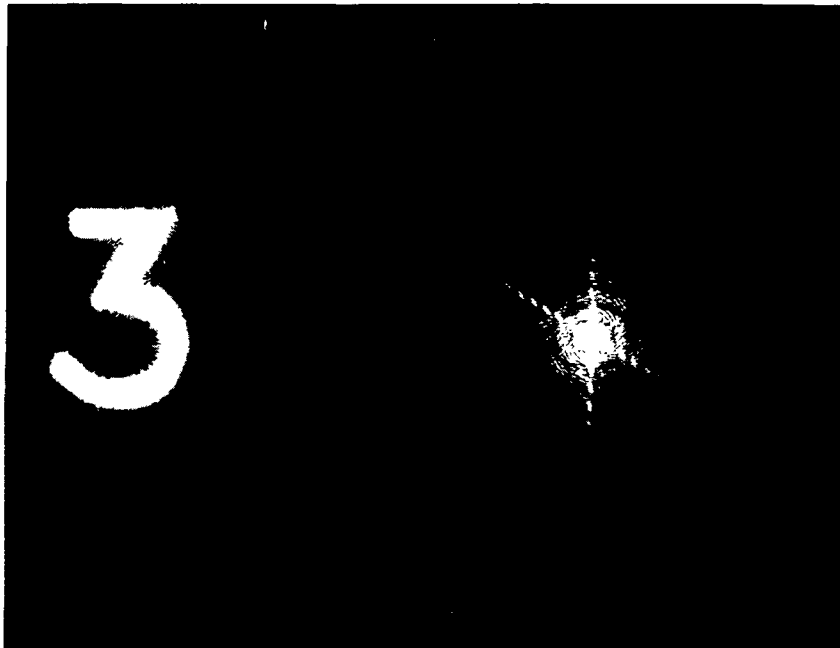


Figure 3-10. Optically obtained Fourier spectrum of the character '3'

It is to be supposed that further optical processing of the signal is possible (filtering, for example) but application to the kind of information required in power system calculations is difficult to see. Nonetheless, diffraction patterns like that of Figure 3-10 may someday be part of a routinely applied general-purpose signal processing system.

3.2.4 Concluding Remarks

It is impossible in a brief survey such as this to cover adequately the field of optical data processing. No discussion has been given of the wide variety of electro-optical or acousto-optical devices which have been described in the literature.

Nevertheless, it has been shown that logical operations can be performed simultaneously on each element of a two-dimensional array of binary data using very simple apparatus, and a method of obtaining two-dimensional Fourier transforms has been demonstrated. It is hoped that these examples serve to show that optical methods may be better suited than electronic methods to high-speed processing, large data arrays, or very wideband signals. Application of these techniques may result in some significant improvements in the performance of information processing systems.

3.3 POWER SYSTEM APPLICATIONS OF OPTICAL DATA PROCESSING

3.3.1 Introduction

This section addresses a small number of power system applications of optical data processing. The applications are much more specific than the ideas presented in the previous section and therefore of limited scope rather than wide generality.

Three ideas are discussed: transformer protection, transformer fault location, and firing-pulse control for HVDC thyristors. If these specific ideas are generalized, they are seen to represent three classes of data processing: asymmetry detection as a measure of abnormal operation of power apparatus, acousto-optical processing of wide-band data in real time, and optical control of power equipment. It is probable that there are other applications for optical data processing under these general headings, though they may be as narrowly applicable as the present ideas and quite different in implementation.

For the time being, the three versions of optical data processing discussed here will have to serve as examples of the kind of application that may be possible and worthy of further study.

3.3.2 Transformer Protection

Perhaps because of the historical need for simplified design procedures most power apparatus is symmetrical. Thus, for example, power transformers are very symmetrical devices, as can be seen in Figure 3-11.

Because the transformer is symmetrical, there is an inherent degree of symmetry in its leakage flux during normal operation. Although much smaller than the core flux, the leakage flux measured (for example, by a fiber optic sensor) in two or more symmetrically located places inside the transformer tank should be identical.

In the event of an internal fault, the leakage flux in the transformer would certainly become asymmetrical in some dimension, so that a measurement of the symmetry of the leakage flux (rather than its absolute magnitude) would serve as a measurement of the health of the transformer. Symmetrical leakage flux implies a healthy transformer, asymmetrical leakage implies an internal fault.

To what extent symmetry would be maintained for a through fault, and to what extent asymmetry would result from an internal fault is presently not known. If it should prove possible to develop a device to measure the symmetry of leakage flux inside a transformer, the way may be open to provide transformer protection which is independent of any of the normal electrical measurements usually made for this purpose. This would certainly seem like a worthwhile goal.

ORIGINAL PAGE IS
OF POOR QUALITY

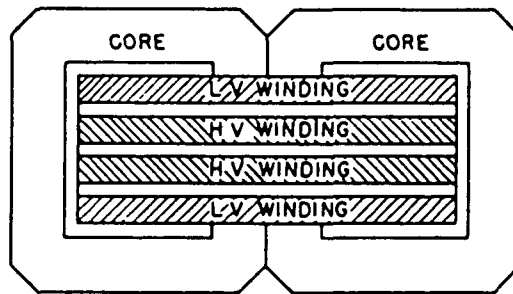
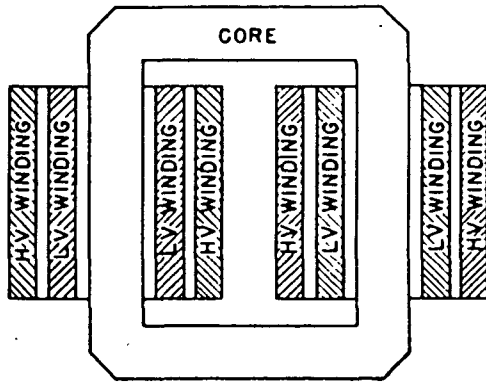


Figure 3-11. Transformer Construction

3.3.3 Transformer Fault Location

It has been known for some time that discontinuities in the dielectric constant of solid insulation can cause field intensification to the point that the insulation breaks down. This effect has been observed in the solid insulation of transformers and cables, and the result has been termed partial discharges, or corona.

Presumably because of the release of thermal energy, the partial discharges give rise to pressure pulses at ultrasonic frequencies. Perhaps the mechanism is similar to the one that produces Trichel pulses [3-7] in gaseous insulation - indeed it may be that the solid insulation contains a void of gas in which Trichel pulses are being generated. Essentially, the process is thought to begin where a heavy positive ion, accelerated by the electric field, dislodges an electron, which moves off in the other direction, and ionizes other atoms by the Townsend (avalanche) process. The positive ions near the original point of impact reduce the field intensity (space-charge effect) and quench the discharge. The process repeats after the positive ions are swept clear by the field. Trichel pulses can have frequencies in the kilohertz or megahertz region and very fast risetimes. The frequency will depend on the geometry of the field and the size of the gaseous region.

In any event, pressure waves at ultrasonic rates and with fast risetimes are detectable in the oil in transformer tanks. These pulses have been used to predict the failure of the transformer insulation [3-8].

A recent refinement has been the introduction of a second ultrasonic sensor into the transformer tank. Information from two sensors can, in principle at least, be used to give an idea of the location of the fault, presumably leading to a simplification of the process of fixing the problem by replacing the insulation. (Transformer rewinding is an expensive business. Power transformers are customarily built with internal supports and bracing, which would have to be removed before the winding insulation could be replaced. If the exact location of the fault were known, only a minimum amount of this work need be done.)

The information from two sensors, combined with a knowledge of the velocity of the sound waves in oil, can be used to locate the fault in the following way. Suppose a fault generates a single pulse at time t_0 , which arrives at sensor a at time t_a and at sensor b a little later at time t_b , as shown in Figure 3-12.

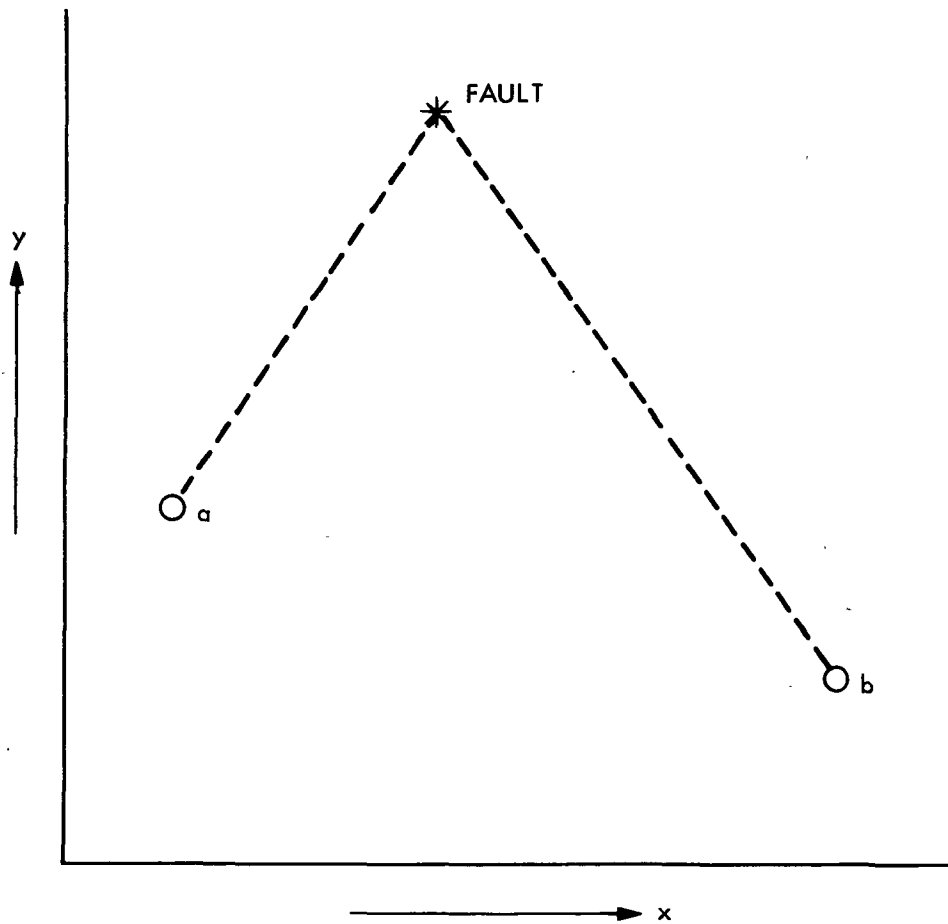


Figure 3-12. Fault location using two sensors

Figure 3-12 is drawn showing the plane through the two sensors and the fault location. The location of the x and y axes is arbitrary, and it has not been assumed that the sensors are along the abscissa or that they have the same ordinate.

The pulse transit time to sensor a is simply

$$\begin{aligned}\tau_a &= t_a - t_o \\ &= \frac{1}{c} \sqrt{(x_f - x_a)^2 + (y_f - y_a)^2}\end{aligned}\quad (3.3.1)$$

where c is the velocity of sound in the oil.

Similarly, the transit time to sensor b is

$$\begin{aligned}\tau_b &= t_b - t_o \\ &= \frac{1}{c} \sqrt{(x_f - x_b)^2 + (y_f - y_b)^2}\end{aligned}\quad (3.3.2)$$

Externally, of course, only the difference in transit times is known, so that the available information is

$$\begin{aligned}\Delta t &= \tau_b - \tau_a \\ &= \frac{1}{c} \left[\sqrt{(x_f - x_b)^2 + (y_f - y_b)^2} - \sqrt{(x_f - x_a)^2 + (y_f - y_a)^2} \right]\end{aligned}\quad (3.3.3)$$

As a fault location technique, the method suffers three disadvantages. First, the velocity of the sound waves in the oil is required, and it has been shown that this parameter is far from constant [3-9]. The velocity appears to depend on the temperature, pressure, gas and moisture content of the oil, as well as the frequency of the sound waves.

Second, even if the velocity of the sound is known exactly, equation (3.3.3) still contains two unknowns. Consequently, there is no unique solution, and the best that can be done is to recast (3.3.3) into a form relating x_f and y_f . The result will obviously be a quadratic equation with the form of a hyperbola.

Third, the analysis was done in a plane passing through the two sensors and the fault, so that only two dimensions were involved. Realistically, the problem is three-dimensional, and would involve unknowns x_f , y_f and z_f .

It is expected that by increasing the number of sensors, the three-dimensional problem can be solved, and without prior knowledge of the velocity. However, the information processing aspects become more difficult, and it is here that optical data processing may be able to play a part.

Suppose there were a third sensor in the situation depicted in Figure 3-12. Then there would exist a third transit time — τ_c — and two additional time differences would be available. As a result, instead of equation (3.3.1), we would have three equations

$$\Delta t_{(ab)} = \frac{1}{c} \left[\sqrt{(x_f - x_b)^2 + (y_f - y_b)^2} - \sqrt{(x_f - x_a)^2 + (y_f - y_a)^2} \right] \quad (3.3.4)$$

$$\Delta t_{(ac)} = \frac{1}{c} \left[\sqrt{(x_f - x_c)^2 + (y_f - y_c)^2} - \sqrt{(x_f - x_a)^2 + (y_f - y_a)^2} \right] \quad (3.3.5)$$

$$\Delta t_{(bc)} = \frac{1}{c} \left[\sqrt{(x_f - x_c)^2 + (y_f - y_c)^2} - \sqrt{(x_f - x_b)^2 + (y_f - y_b)^2} \right] \quad (3.3.6)$$

which can be solved for x_f , y_f , and (if desired) c . It can be shown that the addition of a fourth sensor, out of the plane, would enable a solution to be found for z_f . There would be three additional time differences Δt available, for the addition of only one unknown, z_f . The simultaneous solution of any four of the equations, which would be of the form

$$\begin{aligned} \Delta t_{(ij)} = \frac{1}{c} \left[\sqrt{(x_f - x_j)^2 + (y_f - y_j)^2 + (z_f - z_j)^2} \right] \\ - \frac{1}{c} \left[\sqrt{(x_f - x_i)^2 + (y_f - y_i)^2 + (z_f - z_i)^2} \right] \end{aligned} \quad (3.3.7)$$

would yield the required values for x_f , y_f , and z_f .

Implementation of the solution can be broken into two parts. First, it is necessary to find values for the time differences. Since the ultrasonic pulses are not produced singly, but appear as pulse trains in the presence of noise, it will almost certainly be necessary to perform some kind of correlation on the information from the sensors in order to be sure that the correct signal is being analyzed. Second, it is necessary to process the information from the correlation to find the fault location. The arrangement is shown conceptually in Figure 3-13.

The correlation of fast wideband signals, such as the signals coming from the ultrasonic sensors, would be extremely difficult to perform using conventional signal analysis methods. It may be possible to use acousto-optical methods instead.

The simultaneous solution of a handful of simultaneous quadratic equations should not be difficult using only a small computer. This processing need not be done in real time (unlike the correlations) and a good locator would probably use the available redundant information, and several successive solutions to improve accuracy and reduce the false-alarm rate.

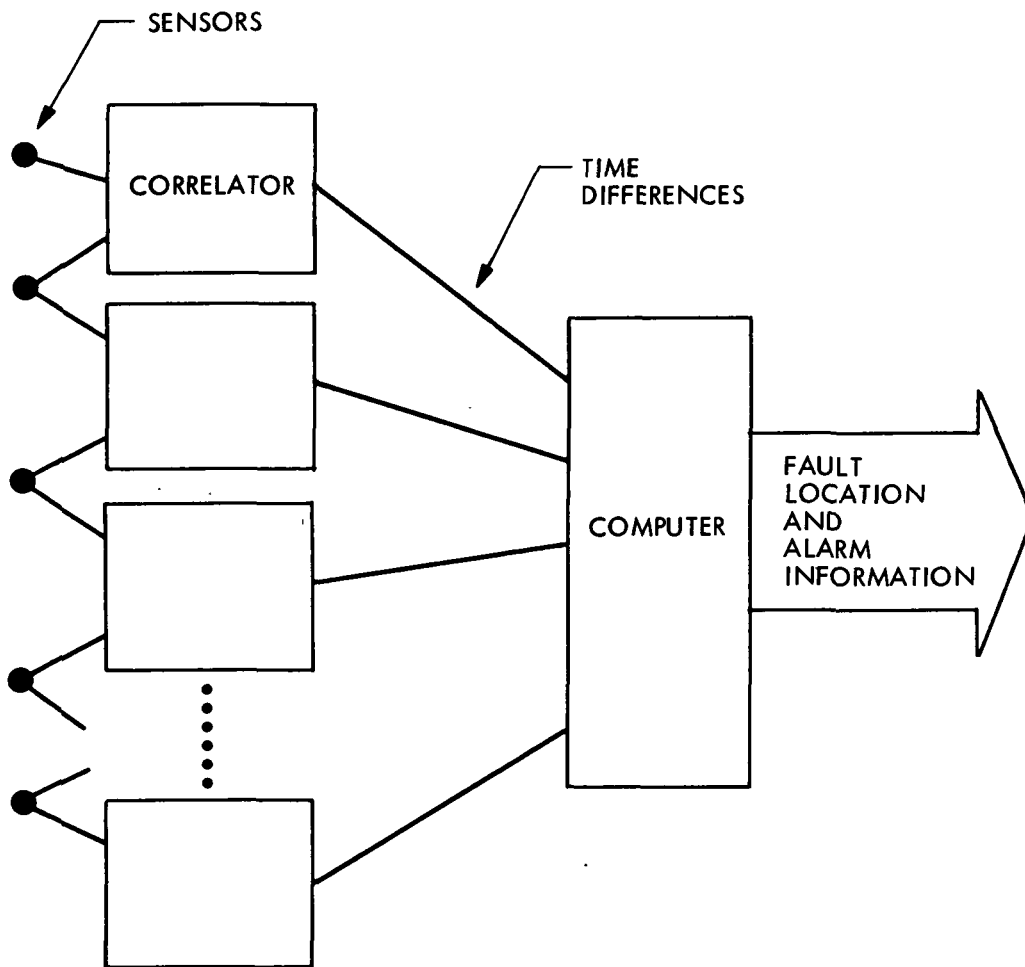


Figure 3-13. Conceptual diagram of three-dimensional fault identification and location system

3.3.4 HVDC Control Pulse Generation

In the two applications of optical data processing described earlier in this section, information was obtained from sensors and processed to yield some useful result. The next application is different, because the light itself is originally only a source of energy, and meaning is added to it by the processing. The light is then used to fire SCRs.

The technique could be applied to the generation of firing pulses for HVDC light-fired thyristors.

At present, light-fired thyristors are being developed for HVDC because of the potential simplicity of coupling the firing pulses to the thyristors. In an HVDC bridge there will normally be many thyristors in series, and electrical firing methods have the problem of coupling a relatively small firing voltage across a relatively large common-mode voltage. Within limits this can be done with pulse transformers, but in applications where the thyristors require reverse gate bias during the blocking period, a separate supply of power to each gate is required. This can be an expensive proposition.

Thyristors have been developed which are light-sensitive and which can be fired with relatively little light energy [3-10]. Such thyristors can, of course, be connected in series for HVDC use, and advantage can be taken of the isolation afforded by fiber optics to provide firing pulses from a single light source.

In operation, each thyristor in a series group must be fired simultaneously. This is easily done by generating the required light pulse in a single source for each group. The requirement for rapid turning on (and off) restricts the kind of light source that can be used. Present technology favors arc lamps with special control of the vapor pressure and temperature to ensure reliable firing [3-11].

However, it happens that firing pulses are applied to only two valve groups in a bridge at any one time. The pulses are switched from group to group in sequence and cause the current to commutate from group to group, but the total energy in the firing pulses is constant. It follows, therefore, that a light source of constant output could be used if the light energy could be switched from group to group by some other means. Figure 3-14 compares the two methods of generating pulses to fire light-activated SCRs.

A number of methods could be used to perform the required optical switching. The choice would depend largely upon the nature of the light source used and, as explained above, there are many possibilities for this, once the restriction for rapid turn-on and turn-off is relaxed. Interferometric methods could be used to switch the light and create pulses. Two possibilities exist. First, a Mach-Zehnder type interferometer could be used, as shown in Figure 3-15.

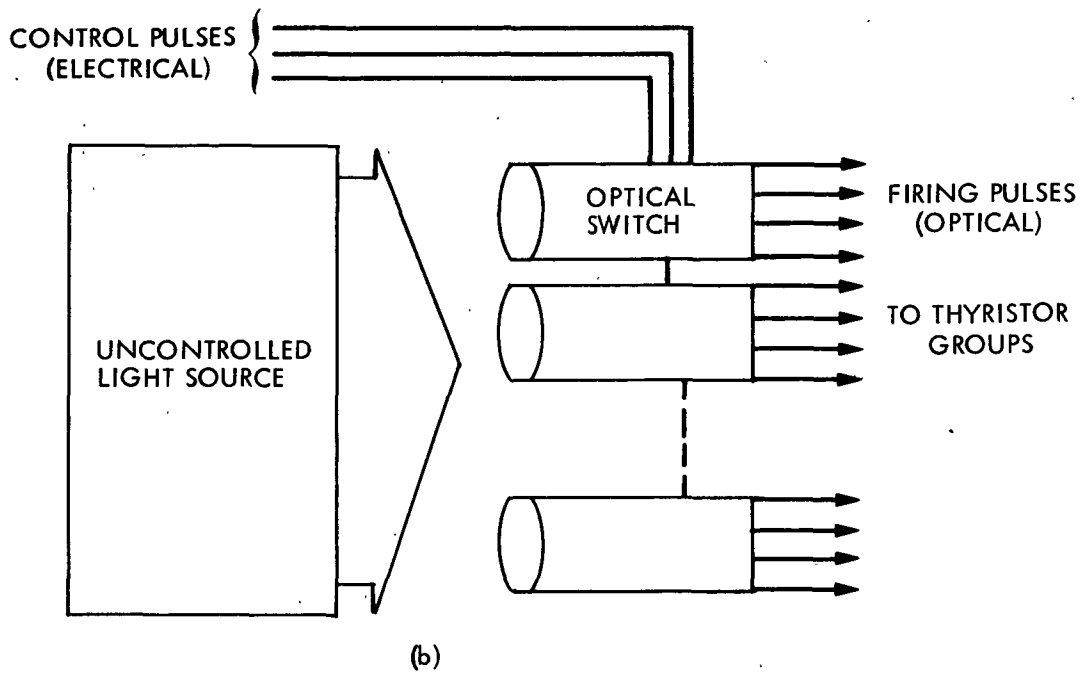
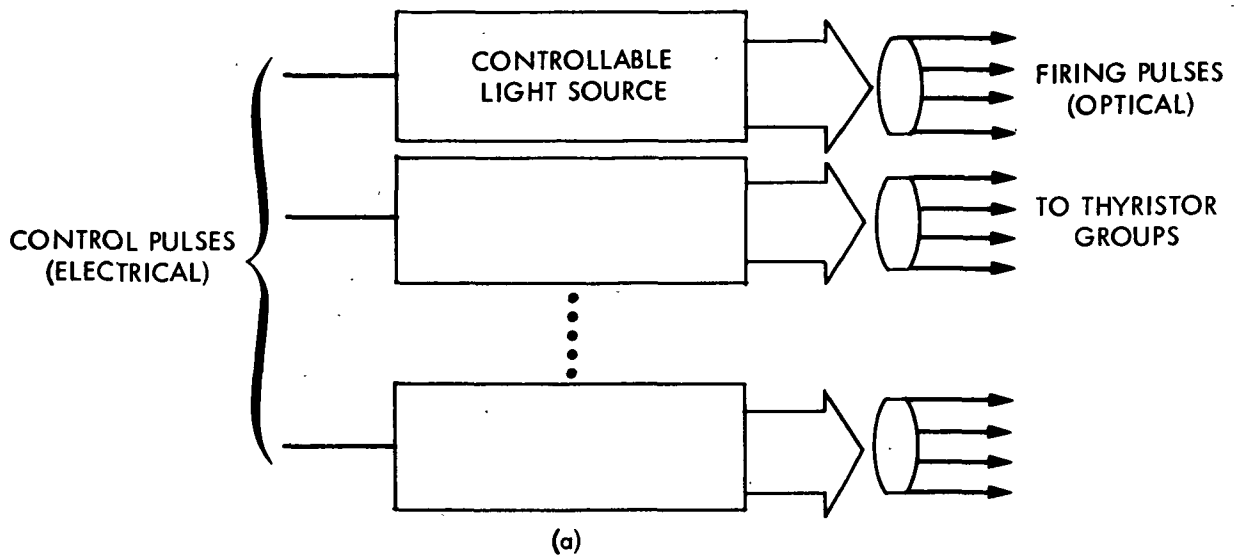


Figure 3-14. Generation of optical firing pulses
 (a) by switching light source on and off
 (b) by optical switching

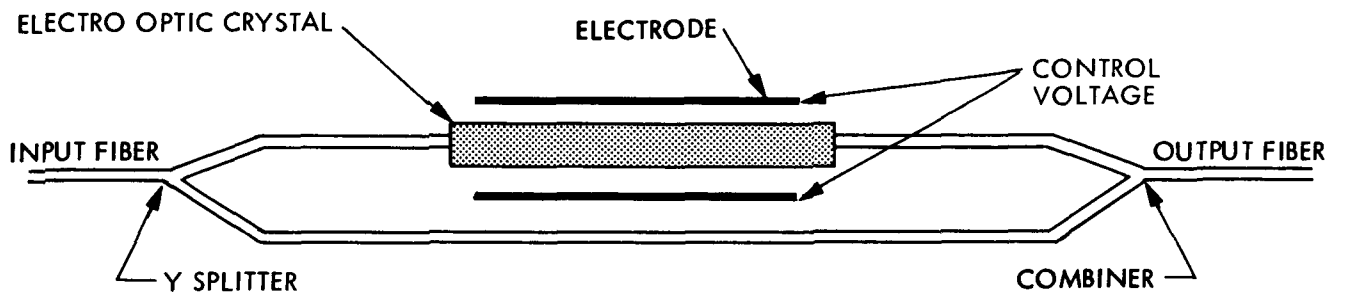


Figure 3-15a. Mach-Zehnder interferometer with electro-optic delay arm

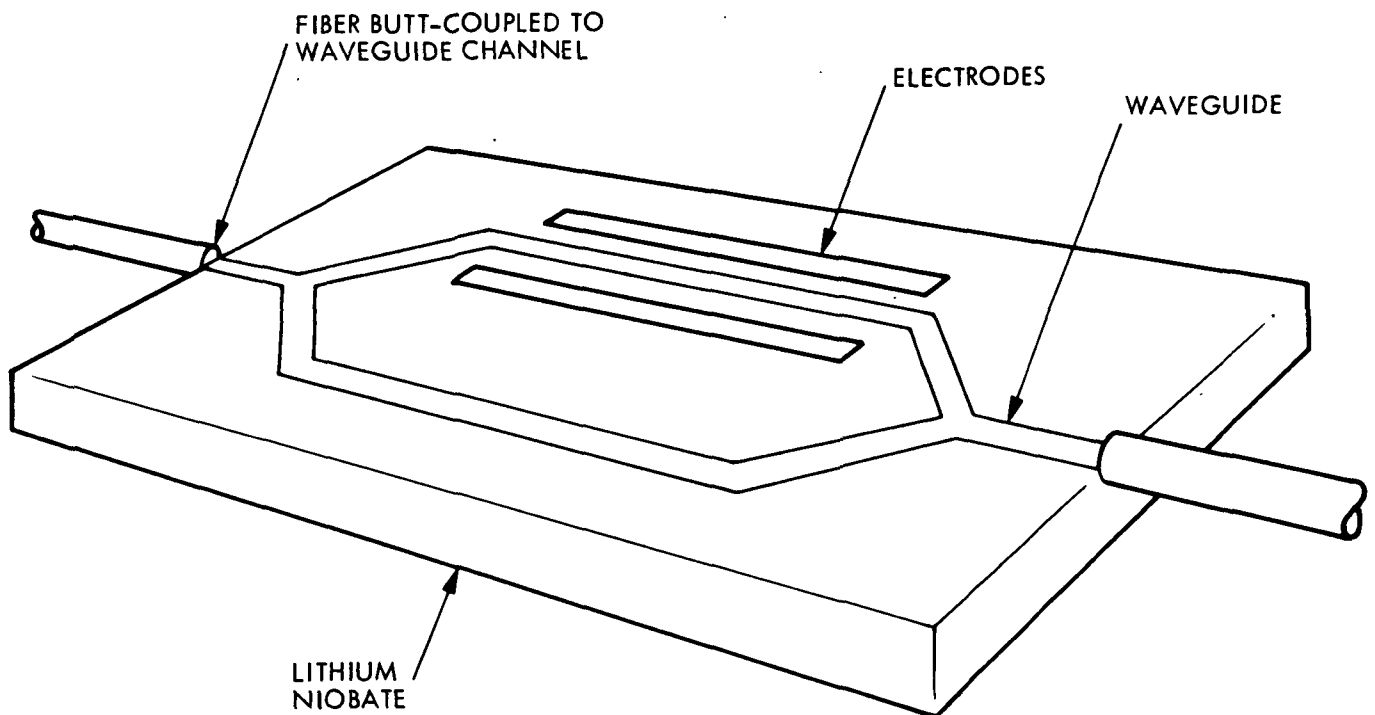


Figure 3-15b. Implementation of Mach-Zehnder interferometer by photolithography on planar substrate

In Figure 3-15, the incoming light is split by a Y into two fibers. A voltage applied to the material that comprises one arm of the interferometer produces a phase retardation ϕ depending on the length of the electrode, l , and the voltage:

$$\phi = KlV$$

where K depends on the geometry and the material used. In practice, a phase shift of π can be produced in lithium niobate (LiNbO_3) with a length of only a few mm and potential only a few volts. Of course, when $\phi = \pi$, no power is transmitted. The re-combined light interferes destructively and does not appear in the output fiber. With no voltage applied, there is no phase shift, so the interference is constructive and all the input energy is coupled to the output (apart from an insertion loss of a dB or so).

Second, the Fabry-Perot (discussed in Section 3.2.1) can also be used as an electro-optical switch. In this instance a linear material could be used (as opposed to the nonlinear material required for the optical transistor described earlier) and operation at room temperature is readily possible. The interferometer is then quite straightforward — probably lithium niobate could be used, with partially reflecting mirrors plated onto the end faces and electrodes plated onto two sides. Figure 3-16 shows the arrangement.

Interferometric methods may not provide sufficient on/off ratio, and other techniques may be worth investigating. One possibility is to use a switch based on the Kerr, Pockels, or Faraday effect. In other words, the switching action can be based on a change in the polarization of the light. In such a switch, the electro-optic material (or magneto-optic material) is placed between polarizers as shown in Figure 3-17.

3.3.5 Concluding Remarks

It is not obvious that any one of the three methods of switching described above has a clear advantage over the others. Nor is it obvious just what the requirements for safe switching of light-fired thyristors would be in terms of maximum light that will not fire any unit and minimum light that will fire all units. These parameters are crucial in the design of a switched-typed light-fired system. It is thought that further investigation of the concept is warranted.

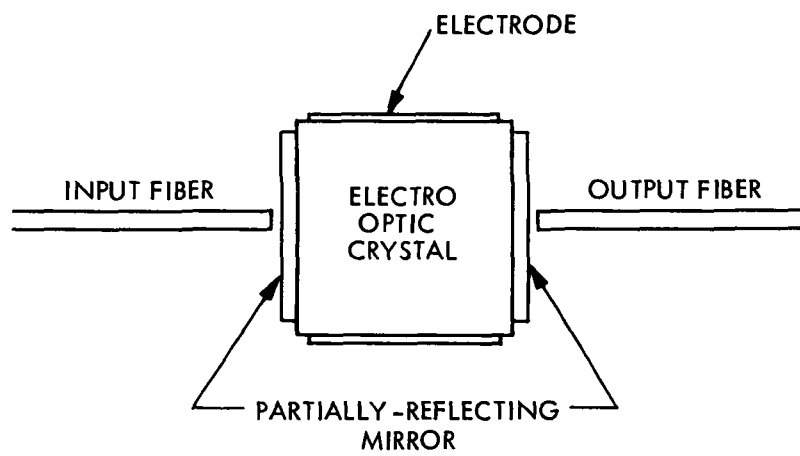


Figure 3-16. Fabry-Perot interferometer as an electro-optical switch

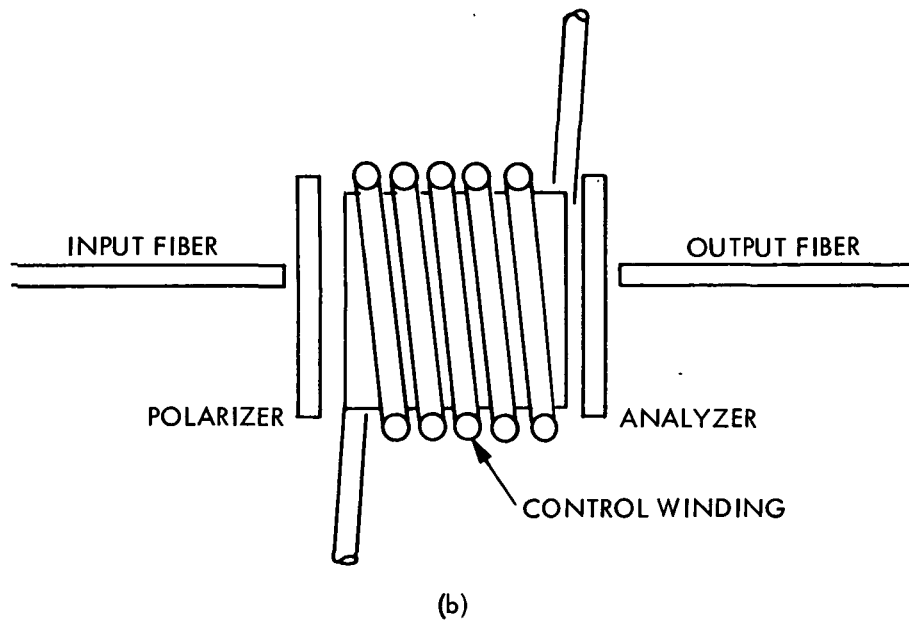
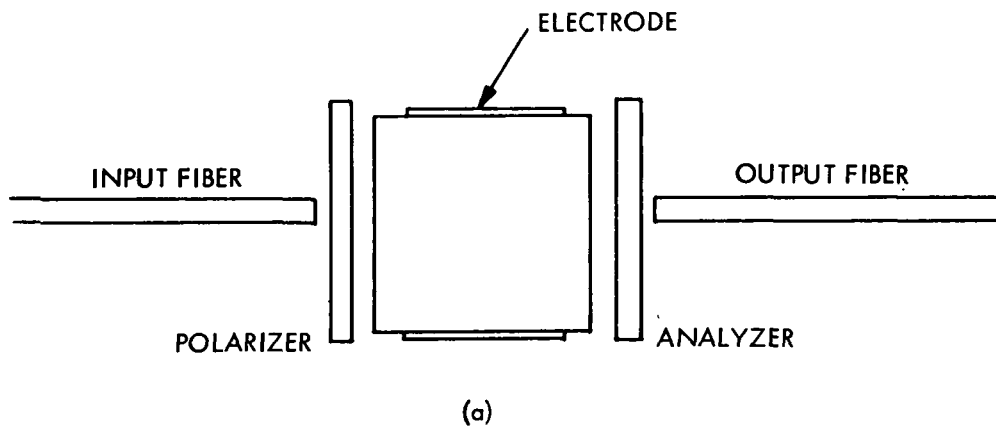


Figure 3-17. Polarization-type optical switching
 (a) electro-optical
 (b) magneto-optical

3.4 REFERENCES

- 3-1 Abraham E. and Seaton C.I. and Smith S.D., 'The Optical Computer', Scientific American, February 1983, pp 85-93.
- 3-2 Garmire E., 'Signal Processing with a nonlinear Fabry-Perot', SPIE, Vol. 269, Integrated Optics (1981), pp 69-74.
- 3-3 Lohmann A.W., 'Chances for Optical Computing', Proceedings of 10th International Optical Computer Conference, April 6-8, 1983, pp 1-5.
- 3-4 Tanida J. and Ichioka Y., 'Optical Logic Array Processor', *ibid* pp 18-23.
- 3-5 Bahcall J.N. and Spitzer L. Jr., 'The Space Telescope', Scientific American, Vol. 247, No. 1, July, 1982, pp 40-51.
- 3-6 Goodman J.W., Introduction to Fourier Optics, McGraw-Hill, San Francisco, CA 1968.
- 3-7 Trichel G. W., Phys. REV. Vol. 54, p. 1078 (1938).
- 3-8 Kawada H., Honda M., Inoue T., and Amemiya T., 'Partial Discharge Automatic Monitor for Oil-filled Power Transformer', paper 83 SM 434-8 at IEEE PES 1983 Summer Meeting, July 17-22, Los Angeles CA.
- 3-9 Howells E. and Norton E.T., 'Parameters Affecting the Velocity of Sound in Transformer Oil', paper 83 SM 435-5 at IEEE PES Summer Meeting, July 17-22, Los Angeles CA.
- 3-10 a) Temple V.A.K., 'Development of a 2.6 kV Light-Triggered Thyristor for Electric Power Systems', IEEE Trans. Electron Devices, Vol. ED-27, 1980, p. 583.
- b) Temple, V.A.K., 'Thyristor Devices for Electric Power Systems', IEEE Transactions on Power Apparatus and Systems, Vol PAS-101, No. 7, July 1982, pp. 2286-2291.
- 3-11 'Development of a Cesium-Vapor-Lamp System for Triggering Photothyristors', EL-3140, Final Report of Research Project 1291-2, June, 1983. Prepared by the General Electric Company, Schenectady, NY, for Electric Power Research Institute, Palo Alto, CA.

SECTION FOUR

**POWER SYSTEM APPLICATIONS
OF
OPTICAL POWER TRANSFER**

by

Taher Daud, Sandra Hyland, and Harold Kirkham

SECTION FOUR

POWER SYSTEM APPLICATIONS OF OPTICAL POWER TRANSFER

4.1 INTRODUCTION

Recent advances in low-cost optical fibers with very low loss figures have created widespread interest in using such fibers to transmit information from point to point. In the power industry, interest has been further stimulated by two additional features of optical fibers as data links, namely their insulating properties and their immunity to external noise. Power substations are examples of environments in which advantage can be taken of the ability of a glass fiber to withstand electrical stress and electromagnetic noise.

An optical fiber data link may not solve all the insulation or noise problems in a given installation. Suppose, for example, that a measurement is being made in a noisy substation, and the measuring equipment includes some low-power electronics connected to a high-voltage bus. (A representative example might be a solid-state multiplier used to calculate power from voltage and current signals.) The data are encoded digitally and transmitted to ground over an optical fiber. Figure 4-1 shows the arrangement.

The somewhat unusual measurement method of Figure 4-1 may be justified if, for example, a suitable current transformer is not available — such as for experimental ultra high voltage (UHV) use — or if the data requirements are reduced by performing some local data processing.

Two possible problems remain with the arrangement of Figure 4-1. First, there is a need to obtain a small amount of power for the electronics, and this could prove costly. At least enough power must be available to generate the light to be used to transmit the data, using an LED, or to modulate or encode the light beam in the case of a round-trip light beam. If the voltage is very high, a low-power transformer of suitable BIL may not be available and may have to be wound specially. Alternatively, it may be possible to tap a small amount of power off the high-voltage bus.

In either event, if the power is derived electrically, while the data link itself may be immune to external noise, the electronics may be subjected to a considerable power-supply noise, either from voltage variations or bus current variations. Further, if the installation is outdoors (i.e., not enclosed in a building), the data link and the power supply must be furnished with outdoor-rated insulation. A post insulator with rain sheds is shown in Figure 4-1 as representative.

If it were possible to transmit the power for the electronics over a fiber, use could be made of the same weather protection for power and data. The incremental cost of the fiber would be very small, actually zero if the same fiber were somehow used. The question is, can enough power be transmitted over an optical fiber to be useful, and what are the costs and problems associated with such a scheme?

Figure 4-2 shows two ways of optically powering a data link.

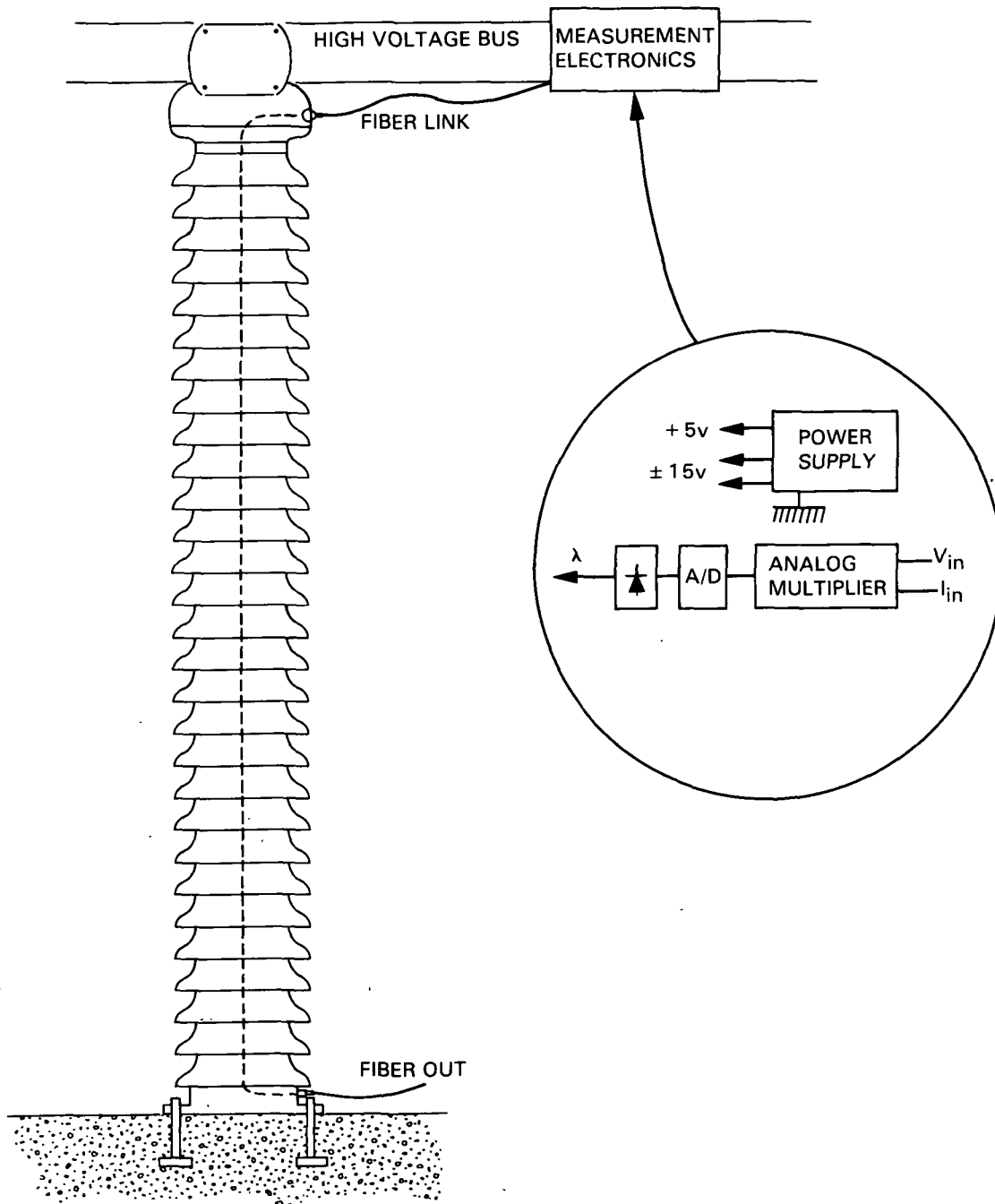


Figure 4-1. Digital data link in high voltage bus

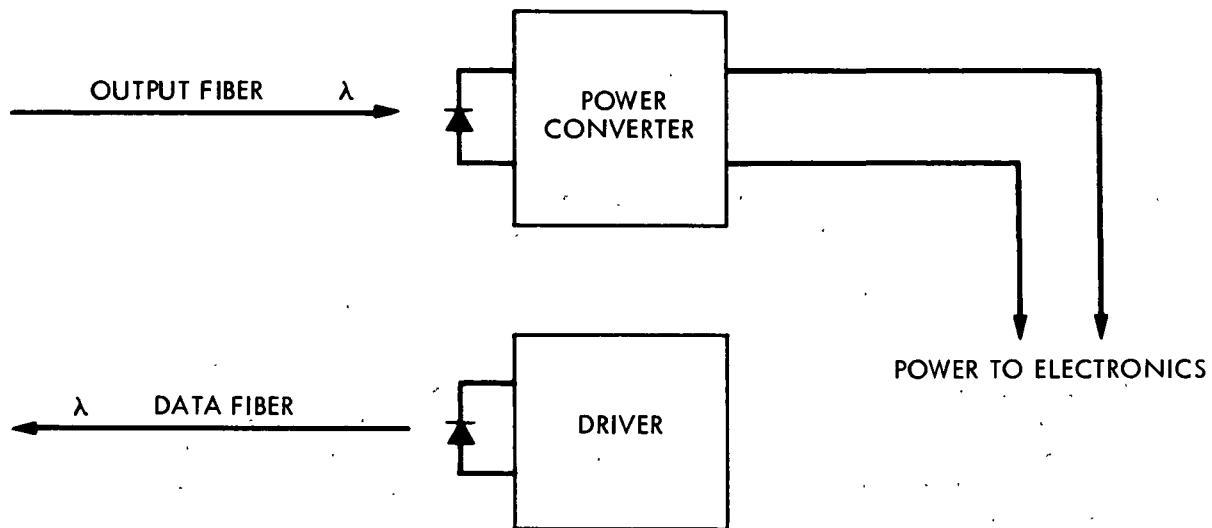


Figure 4-2a. Optical data link with power supplied over separate fiber

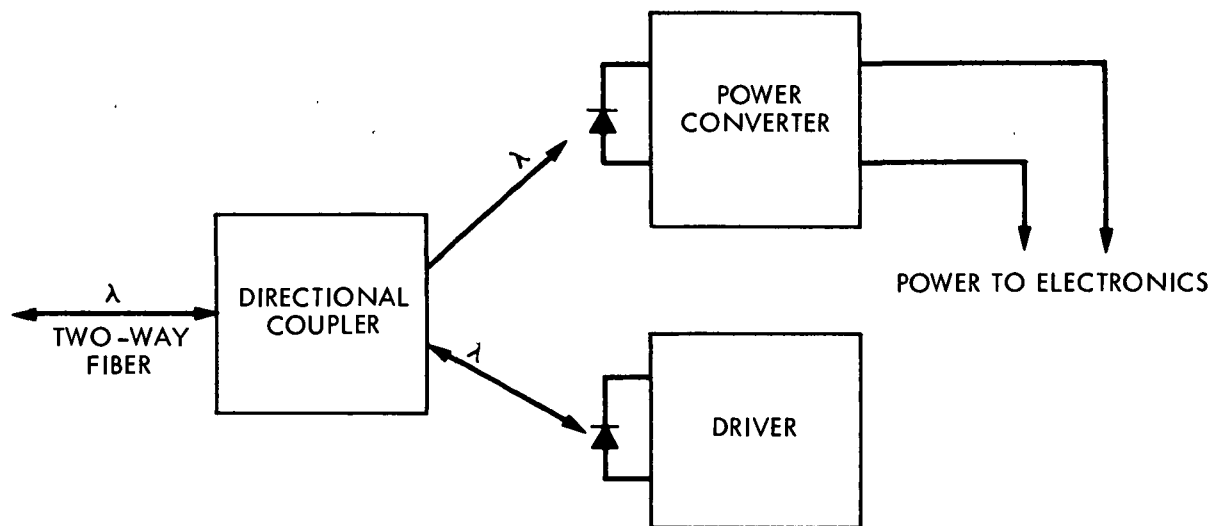


Figure 4-2b. Optical data link with power transmitted in same fiber

The study reported in this section was a small effort with the purpose of providing a background to understanding the limitations of optically-transmitted power and of initiating the design process so that power couplers can be made available in support of the other fiber optics tasks of the Communications and Control Project. The study was designed to take advantage of JPL facilities that had been developed as part of the Photovoltaics Program of the Department of Energy. These facilities included the necessary equipment to fabricate and evaluate silicon photodiodes and computer programs to aid in the design of 'solar cells'. Some sample cells were designed and made. This work is described in Section 4.3.

Section 4.2 describes the components of systems that could be made to transmit power in optical form. The remainder of Section 4.1 presents some applications for optically transmitted power.

4.1.1 Other Applications

Another application area for optically transmitted power exists in high-voltage direct current (HVDC) converters. Typically, HVDC converter valves are constructed by connecting thyristors in series and parallel. The thyristors should be reverse biased to prevent inadvertent firing. With series thyristors, a large common mode voltage appears across the firing circuit power supplies.

Considerable ingenuity has been demonstrated in developing power for the bias and firing circuits. For example, rotating insulating rods, driven by a motor and with a number of small generators attached, have been used, as have insulating rods with piezo-electric transducers and turbine generators rotated by fan-driven air.

While a considerable amount of effort is presently being expended to develop optically fired thyristors, optically coupled power provides an alternative. It should be possible to use an optical fiber to couple enough power to a suitable firing circuit to reverse bias the SCR during the non-conducting period and to apply a suitably large pulse train to guarantee firing during the conducting period. In this way the benefits of optical firing would be achieved with the reliability and low cost of conventional SCRs. Figure 4-3 shows a possible arrangement.

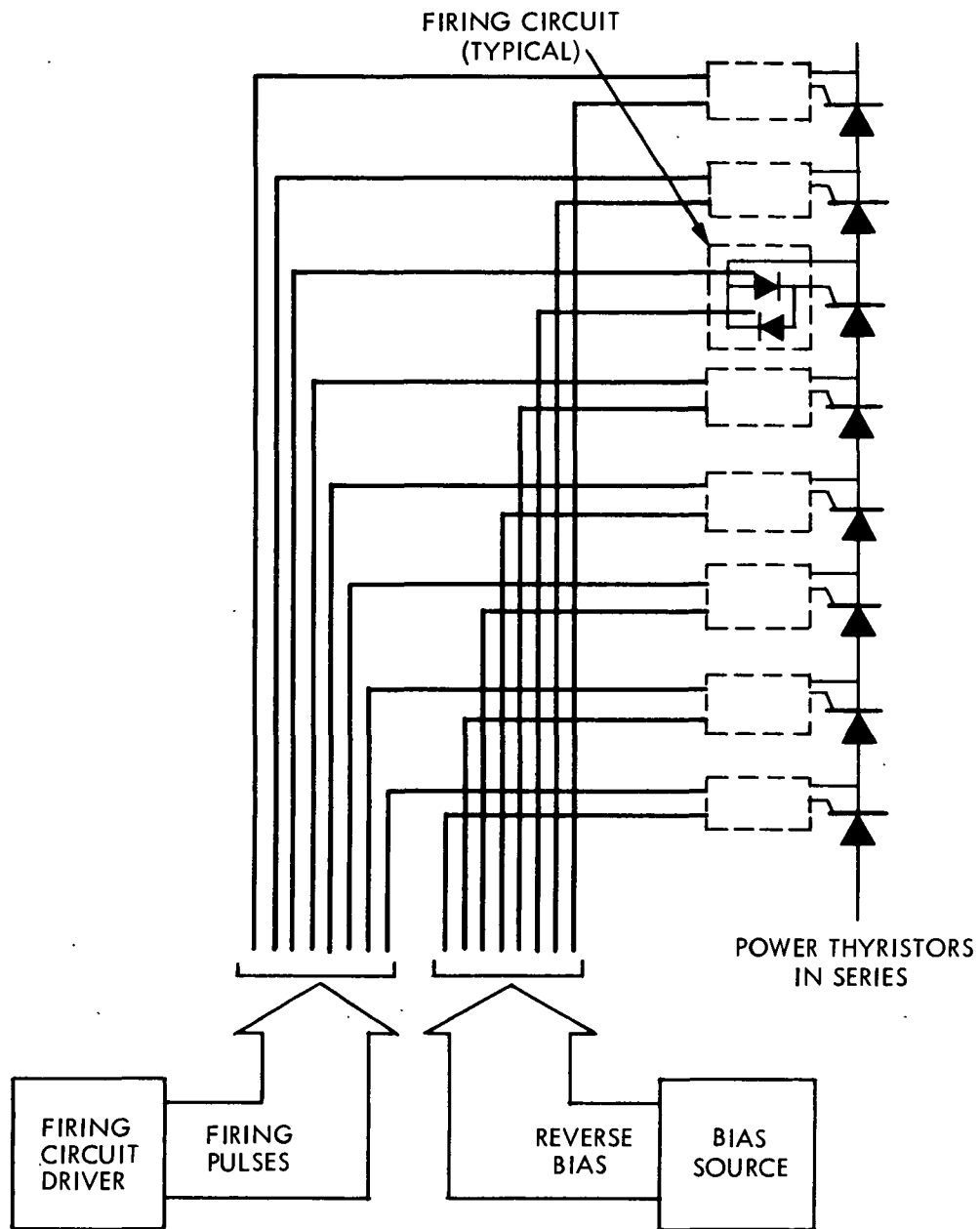


Figure 4-3. Optically-transmitted power in HVDC application

4.2 SYSTEM DESCRIPTION

4.2.1 Overall Design

It was indicated in Section 4.1 that there are situations in which it might be advantageous to transmit a small amount of electrical power optically, rather than by means of a transformer. This section will continue with a discussion of the overall design of a system suitable for transmitting a small amount of electric power optically and an examination of the various sources of inefficiency in optical transfer.

Figure 4-4 shows a suitable power transfer system in block diagram form. The system consists of a converter to change the incoming electrical energy to optical form, a coupler to insert this energy into the fiber which is used to provide isolation, the fiber itself, hardware to couple the energy emerging from the fiber into a receiver, and the receiver itself. Each of the elements in this block diagram could take many forms in practice, and each will be discussed in turn.

4.2.2 Electrical To Optical Conversion

The conversion of energy from electrical to optical form energy is usually a very inefficient one. Since we are concerned here with power and not data rate, speed is of no importance (unlike the situation in a communications application), and there are a number of possible mechanisms that could be employed, such as the ordinary incandescent lamp, the fluorescent lamp and high- or low-pressure gas discharge lamps. It is also possible to use lasers of various forms. The efficacies, in terms of output light to input power, of these devices vary considerably, as does their average (or cw) power, as is shown in Table 4-1.

The quantity 'lumens' is defined with respect to the response of the average human eye. A light source of high efficacy will produce a maximum amount of its output near the peak in the spectral response of the eye — around 555 nm. A light whose output energy is entirely in the infra-red (or the ultra-violet) region will have an efficacy of zero, since its output is not visible.

In terms of our application, it is convenient that the spectral response of the (silicon) photodiode to be used as detector is somewhat similar to the spectral response of the eye. Because of this, the efficacy of a light source can be used as a guide to the conversion efficiency at the receiver.

If we made the assumption that half the input power to a filament lamp is dissipated as heat lost to the surroundings and half available as radiated energy, the amount of that energy recoverable by a photodiode will depend on the efficiency with which the radiant energy can be coupled into the fiber, and the match between the spectrum of the light and the spectral response of the cell, i.e. its efficacy.

Since in a power system application it may be reasonably assumed that there is a plentiful supply of electrical power available at ground potential, it follows that the inefficiencies of some of the sources shown in Table 4-1 can

be tolerated. The wasted energy is dissipated as heat, and means of removing the heat are probably easy to set up on the ground. Consequently, it is not always essential to use a highly efficient light source to provide power to insert into the fiber. This would be especially true if higher average power levels are required.

TABLE 4-1. LAMP DATA

LAMP	EFFICACY (lm/W)	LUMINOSITY (lm/mm ²)	POWER RANGE (W)
Tungsten	5-15	1.0	1-2000
Tungsten halogen	15-25	0.75	25-2000
Mercury fluorescent	30-80	0.1	5-125
High pressure mercury	50-80	2.5	15-1000
Metal halide	60-120	3.0	75-10,000
Compact Source Iodide	80-100	16.0	1000-2000
High pressure sodium	80-125	7.0	50-1000
Low pressure sodium	100-150	1.5	35-225
Laser (solid state)	?	large	-5

Note: Data are for commonly available general purpose lamps, and are approximate.

4.2.3 Source to Fiber Coupling

It is somewhat misleading to consider the efficiency of the source device on its own, since it is necessary to couple the output energy into a very small fiber. If the source is physically large, it may be impractical to collect more than a small fraction of its output energy and focus it into an optical fiber. The light entering a fiber need not be well collimated. The acceptance cone half-angle for a step index fiber is given by

$$\theta_a = \sin^{-1} (n_1^2 - n_2^2)^{0.5}$$

where n_1 is the refractive index of the core and n_2 is the refractive index of the cladding.

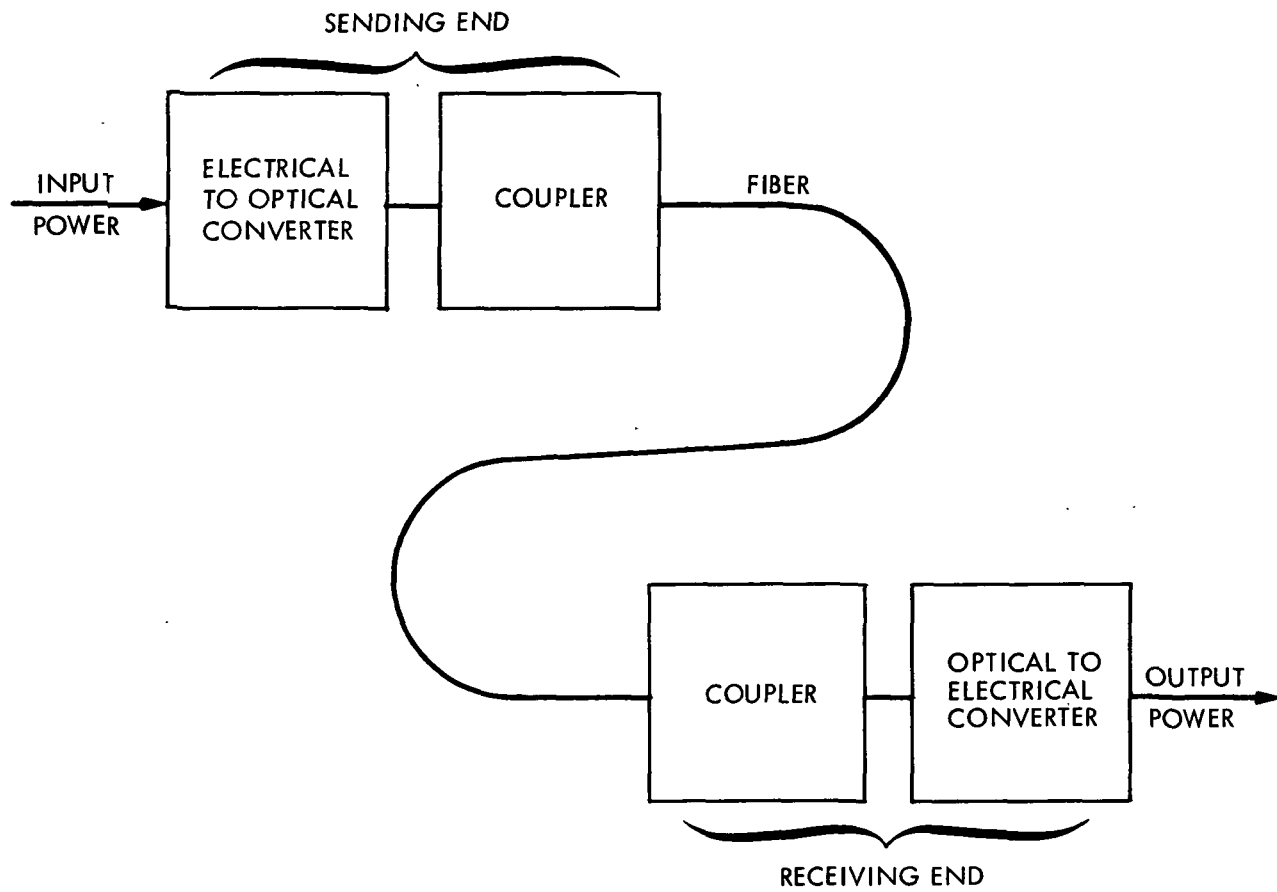


Figure 4-4. Block diagram of optical power transfer system

If we assume values for the refractive index of 1.45 and 1.47, the half-angle of the acceptance cone is about 14° . The effect can be seen in the large cone of light which emerges from the end of a fiber. Figure 4-5 shows the light cone at the end of a transmitting fiber.

The efficiency of the source to fiber coupling device, which is typically a lens, will depend upon the nature of the source. For example, if the source is highly dispersed, such as a fluorescent light bulb might be, it may be difficult to collect much of its light output. On the other hand, a concentrated and collimated source, such as a laser, couples more easily into an optical fiber. It is to be expected that sources with high luminosity (see column two of Table 4-1) will couple most effectively into optical fibers.

4.2.4 Fiber

Very efficient fibers are now available, developed primarily for the long-distance transmission of information. Losses as low as 10^{-3} dB/km are anticipated for fibers operating with wavelength above 3 nm. While the availability of such extremely low-loss fibers is, at this point, somewhat speculative, fibers are presently available with losses so low that fiber loss need be of no concern as far as transmitting the small amount of power under discussion here over the distances (a few meters) anticipated for power system use. The transmission of power over longer distances might be important in, for example, submarine cables with regenerators (repeaters), but in such applications, the electrical isolation problem is not as severe as in the power system, and use of a dc cable to provide power for the submerged electronics should be easily possible. With losses below 0.001 dB/km, regeneration of the signal may not be necessary, even on the longest submarine cable.

4.2.5 Receiving End

There are fewer choices for receiving-end equipment than there were for the sending end. Whereas a large number of devices will generate light, they cannot, generally speaking, be used in a reciprocal fashion. A wire filament irradiated by a small amount of light will not generate electricity, a laser diode does not work 'backwards'.

The physical effect of most interest for generating a small amount of electricity from light energy is the photovoltaic effect. Considerable public attention has been devoted to photovoltaic devices in recent years as possible generators of 'solar electricity'. The Jet Propulsion Laboratory has been a photovoltaic Lead Center, with facilities for designing, fabricating, and testing photovoltaic cells. Because of this it was decided to take advantage of these facilities and produce some photovoltaic cells 'optimized' for use with fiber optics power converters.

This topic is taken up in the next section of this report. For convenience, laser light at 850 nm was assumed as input.

ORIGINAL PAGE IS
OF POOR QUALITY



Figure 4-5. Light cone emerging from the end of an optical fiber

4.3 DEVICE FOR ENERGY CONVERSION AT 0.85 μm

4.3.1 Review

In a semiconductor at low temperatures, the valence band is full, and the conduction band is empty. Between these two is a band gap which is inaccessible to electrons — the forbidden band. Although, in an isolated atom, energies associated with the valence shell and the conduction shell have well-defined values, in a crystal the number of allowable states within the band increases as the number of atoms in the crystal, so that for all practical purposes each band consists of a continuum of states.

Consequently, when a photon of light energy is incident on a semiconductor crystal, photons over quite a wide range of energies can move an electron from the valence band to the conduction band, creating a hole-electron pair, and giving rise to conduction in the otherwise insulating material.

A photodiode can be made from a p-n junction in a semiconductor material. Photons are absorbed in the semiconductor, and hole-electron pairs are created. These carriers are separated by an electric field, such as exists in the depletion region of the p-n junction, and give rise to current in the external circuit.

To convert light into electricity efficiently, the material band-gap must match the energy of the incoming photons. Since the bands either side of the gap are rather broad, a broad range of incoming colors will be usable. The photon-generated carriers move by two processes: diffusion and drift. Diffusion is so slow that it can be neglected. Drift is caused by any internal field, so efficiency is improved by ensuring that incident photons are absorbed in the relatively high field of the depletion region.

In the design of a diode there are a number of parameters that can be traded off. Response speed, conversion efficiency, and usable spectrum can be adjusted, within limits, in the design process.

The development of silicon devices for conversion of light transmitted through a fiber at 0.85 μm wavelength was approached both from device fabrication and theoretical modelling viewpoints.

4.3.2 Device Design

To design a device for maximum conversion efficiency at 0.85 μm , the device was divided into three elements, each of which was addressed separately, although there is considerable interaction between the elements. The three elements were: (1) the silicon, including the base material and the device junction, (2) the metallization or contact design, and (3) the anti-reflective coating (Figure 4-6). Each of these is discussed below.

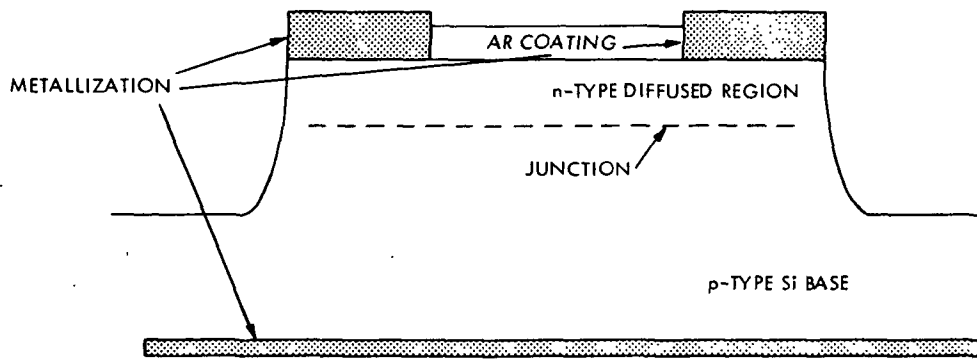


Figure 4-6 Device Design

4.3.2.1 The Silicon. Silicon for the base material can be either p-type or n-type and comes in a variety of doping levels or resistivities. There seems to be little difference in the performance of devices made on either p- or n-type bases, so the decision to use p-type silicon was made for ease in handling and processing. The choice of resistivity has more direct effect on the efficiency of the power conversion. High resistivity (low doping) material has a long minority carrier lifetime, meaning a higher current collecting efficiency, but the voltage expected from this material is low. Low resistivity (high doping) material has a shorter minority carrier lifetime and a lower current collection efficiency, but the voltage expected is higher. Both these materials were tried, with the result that the lower resistivity material was chosen.

Since light is absorbed exponentially in silicon, with the shorter wavelength light being absorbed nearer the surface of the device, the depth of the junction influences the amount of light absorbed in the n-type diffused region (Figure 4-6). Comparatively, this region is highly stressed due to heavy doping, and hence the generated carrier lifetime is short. Thus, the deeper the junction, the worse the collection efficiency for short wavelength radiations. This is also true of the longer wavelength radiation, although the influence is less marked. The junction depth also determines the maximum unmetallized area of the device that can collect current without conversion efficiency degradation. For example, a shallower junction ($\sim 0.15 \mu\text{m}$) will have a high sheet resistance for the n-region ($> 100 \Omega/[\]$) and will require metal gridlines for current collection that are close together to avoid high series resistance. However, the metal gridlines can be far apart (0.2 mm) for a deeper junction ($\sim 0.4 \mu\text{m}$) device which has comparatively lower sheet resistance ($< 25 \Omega/[\]$) without efficiency degradation due to lower series resistance. The design of the junction, then, must trade off between having a larger gridline spacing (or larger active area within the surrounding metal) with a deeper junction which will offer less series resistance but poorer short wavelength response, and a shallower junction with closer gridline spacing (or smaller area within the surrounding metal). For this study, we have used both shallow and deep junction devices and modelled both by computer to determine the optimum configuration for this application.

4.3.2.2 Metallization or Contact Design. The metallization or contact design is generally dictated by the junction depth and the device active area required. For this case, it is possible to make the device active area small and so not require any metallization in the illuminated area. This eliminates shadowing. The design for the device then becomes like a doughnut, with the active area in the center and the contact metallization surrounding it.

4.3.2.3. The Anti-Reflection Coating. It is known from the extensive work done at JPL on silicon solar cells that approximately 32% of incident light is reflected by the silicon surface. This reflection is reduced by applying one or more quarter wavelength thick anti-reflective coatings to the surface of the device. For devices designed for use under white light illumination, the anti-reflection (AR) coating is designed for the least reflection at 0.6 μm wavelength, or approximately the peak in radiation from the sun on earth. The decrease in reflectance over the entire spectrum is about 40% with this coating. For the present application, a quarter wavelength AR coating must be developed to minimize reflection at 0.85 μm , with an estimated decrease in reflection of greater than 50%.

4.3.2.4. Computer Modelling. Various computer programs have been developed to model the performance of solar cells under illumination. One of these programs was used to determine the optimum junction depth for use at 0.85 μm and the predicted current at that wavelength and the other wavelengths which may be of interest.

To predict a reasonably achievable device conversion efficiency, we have chosen an open-circuit voltage (V_{oc}) of 0.58 volts and curve fill-factor (CFF) of 0.8 that have been attained on solar cells today. A computer program that calculates the amount of short-circuit current (I_{sc}) that can be collected from a device at a given wavelength for a given input power was used to get an approximate value for I_{sc} for our devices. For an input at 0.8 μm of 1 mW (see testing conditions) the possible I_{sc} was determined to be 0.55 mA. With a V_{oc} of 0.58 V and a CFF of 0.8, the maximum predicted conversion efficiency is $(0.58 \times 0.55 \times 0.8)/1 \text{ mW} = 25.5\%$ (Figure 4-2). At 0.6 μm and 0.5 mW input power, the predicted I_{sc} is approximately 0.4 mA.

At 100 mW of 0.85 μm , the predicted I_{sc} is approximately 80 mA, resulting in a predicted device conversion of 37.8%. However, due to the fact that the light intensity is concentrated in a small area, there may be factors affecting the I_{sc} which are not included in this computer model.

4.3.3 Device Fabrication and Measurements

Two lots of devices were fabricated. One lot, #144, was a deep junction on 7-10 $\Omega\text{-cm}$ p-type material. These devices were 0.1-in (2.5-mm) in diameter in active area, 0.3-in (7.5-mm) in diameter in total area. The second lot, #164, was a shallow junction on 2-4 $\Omega\text{-cm}$ p-type material. The size of these diodes was 0.014-in (0.35-mm) diameter active area, 0.027-in (0.69-mm) diameter total area.

The devices were measured in a variety of ways, none of them reliable for predicting the behavior of these devices under 0.85 μm , 100 mW illumination. The three test conditions used were: 0.85 μm light, 1 mW; white light, 100 mW/cm²; and 0.6 μm light, 0.48 mW.

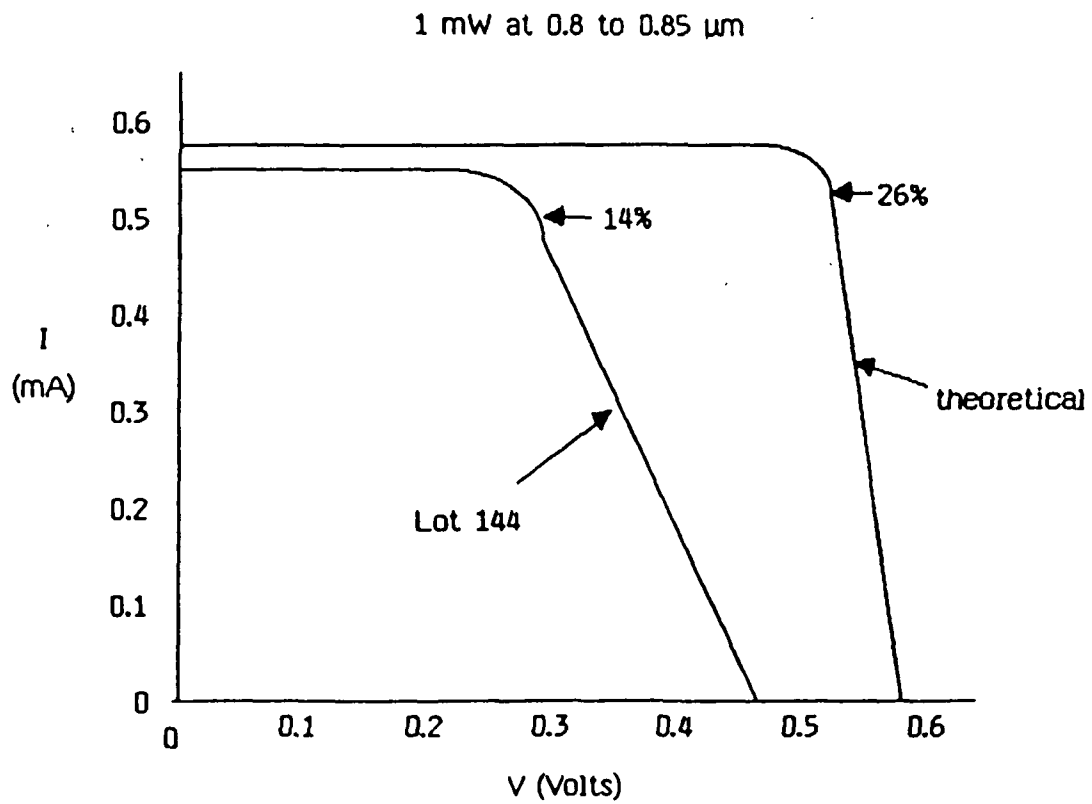


Figure 4-7 Current-Voltage Curves,
Measured and Theoretical

Lot 144, the deep junction, larger area devices, yielded a 14% conversion efficiency under 0.85 μm , 1 mW illumination (see Figure 4-7). It was felt that the low testing illumination level and the high resistivity substrate caused the open-circuit voltage (V_{oc}) to be low. The low testing illumination also caused the curve fill factor (CFF) to be low. However, the current collection ($I_{sc} \sim 0.55 \text{ mA}$) was close to that maximum predicted by the computer model. Tests under Air Mass 1 (AM1) white light illumination (100 mW/cm^2) gave a 12.1% conversion efficiency. Low-level white light tests showed the expected decrease in V_{oc} with decreasing illumination level, from $V_{oc} = 0.46 \text{ V}$ at AM1 to $V_{oc} = 0.39 \text{ V}$ at $\sim 3\%$ AM1 (see Table 4-2).

Lot 164, the smaller, shallow junction devices, showed 13.5% to 15.8% efficiency under AM1 illumination (see Table 4-3). Testing of these diodes at 0.6 μm wavelength and 0.48 mW input power showed (see Table 4-4) a maximum conversion efficiency of 18.5%. In the first set of diodes, Lot 144, several devices were fabricated before any computer modelling was done. The results of the computer modelling indicated that, even at 0.85 μm wavelength, the device junction should be shallow for maximum current collection. This was incorporated into the second set of diodes, Lot 164. In addition, it was seen that low resistivity material did not affect the current collection but did increase the V_{oc} considerably.

4.3.4 Test Results

The following pages summarize the test results of the silicon cells that were fabricated.

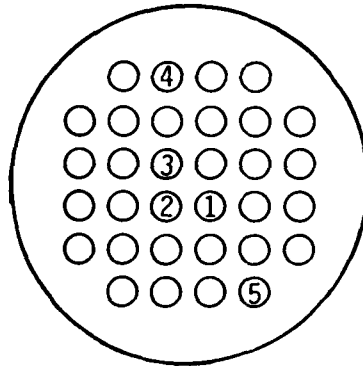
Table 4-2. Light intensity variation test

Lot #144, Diode 1

Test No.	% AMI Intensity (100 mW/cm ²)	V _{oc} (volts)	I _{sc} (mA)	P _{max} (mW)	F.F.	%η
1	3	0.39	0.058	0.0168	0.74	10.98
2	6	0.42	0.100	0.0315	0.75	10.65
3	9	0.42	0.155	0.0468	0.72	10.19
4	15	0.425	0.25	0.0864	0.77	11.60
5	100	0.462	1.715	0.617	0.78	12.10

Diode Area = 0.051 cm²
 Intensity Readings at Low Levels Are Approximate
 Efficiency Increases at Higher Intensities

Table 4-3. Lot #164 (ID-2510)



Cell No.	Cell Active Area (cm ²)	V _{oc} (Volts)	I _{sc} (mA)	P _{max} (mW)	F.F.	%η
1	0.049	0.472	1.84	0.662	0.762	13.5
2	0.049	0.475	1.92	0.728	0.797	14.8
3	0.045	0.474	1.90	0.717	0.796	15.8
4	0.045	0.472	1.83	0.693	0.805	15.3
5	0.049	0.471	1.85	0.694	0.796	14.1

$$\text{Fill Factor, F.F.} = P_{\max} / V_{oc} \cdot I_{sc}$$

$$\text{Efficiency, \%}\eta = \frac{P_{\max} \cdot 100}{P_{in}} = \frac{P_{\max} \cdot 100}{\text{Area}(\text{cm}^2) \cdot 100 \text{ mW/cm}^2} \text{ at AM1}$$

Table 4-4. Lot #164 (ID-2082)

Test with 0.48 mW, 6328 Å Laser

Cell No.	V _{oc} (volt)	I _{sc} (μA)	P _{max} (μW)	F.F.	%η
1	0.575	199	85.5	0.747	17.8
2	0.578	196.5	86.9	0.765	18.1
3	0.578	198	88.7	0.775	18.5
4	0.578	200	88.2	0.763	18.4
5	0.579	197.5	88.7	0.776	18.5

Assumption: All Radiation (0.48 mW) Concentrated within Diode Surface Area.

4.4 FUTURE WORK

It is felt that low light level conditions are misleading in terms of predicting the performance of the devices at 0.85 μm and, (say), 100 mW. This high power input may dictate changes in the device structure in terms of device area, metallization, junction depth, etc. Reliable operation at this high-light concentration may demand even further changes.

Recommendations for future work include borrowing or constructing a measurement set-up that will allow examination of device operation at light wavelengths and intensities close to those expected for device use, i.e., 100 mW at 0.85 μm . Once the devices can be measured under the predicted operating conditions, there are several device structures which can be studied.

One study involves the device area. At high concentration levels there is some degradation of device performance. Devices would be constructed in a range of sizes to find the optimum active area for maximum energy conversion. Computer simulation of devices working under high-injection conditions will be used to understand the behavior of the devices under high light concentration and to lead to the development of the best possible device area for the application.

Another device structure that can be studied is one where the diffused junction is deep below the metallization but is shallow in the device active area. It is felt that this structure will allow a very shallow junction where it is needed, in the active collection area, but the deep junction under the metallization will reduce the sheet resistance and allow for sintering to produce a good metal/silicon contact without the possibility of the metal diffusing into the junction and degrading the V_{oc} . It is also considered that this design will allow the device to work at high light concentration and elevated temperatures for a longer time.

In addition, the AR coating required for this application must be developed. This will entail determining the thickness of the coating needed for maximum transmission and may also involve investigation of conducting oxides to act both as an AR coating and also as a conductive path, reducing the device sheet resistance.

Further, the question of lifetime and reliability of these devices will require study once a design has been reached.

One more point to remember is that the best silicon response is obtained at about 0.6 μm wavelength radiation, rather than at 0.85 μm . It may, therefore, be advantageous to consider change of wavelength. This may not alter the cell structure but will alter the AR coating thickness. Another possibility would be to change the material (presently silicon) to a material with peak sensitivity at 0.85 μm . For example, it might seem natural to use a gallium arsenide photocell with a gallium arsenide laser. However, the spectral response of silicon is quite broad, so that significant improvement in efficiency is unlikely, and AR coating thickness may be more important.

APPENDIX

**SOLUTION OF POISSON'S EQUATION
IN CYLINDRICAL COORDINATES**

APPENDIX

SOLUTION OF POISSON'S EQUATION IN CYLINDRICAL COORDINATES

We start with Poisson's equation:

$$\text{div grad } V = \Delta V = \frac{-\rho}{\epsilon_0} \quad \text{A.1}$$

where V is the potential, ρ the charge density and ϵ_0 the permittivity of space. We expand in cylindrical coordinates:

$$\Delta V = \frac{\partial^2 V}{\partial r^2} + \frac{1}{r} \frac{\partial V}{\partial r} + \frac{1}{r^2} \frac{\partial^2 V}{\partial \phi^2} + \frac{\partial^2 V}{\partial z^2} \quad \text{A.2}$$

With axial (z) and circumferential (ϕ) symmetry this becomes

$$\Delta V = \frac{d^2 V}{dr^2} + \frac{1}{r} \frac{dV}{dr} = \frac{-\rho}{\epsilon_0} \quad \text{A.3}$$

We have, from physical considerations

$$J = \rho v \quad \text{A.4}$$

$$v = \mu E \quad \text{A.6}$$

and

$$J = \frac{I}{2\pi r} \quad \text{A.7}$$

where J is the current density, v the drift velocity of the space charge, μ the mobility of the ions, E the field gradient, I the ion current and r the radius. It follows that

$$J = \rho \mu E = \frac{I}{2\pi r} \quad \text{A.7}$$

Rearranging:

$$\rho = \frac{I}{2\pi \mu E r} \quad \text{A.8}$$

and hence

$$\frac{d^2 V}{dr^2} + \frac{1}{r} \frac{dV}{dr} = \frac{-I}{2\pi \mu E r \epsilon_0} \quad \text{A.9}$$

Since the field changes only in the r direction, we can substitute $E = -dV/dr$ to obtain a first order equation

$$\frac{dE}{dr} + \frac{E}{r} = \frac{I}{2\pi\mu E r \epsilon_0} \quad \text{A.10}$$

whence

$$\frac{dE}{dr} = \frac{1}{r} \left[\frac{I}{2\pi\mu\epsilon_0 E} - E \right] \quad \text{A.11}$$

Thus

$$\frac{E dE}{\left[\frac{I}{2\pi\mu\epsilon_0} - E^2 \right]} = \frac{dr}{r} \quad \text{A.12}$$

This can be integrated by means of a substitution:

$$s = \frac{I}{2\pi\mu\epsilon_0} - E^2 \quad \text{A.13}$$

so that, for constant ion current I

$$ds = -2E dE \quad \text{A.14}$$

Equation A.12 then becomes

$$\frac{dr}{r} = - \frac{ds}{2s} \quad \text{A.15}$$

Integrating:

$$\ln r + k_1 = - \frac{1}{2} \ln s \quad \text{A.16}$$

where k_1 is a constant of integration. A little algebra will yield the desired result:

$$\ln r + \ln (s)^{1/2} = k_2 \quad \text{A.17}$$

where $k_2 = -k_1$. Thus:

$$\ln r s^{1/2} = k_2 \quad \text{A.18}$$

$$r s^{1/2} = \ln^{-1} k_2 \quad \text{A.19}$$

$$s^{1/2} = \frac{\ln^{-1} k_2}{r} \quad \text{A.20}$$

or

$$s^{1/2} = \frac{k_3}{r} \quad \text{A.21}$$

where $k_3 = \ln^{-1} k_2$. Squaring both sides, we have

$$s = \frac{k_3^2}{r^2} \quad \text{A.22}$$

or, substituting for s

$$\frac{I}{2\pi\mu\epsilon_0} - E^2 = \frac{k_3^2}{r^2} \quad \text{A.23}$$

or

$$E^2 = \frac{I}{2\pi\mu\epsilon_0} + \frac{b}{r^2} \quad \text{A.24}$$

where $b = -k_3^2$ and was derived from the constant of integration in (A.16).

In the absence of a space charge, the ion current is zero and the first term of (A.24) vanishes. The result is that the gradient falls as $1/r$, which is the result to be expected from Laplace's equation. The ion current term in (A.24) has the effect of modifying the reciprocal distribution of the gradient.

In the high voltage test cage, it is the voltage which is constant. If there is an ion current varying because of environmental conditions, the gradient distribution will change. In this situation, the b coefficient in (A.24) must change. Rearranging (A.24) to find the gradient gives:

$$E = \left[a + \frac{b}{r^2} \right]^{1/2} \quad \text{A.25}$$

where a is the field contribution due to the ion current term, that is $a = I/2\pi\mu\epsilon_0$.

The system constraint that the voltage be constant can be represented by integrating (A.25):

$$V = -\int \left[a + \frac{b}{r^2} \right]^{1/2} dr \quad \text{A.26}$$

Equation (A.26) is deceptively simple — and has proved difficult to solve. Rearranging yields

$$-V = \int \frac{(ar^2 + b)^{1/2}}{r} dr \quad \text{A.27}$$

We can substitute as follows:

$$y^2 = ar^2 + b \quad \text{A.28}$$

so that

$$y \, dy = ar \, dr \quad \text{A.29}$$

$$dr = \frac{y \, dy}{ar} \quad \text{A.30}$$

and

$$r^2 = \frac{y^2 - b}{a} \quad \text{A.31}$$

Substituting in (A.27) yields

$$-V = \int \frac{y}{r} \frac{y \, dy}{ar} \quad \text{A.32}$$

$$= \int \frac{y^2 \, dy}{y^2 - b} \quad \text{A.33}$$

$$= \int \left[1 + \frac{b}{y^2 - b} \right] dy \quad \text{A.34}$$

$$= y + b \int \frac{dy}{y^2 - b} \quad \text{A.35}$$

Expanding, we obtain

$$-V = y + \frac{b}{2\sqrt{b}} \int \left[\frac{1}{y - \sqrt{b}} - \frac{1}{y + \sqrt{b}} \right] dy \quad \text{A.36}$$

$$= y + \frac{\sqrt{b}}{2} \ln \left[\frac{y - \sqrt{b}}{y + \sqrt{b}} \right] + C \quad \text{A.37}$$

where C is the constant of integration. Resubstituting for y gives

$$-V = \sqrt{ar^2 + b} + \frac{\sqrt{b}}{2} \ln \left[\frac{\sqrt{ar^2 + b} - \sqrt{b}}{\sqrt{ar^2 + b} + \sqrt{b}} \right] + C \quad \text{A.38}$$

The constant C can readily be found. If we set the cage wall voltage to zero, and designate $r = r_1$ at this radius, we find

$$C = -\sqrt{ar_1^2 + b} - \frac{\sqrt{b}}{2} \ln \left[\frac{\sqrt{ar_1^2 + b} - \sqrt{b}}{\sqrt{ar_1^2 + b} + \sqrt{b}} \right] \quad \text{A.39}$$

so that the voltage is given by

$$V(r) = \sqrt{ar^2 + b} - \sqrt{ar_1^2 + b} + \frac{\sqrt{b}}{2} \ln \left[\frac{\sqrt{ar^2 + b} - \sqrt{b}}{\sqrt{ar^2 + b} + \sqrt{b}} \right] - \frac{\sqrt{b}}{2} \ln \left[\frac{\sqrt{ar_1^2 + b} - \sqrt{b}}{\sqrt{ar_1^2 + b} + \sqrt{b}} \right] \quad \text{A.40}$$

Equation (A.40) can be solved for $V(r)$ by specifying the coefficient a (the contribution due to ion current) and finding the coefficient b . At the surface of the center conductor, say radius r_2 , the left-hand side of (A.40) can be set equal to the applied voltage. While a closed form solution for b does not seem possible, numerical methods can be used to find the value, so that (A.25) can be used to obtain a gradient profile.

Even the problem of writing a computer program to find the coefficient b proved to be a challenge: using a BASIC program and an 8-bit computer difficulty was experienced in implementing an iterative solution of equation (A.40) to find b . The problem was traced to the logarithm function, which was executed on the difference between two square-roots. With the 8-bit machine, the square root function was returning the same value for successive calls which were almost identical, and this was giving problems in the subsequent logarithm call. The solution was to test the difference between the values whose square roots were going to be subtracted from one another. If the difference was small (less than an arbitrary breakpoint, set at 0.1%) the square root call was replaced by an evaluation based on the binomial expansion. It will be recalled that the expansion of $(1 + x)^n$ for $n = 1/2$ is

$$1 + \frac{1}{2}x - \frac{1}{8}x^2 \dots \dots \dots \quad \text{A.41}$$

so that, in the terms used in (A.40)

$$\sqrt{ar^2+b} - \sqrt{b} = \sqrt{b} \left[1 + \frac{ar^2}{2b} \dots \dots \dots \right] - \sqrt{b} \quad \text{A.42}$$

$$= \frac{1}{2} \frac{ar^2}{\sqrt{b}} \quad \text{for } ar^2 \ll b \quad \text{A.43}$$

to a first approximation, since the first term in (A.41) cancels in (A.42). This approximation resulted in satisfactory program execution: further terms were retained in the final version of the program, but the results were very similar, and did not change when terms beyond the third were dropped.

The program consists of two segments. First, the value of b was computed so that, for any value of ion current in (A.40) the required conductor voltage (500 kV in the final version) was obtained. Using this value of b the gradient was calculated from equation (A.25) at various radii.

The ion currents and radii were specified in a DATA statement, and the b coefficients calculated one at a time. The program listing is shown in Table A.1, and the program output is given in Table A.2.

Program results are presented graphically in Section 2.3.2.

TABLE A.1
PROGRAM LISTING

```

10 REM          PROGRAM FOR FIELDS          FILENAME "B:POISSON"
20 REM          SOLVES POISSON'S EQUATION IN CYLINDRICAL COORDINATES
30 REM          WITH A FIXED APPLIED VOLTAGE AND VARIOUS ION CURRENTS.
40 REM INIT
50 DIM A(10),C(10),GRAD(8),R(8)
60 REM  DATA FOR VALUES OF CURRENT
70 DATA .000001,.02,.05,.1,.2,.5,1,2,5,10
80 REM THE LOWEST VALUE OF CURRENT IS USED INSTEAD OF ZERO
90 REM WHICH WOULD MAKE THE PROGRAM BLOW UP!
100 REM
110 REM DATA FOR RADII AT WHICH TO CALCULATE FIELD
120 DATA .05,.1,.2,.5,1,2,5,10
130 B=8900
140 REM FIRST GUESS B
150 R1 = 10
160 R = .05
170 REM          THE PROGRAM IS IN TWO PARTS.  THE FIRST PART FINDS THE
180 REM          VALUE OF THE COEFFICIENT B IN EQUATION A.40 SO THAT
190 REM          THE VOLTAGE CONDITIONS ARE MET AT THE BOUNDARIES.
200 FOR I = 1 TO 10
210 READ C(I)
220 REM NEED TO CONVERT THE ION CURRENT VALUES (IN MICRO AMPS)
230 REM INTO THE PROPER UNITS.  THE COEFFICIENT A IN EQUATION
240 REM A.25 IS GIVEN BY  $I/(2*PI*MU*E-ZERO)$ .  WITH ONE MICRO AMP,
250 REM AND THE RIGHT VALUES FOR THE CONSTANTS, A WORKS OUT TO
260 REM BE 1.7983609E8 IN  $(V/M)^2$ .  TO EXPRESS THE VALUE IN
270 REM  $(KV/M)^2$  WE NEED TO MULTIPLY THE ION CURRENT IN
280 REM MICRO AMPS BY 179.836.  THEREFORE.....
290 A(I)=C(I)*179.836
300 NEXT I
310 FOR J=1 TO 8
320 READ R(J)
330 NEXT J
340 REM FIRST SOLVING FOR B BY HOLDING CONSTANT V
350 FOR I=1 TO 10
360 T1 = SQR(A(I)*R^2+B)
370 T2 =SQR(A(I)*R1^2+B)
380 TB=SQR(B)
390 BRK=(T2-TB)/TB

```

TABLE A.1 (Cont.)

```

400 REM TEST THE VALUES TO SEE IF WE CAN USE THE BASIC SQR FUNCTION
410 REM OR WHETHER WE HAVE TO MAKE AN APPROXIMATION USING THE
420 REM BINOMIAL THEOREM TO EXPAND THE SQUARE ROOT.
430 REM THE SQR CALL WORKS OK, BUT THE SUBSEQUENT LOG CALL
440 REM CRASHES IF ASKED FOR THE LOG OF A SMALL ENOUGH NUMBER.
450 IF BRK<.001 GOTO 480
460 T5=LOG(T2-TB)
470 GOTO 510
480 T5=.5*A(I)*R1^2/TB
490 T5=T5-.5*T5^2/TB+.5*T5^3/B
500 T5=LOG(T5)
510 T6=LOG(T2+TB)
520 BRK=(T1-TB)/TB
530 IF BRK<.001 GOTO 560
540 T7=LOG(T1-TB)
550 GOTO 590
560 T7=.5*A(I)*R^2/TB
570 T7=T7-.5*T7^2/TB+.5*T7^3/B
580 T7=LOG(T7)
590 T8=LOG(T1+TB)
600 T9=T5-T6
610 T10=T7-T8
620 C=T2+(TB/2)*T9
630 V=T1+(TB/2)*T10-C
640 VERR =V+500
650 REM THIS IS A GOOD PLACE TO PUT DIAGNOSTICS IF THE PROGRAM BOMBS.
660 IF ABS(VERR)<.001 GOTO 730
670 B=B+15*VERR
680 GOTO 360
690 REM      AT THIS POINT WE GOT A VALUE FOR B
700 REM      THE SECOND MODULE USES THE VALUE OF B TO CALCULATE
710 REM      VALUES FOR THE FIELD AT VARIOUS RADII.
720 REM
730 B(I)=B
740 FOR J=1 TO B
750 GRAD(J)=SQR(A(I)+B(I)/R(J)^2)
760 NEXT J
770 REM REALLY NOT MUCH TO FINDING THE GRADIENT ONCE THE
780 REM VALUES OF THE COEFFICIENTS HAVE BEEN FOUND!
790 LPRINT
800 LPRINT "ION CURRENT IN MICROAMPS";C(I)
810 LPRINT "RADIUS      .05      .1      .2      .5"
820 LPRINT "GRADIENT ";GRAD(1);"      ";GRAD(2);"      ";GRAD(3);"      ";GRAD(4)
830 LPRINT "RADIUS      1      2      5      10"
840 LPRINT "GRADIENT ";GRAD(5);"      ";GRAD(6);"      ";GRAD(7);"      ";GRAD(8)
850 NEXT I
860 END
870 REM WRITTEN BY HAROLD KIRKHAM, MARCH 1984

```

TABLE A.2
PROGRAM OUTPUT

ION CURRENT IN MICROAMPS .000001				
RADIUS	.05	.1	.2	.5
GRADIENT	1887.39	943.695	471.847	188.739
RADIUS	1	2	5	10
GRADIENT	94.3695	47.1847	18.8739	9.43696
ION CURRENT IN MICROAMPS .02				
RADIUS	.05	.1	.2	.5
GRADIENT	1883.81	941.906	470.956	188.39
RADIUS	1	2	5	10
GRADIENT	94.2094	47.1333	18.9333	9.60806
ION CURRENT IN MICROAMPS .05				
RADIUS	.05	.1	.2	.5
GRADIENT	1878.47	939.241	469.628	187.871
RADIUS	1	2	5	10
GRADIENT	93.9714	47.0574	19.0225	9.85942
ION CURRENT IN MICROAMPS .1				
RADIUS	.05	.1	.2	.5
GRADIENT	1869.68	934.849	467.439	187.016
RADIUS	1	2	5	10
GRADIENT	93.5801	46.9339	19.1717	10.2653
ION CURRENT IN MICROAMPS .2				
RADIUS	.05	.1	.2	.5
GRADIENT	1852.45	926.242	463.15	185.342
RADIUS	1	2	5	10
GRADIENT	92.8162	46.6978	19.4711	11.0343
ION CURRENT IN MICROAMPS .5				
RADIUS	.05	.1	.2	.5
GRADIENT	1803.08	901.577	450.863	180.555
RADIUS	1	2	5	10
GRADIENT	90.65	46.063	20.372	13.0841
ION CURRENT IN MICROAMPS 1				
RADIUS	.05	.1	.2	.5
GRADIENT	1726.4	863.278	431.795	173.155
RADIUS	1	2	5	10
GRADIENT	87.3529	45.1942	21.8601	15.9481
ION CURRENT IN MICROAMPS 2				
RADIUS	.05	.1	.2	.5
GRADIENT	1586.22	793.279	396.98	159.74
RADIUS	1	2	5	10
GRADIENT	81.5414	43.9546	24.7234	20.5564
ION CURRENT IN MICROAMPS 5				
RADIUS	.05	.1	.2	.5
GRADIENT	1215.56	608.333	305.273	125.164
RADIUS	1	2	5	10
GRADIENT	67.756	42.6861	32.355	30.5957
ION CURRENT IN MICROAMPS 10				
RADIUS	.05	.1	.2	.5
GRADIENT	642.227	323.207	165.724	76.8436
RADIUS	1	2	5	10
GRADIENT	53.1508	45.3323	42.8885	42.528